THESIS

# ANOMALOUS DIFFUSION OF MRNA IN THE CYTOPLASM OF HELA CELLS

Submitted by

Ryan Roessler

School of Biomedical Engineering

In partial fulfillment of the requirements

For the Degree of Master of Science

Colorado State University

Fort Collins, Colorado

Spring 2024

Master's Committee:

Advisor: Diego Krapf

Tim Stasevich
Ashok Prasad

ABSTRACT

ANOMALOUS DIFFUSION OF MRNA IN THE CYTOPLASM OF HELA CELLS

Information about the diffusive motion of RNA would provide insights into intracellular structures and functions, as well as gene expression and genetic regulation. We study the motion of individual messenger RNA molecules in the cytoplasm of HeLa cells. RNAs are imaged in live cells via total internal reflection (TIRF) microscopy. In order to visualize individual RNA molecules expressing the MYH9 gene, they were labeled via MS2 stem loops bound to coat proteins tagged with the HaloTag-JF646 fluorophore. We then used single-particle tracking to obtain trajectories of individual molecules. Trajectories were analyzed in terms of their mean-squared displacement (MSD) and power spectral density (PSD). We observed non-ergodic, subdiffusive behavior, with statistics that depend on observation time, i.e., aging. Additionally, we observe stochastic switching between two mobility states with an order of magnitude difference in diffusivity. This switching process is responsible for the aging nature of the system. When compared to the cytoplasmic motion of synthetic nanoparticles, the analysis of RNA trajectories gives rise to discrepancies that raise questions about specific intracellular interactions.

# ACKNOWLEDGEMENTS

First and foremost, I would like to thank Dr. Diego Krapf for giving me the opportunity to be involved in his lab and for being an outstanding mentor and advisor. I would like to thank Carsten Dietvorst for being another fantastic mentor and friend to me during my research. I would also like to thank our collaborators O'Neil Wiggan and Dr. Tim Stasevich for their support, advice and guidance. Thank you to all of my comittee members for taking the time and interest to review this work. This material is based upon work supported by the National Science Foundation under Grant No. 2102832. Any opinions, findings, and conclusions or recommendations expressed in this material are those of the author and do not necessarily reflect the views of the National Science Foundation.

# DEDICATION

*I would like to dedicate this thesis to my mother. You always took an interest in my life and goals, and I don't know where I'd be without your love and support.*

TABLE OF CONTENTS

LIST OF FIGURES

# Chapter 1

# Introduction

A wide range of biological processes involve diffusion, and many biological systems would cease to exist without it. Some of these processes include but are not limited to the movement of gasses across capillary beds from the lungs to the blood stream [9], the scent of a flower permeating through space, the passive transport of water and nutrients across the membrane of a cell [10], the motion of macromolecules like proteins and nucleic acids in a cell or cell membrane [11–13], surface interactions of implanted biomaterials and biosensors, biomolecular recognition and biochemical reactions [14]. Understanding how certain molecules diffuse in biological systems like living cells can elucidate the molecular mechanisms and interactions that govern their motion, as well as intracellular structures, physiology, and more complex interactions like genetic regulation [15].

## 1.1 Diffusion & Brownian Motion

Perhaps one of the earliest accounts of diffusion comes in 60 BCE from the Roman poet and philosopher Titus Lucretius, who while observing the motion of dust particles in a beam of light, stated the following [16]: "Thou turn thy mind the more unto these bodies which here are witnessed tumbling in the light: namely, because such tumblings are a sign that motions also of the primal stuff secret and viewless lurk beneath, behind. For thou wilt mark here many a speck, impelled by viewless blows, to change its little course, ... And then those bodies built of unions small and nearest, as it were, unto the powers of the primeval atoms, are stirred up by impulse of those atoms' unseen blows, ... Thus motion ascends from the primevals on, and stage by stage emerges to our sense, until those objects also move which we can mark in sunbeams, though it not appears what blows do urge them." In this incredible depiction, Lucretius both postulates the existence of atoms, as well as observes/hypothesizes the macroscopic emergence of microscopic thermal fluctuations, later to be known as Brownian motion [17].

Diffusion is the 'mixing' or 'spreading out' caused by the Brownian motion of surrounding atoms or molecules [18]. The atomic-scale "self diffusion" of atoms and molecules is evident in all states of matter, with their motion becoming increasingly rapid from solids ($\sim$ nm/s, or $\sim \mu\mathrm{m/s}$ near the melting temperature of a metal) to liquids ($\sim$ mm/s) to gases ($\sim$ cm/s), respectively [18].

To quote the French scientist Georges Gouy: "Brownian motion, unique among physical processes, makes visible the constant state of internal restlessness of bodies in the absence of any external cause ... It is a weakened and remote testimony of thermal molecular motions." [18]. Take for example a solution of pure water; on a microscopic/atomic scale, the water molecules ($\sim$ 3 Å in diameter) are dancing and bumping into one another in continuous random motion, the root cause of which is thermal energy [18]. This motion is invisible both to the naked eye, and even with the help of a light microscope. However, as Robert Brown observed in 1827, when a relatively macroscopic pollen granule ($\sim 5\ \mu\mathrm{m}$ in diameter) is immersed in water, the microscopic movement of the water molecules gives rise to the random motion of the pollen, which Brown observed under a microscope, stating the following: "While examining the form of these particles immersed in water, I observed many of them very evidently in motion ... These motions were such as to satisfy me, after frequently repeated observation, that they arose neither from currents in the fluid, nor from its gradual evaporation, but belonged to the particle itself" [18]. Brown's observation is most likely the same phenomenon that Lucretius observed with dust particles in the air.

Mathematically speaking, Brownian motion is the solution to the diffusion equation

$$\frac{\partial P}{\partial t} = D\left(\frac{\partial^2 P}{\partial x^2} + \frac{\partial^2 P}{\partial y^2}\right) \tag{1.1}$$

where $D$ is the diffusion coefficient, and $P$ is either a particle concentration or probability of finding a particle at location $(x, y)$ at time $t$ [19]. In the event that a particle is at the origin at time zero, the solution to Eq (1.1) is the Gaussian function

$$P\left(\mathbf{r}, t\right) = \frac{1}{4\pi D t} e^{r^2/(4Dt)} \tag{1.2}$$

where $r^2 = x^2 + y^2$ and $P(\mathbf{r}, t)$ is the probability of finding the particle at location $\mathbf{r}$ at time $t$. Classical Brownian motion is characterized by independent and uncorrelated increments [19].

## 1.2 Mean Square Displacement

The diffusion coefficient is often of interest, and essentially represents the speed at which the object diffuses. A common way of estimating the diffusion coefficient is via the mean square displacement (MSD), which can be calculated by averaging experimental measurements [19]. From Eq (1.2), the MSD in two dimensions is [19]

$$\langle r^2 \rangle = \int_0^\infty (2\pi r)\, P\left(\mathbf{r}, t\right) r^2 dr = 4Dt. \tag{1.3}$$

Typically, the time-averaged (TA) MSD is taken, requiring only a single particle or trajectory

$$\overline{\delta^2\left(\mathrm{t_{lag}}\right)} = \frac{1}{T_m - t_{\mathrm{lag}}} \int_0^{T_m - t_{\mathrm{lag}}} \left[\mathbf{r}\left(\tau + t_{\mathrm{lag}}\right) - \mathbf{r}\left(\tau\right)\right]^2 \mathrm{d}\tau, \tag{1.4}$$

where $T_m$ is the experimental observation time, or measurement time, $t_{\mathrm{lag}}$ is the lag time, and $r(t)$ is the position at time $t$ [19, 20]. Alternatively, there is the ensemble-averaged (EA) MSD, requiring an ensemble of observations

$$\left\langle r^2\left(t_{\mathrm{lag}}\right)\right\rangle = \frac{1}{N} \sum_{n=1}^{N} \left[r_n\left(t + t_{\mathrm{lag}}\right) - r_n\left(t\right)\right]^2 \tag{1.5}$$

where $N$ is the number of observed trajectories and $t$ is the starting time relative to the first point in the trajectory [21]. There is an important distinction in notation between Eq 1.4 and 1.5, namely, brackets versus a bar on the left hand sides. Bracket notation refers to an ensemble average, whereas bar notation refers to a time average; this notation will be used consistently throughout this document. When both the TA (in the limit of infinite time) and EA (in the limit of infinite particles) MSDs converge, the process is said to be ergodic, i.e., the mean values of various observables are independent of the averaging method. Normal diffusion processes (e.g. Brownian motion) are ergodic, and also follow the Gaussian central limit theorem (CLT), which states that if

a random time series $x(t)$ is the sum of random, identically distributed increments with a stationary distribution, have finite variance, and are independent, then the probability density function (PDF) of $x$ at time $t$ is Gaussian in shape. Thus, the EA-MSD obeys $\langle x^2(t)\rangle \propto t$ at long times [19,22,23].

A more statistically robust approach to calculating the average MSD is a combination of Eqs. (1.4) and (1.5), deemed the ensemble-time averaged (ET) MSD

$$\overline{\langle \delta^2 \left(t_{\mathrm{lag}}\right)\rangle} = \frac{1}{T_m - t_{\mathrm{lag}}} \left\langle \int_0^{T_m - t_{\mathrm{lag}}} \left[\mathbf{r}\left(\tau + t_{\mathrm{lag}}\right) - \mathbf{r}\left(\tau\right)\right]^2 \mathrm{d}\tau \right\rangle, \tag{1.6}$$

where $t_{\mathrm{lag}}$ is the time between steps (or frames) [24].

## 1.3 Power Spectral Density

Power spectral density (PSD) is another powerful tool for characterizing random processes. Traditionally, the PSD is an ensemble averaged property taken over an infinitely large observation time; specifically, it is the Fourier transform of the covariance function of a given signal [25]. Many physical and biological systems experience correlations that exist as a broad spectrum of relaxation times with a $1/f^{\beta}$ decay in their power spectrum [24]. This behavior is observed in systems including but not limited to nano-scale electrodes [26], semi-conductor devices [27], quantum dots [28], DNA sequences [29], earthquakes [30], and even heartbeats [31].

The PSD is given by the following general formula

$$S_{T_m}\left(\omega\right) = \frac{1}{T_m} \left| \int_0^{T_m} x\left(t\right) e^{-i\omega t} dt \right|^2 \tag{1.7}$$

where $T_m$ is the measurement time [25, 32].

## 1.4 Wiener-Khinchin Theorem

The Wiener-Khinchin theorem is a useful mathematical tool for relating the time and frequency portrayals of a fluctuating process. Given either a measured autocorrelation function $C(\tau)$ of a stationary random signal $x(t)$

$$C(\tau) = \langle x(t+\tau)\, x(t) \rangle \tag{1.8}$$

or PSD (recall Eq. 1.7), the Wiener-Khinchin theorem

$$S(\omega) = \int_{-\infty}^{\infty} e^{-i\omega\tau} C(\tau)\, d\tau = 2\int_{0}^{\infty} \cos\omega\tau C(\tau)\, d\tau \tag{1.9}$$

states that they are equal, and provides a method for determining the other [32–35].

A problem however arises for nonstationary processes. The Wiener-Khinchin theorem fails for an aging process where the correlation function $C(\tau, t) = \langle x(t+\tau)x(t))\rangle$ and PSD (Eq. 1.7) both depend on observation time.

For a broad class of self-similar processes with an autocorrelation function of the form $\langle x(t+\tau)x(t))\rangle \sim t^{\gamma}\phi_{EA}(\tau/t)$, the time averaged PSD is given in terms of $C(\tau, t)$ as

$$S_{TA}(\omega, T_m) = \frac{2}{T_m}\int_0^{T_m} dt'' \int_0^{t''} \cos\omega t' C\left(t', t'' - t'\right) dt' \tag{1.10}$$

where both arguments of the correlation function are positive by taking $C(-\tau, t+\tau)$, and the time-averaged correlation function is defined as

$$C_{TA}(T_m, \tau) = \frac{1}{T_m - \tau}\int_0^{T_m-\tau} I(t_1)I(t_1+\tau)dt_1 \tag{1.11}$$

Furthermore, the correlation function is related to the PSD via

$$C(\tau, T_m - \tau) = \frac{1}{\pi}\Big[1 + T_m\frac{\delta}{\delta T_m}\Big]\int_0^{\infty} \cos\omega\tau S_{TA}(\omega, T_m)\, d\omega \tag{1.12}$$

for the case where $T_m > \tau$. Consider equations (1.10) and (1.11) a generalization of the Weiner-Khinchin theorem (Eq. 1.9) for nonstationary finite time processes. The nonstationary Weiner-Khinchin theorem allows us to estimate the power spectrum of an aging process in the limit of $T_m \to \infty$ [33, 35].

## 1.5 Anomalous Diffusion in Biological Systems

Whereas Brownian Motion is characterized by a TA-MSD that scales linearly with time, dynamics in living cells often scale non-linearly

$$\overline{\delta^2\left(t_{\mathrm{lag}}\right)} = D{t_{\mathrm{lag}}}^{\alpha}, \tag{1.13}$$

where $D$ is the generalized diffusion coefficient, and $\alpha \neq 1$. Living cells offer a fluid environment heavily crowded with macromolecules, and diffusion in cells is often observed to be anomalous and subdiffusive, i.e., $\alpha < 1$ from Eq. (1.6) [11, 12, 19, 20, 36]. Anomalous diffusion (and sometimes ergodicity-breaking) in living cells or cell membranes manifests as a broad spectrum of varying TA-MSDs for individual trajectories [14, 20].

There are several ways to model anomalous diffusion in living cells; two of the most common ways are fractional Brownian motion (fBM) and continuous time random walks (CTRWs). fBM is a generalization of classical Brownian motion, and is defined not by independent increments, but instead by increments that depend on previous ones. Similar to Eq. (1.2) and consistent with Eq. (1.6) the probability density function (PDF) for fBM is Gaussian, only with a time-dependent diffusion coefficient

$$P\left(x,t\right) = \frac{1}{\sqrt{2\pi D t^{\alpha}}} e^{-x^2/(2Dt^{\alpha})} \tag{1.14}$$

where $\alpha$ is the anomalous exponent, and in this case, $D$ has units of $\mathrm{cm}^2/\mathrm{s}^{\alpha}$. fBM may originate from viscoelastic media, which can result from heavily crowded environments involving transient, intermolecular interactions. In a viscoelastic medium, a particle experiences both positive and negative forces in relation to its instantaneous velocity, which results in antipersistent motion (i.e. having the tendency to backtrack to its past locations) [19, 36].

Another way of representing anomalous diffusion is the CTRW. In a classical random walk, a particle forms a trajectory via random steps which occur at times spaced equally between jumps (constant waiting times). If the step size (i.e. distance between jumps) is either constant, or is ran-

dom with finite mean and variance, the random walk converges to Brownian motion at long times. However, if the waiting times between steps are variable, we say it is a CTRW with "sojourn times" (waiting times) that are independent and identically distributed (i.i.d.) random variables with a probability density function $\Psi(\tau)$. When $\Psi(\tau)$ has a finite mean and variance, the average number of steps in time $t$ is $t/\tau_0$, where $\tau_0$ is the characteristic time of the distribution. In this scenario, diffusion is normal for $t >> \tau_0$. However, if $\Psi(\tau)$ has undefined moments (no characteristic scale), the characteristic time becomes the total observation time of the experiment, and we say the process exhibits aging; in other words, experimental results depend on your measurement time . An example of such a scale-free PDF is a power-law distribution

$$\Psi(\tau) \sim \tau^{-(1+\alpha)}, \tag{1.15}$$

where the mean waiting time $\langle\tau\rangle$ diverges, resulting in aging, ergodicity breaking, and having the potential for very long waiting times between jumps [19, 23, 37].

For a fBM-like process, its autocorrelation function for discrete times *n* is given by

$$\langle x_n x_{n+\Delta n}\rangle = \Delta x^2 \left[n^{2H} + (n+\Delta n)^{2H} - \Delta n^{2H}\right] \tag{1.16}$$

where $H$ is the Hurst exponent [24]. When $2H = 1$, fBM becomes normal Brownian motion. The ensemble-averaged autocorrelation function scales as $C_{EA}(t,\tau) \sim t^{\alpha}$, being independent of lag time, this equals the MSD, resulting in a traditional CTRW exhibiting subdiffusion with anomalous exponent $\alpha$. Using the aging Wiener-Khinchin theorem, an exact solution can be found for the PSD (expanding around $\omega t_m >> 1$), where the leading term scales as

$$\langle S_{2H=1}(\omega, t_{\mathrm{m}})\rangle \sim \frac{1}{t_{\mathrm{m}}^{1-\alpha}\omega^2} \tag{1.17}$$

When $2H \neq 1$, the process develops correlated increments, where $H > 0.5$ corresponds to positive correlations (persistent) and $H < 0.5$ corresponds to negative correlations (antipersistent) [24].

Again, using the aging Wiener-Khinchin theorem, for the case of negatively correlated increments ($H < 0.5$), the PSD scales as

$$\langle S_{H<1/2}(\omega, t_{\mathrm{m}})\rangle \sim \frac{1}{t_{\mathrm{m}}^{1-\alpha}\omega^{2-\alpha+2\alpha H}} \tag{1.18}$$

Additionally, for the case of positively correlated increments, the PSD scales as

$$\langle S_{H>1/2}(\omega, t_{\mathrm{m}})\rangle \sim \frac{2Dt_{\mathrm{m}}^{2\alpha H-1}}{\omega^2} \tag{1.19}$$

where $D$ is the generalized diffusion coefficient [24].

## 1.6 Single Particle Tracking

Almost everything discussed thus far comes from data obtained through observations of single molecules or particles. Single particle tracking (SPT) is an extremely useful tool involving microscopy, and has become an integral, quantitative process in the biological sciences. SPT measurements consist of one or more trajectories (i.e. position as a function of time $r(t)$), and provide a plethora of insights into the underlying mechanisms, interactions and forces that govern the particle's movement; it may also elucidate the structure and physiology of a cell, or even more complex interactions involved in things like genetic regulation [12, 15, 23]. It is often difficult to obtain an ensemble of trajectory measurements, which is why individual time averages are more common [19].

## 1.7 Super-resolution Microscopy

In order to perform SPT experiments, particles on the order of $\mu\mathrm{m}$ or nanometers must be sufficiently resolved. This is a challenge due to what is known as the diffraction limit, or Abbe's resolution limit, which is the smallest distance that can be resolved between two objects by optical instruments [38]. In other words, the resolution of an image is determined by both the diffraction of light through the specimen you are imaging, and the objective lens you are imaging with. The

image of an infinitely small point object appears as a circular Airy disk surrounded by concentric light and dark rings of decreasing intensity. The radius of the first dark ring is given as

$$r_{\text{Airy}} \sim \frac{\lambda_o}{NA_{\text{obj}}}, \tag{1.20}$$

where $r_{\text{Airy}}$ is a distance in the plane of the specimen, $\lambda_o$ is the wavelength of light being used, and $NA_{\text{obj}}$ is the numerical aperture of the objective lens. The image of two adjacent points of equal intensity can only be resolved if the distance $d$ between them is greater than or equal to $r_{\text{Airy}}$ [39]. In other words, if two objects are closer than $\lambda/2NA$, a microscope cannot resolve them [40].

### 1.7.1 Fluorescence Microscopy

One method of overcoming the diffraction limit is through a technique called fluorescence microscopy, in which the sample of interest becomes a fluorescent signal against an otherwise black background, and effectively has an very high signal to noise ratio (SNR). Fluorescence results when a molecule absorbs some wavelength of light (excitation) and transitions to an 'excited state' before undergoing a second transition mere nanoseconds later, emitting a slightly higher wavelength of light (emission). By filtering out your excitation wavelength, you are left seeing only the emission wavelength(s) at a relatively high SNR. Molecules that are used for their fluorescent properties are called fluorophores, and in principle bind to the specimen of interest [2].

### 1.7.2 TIRF Microscopy

One common method of fluorescence microscopy is total internal reflection (TIRF). TIRF works by producing an evanescent field that is produced when light is totally reflected internally at the boundary of the coverslip where the specimen resides. The evanescent field only penetrates approximately 100 nm, so TIRF is useful for imaging things like cell membranes [3]. Variations of TIRF microscopy include oblique illumination and epifluorescence, which allow for deeper penetration than achieved with an evanescent field. In both oblique illumination and epifluorescence,

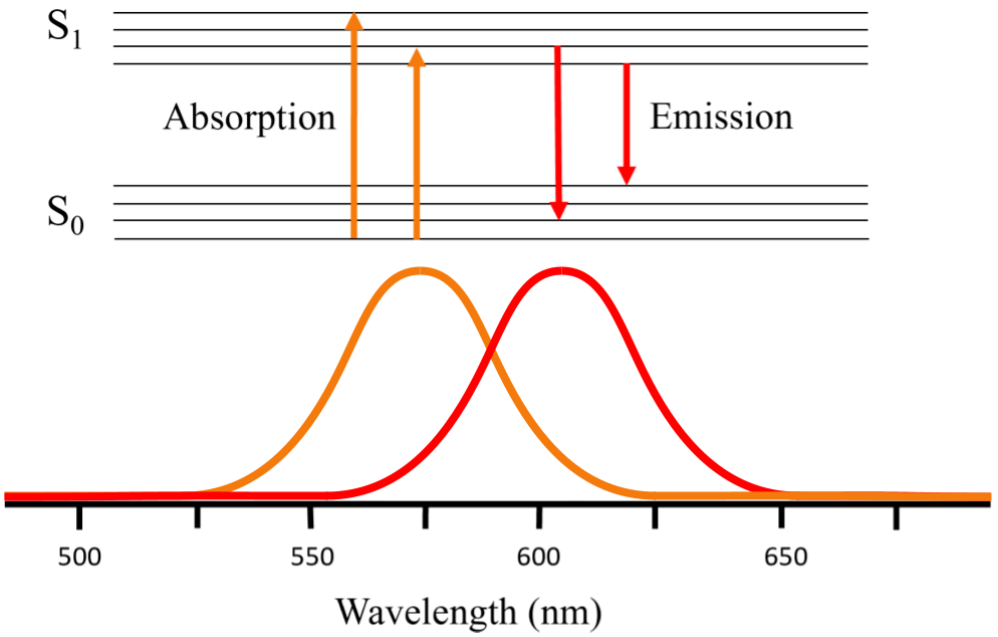


**Figure 1.1:** Diagram showing the absorption of higher energy photons and the emission of lower energy photons by a fluorophore, as well as the corresponding spectrum, where $S_0$ and $S_1$ are increasingly higher atomic excitation states (adapted from [2]).

total internal reflection is broken, and the sample is illuminated with the incident beam directly (this method of imaging was utilized heavily for the experiments in chapters 2 and 3) [4].

### 1.7.3 Confocal Microscopy

Another commonly used technique is confocal fluorescence microscopy, in which your specimen is exposed to some excitation wavelength, whereby only the emitted wavelengths of light pass through a specially selected dichroic filter. The emitted light then passes through a pinhole aperture to mitigate scattering before detection with a camera [5].

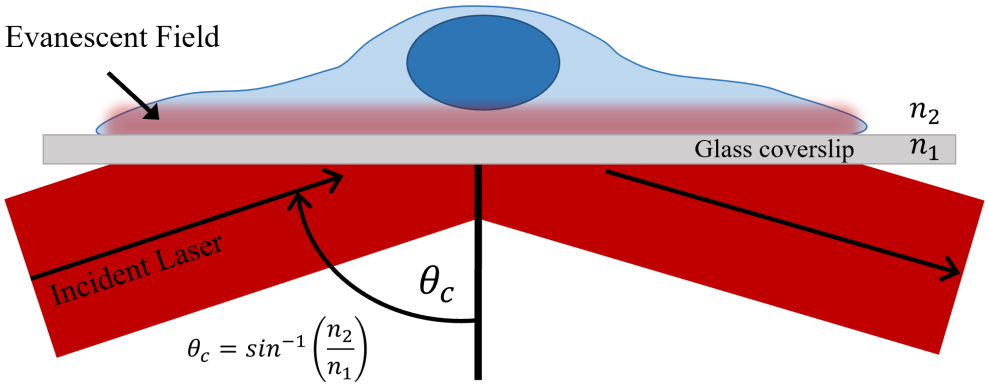


**Figure 1.2:** Diagram showing the principle of TIRF microscopy, where the evanescent field is shown as a thin red strip penetrating the boundary of the cell membrane and the glass coverslip. Quantities $n_1$ and $n_2$ represent the indices of refraction of both media, and $\theta_c$ represents what is known as the critical angle needed to achieve total internal reflection (adapted from [3]).

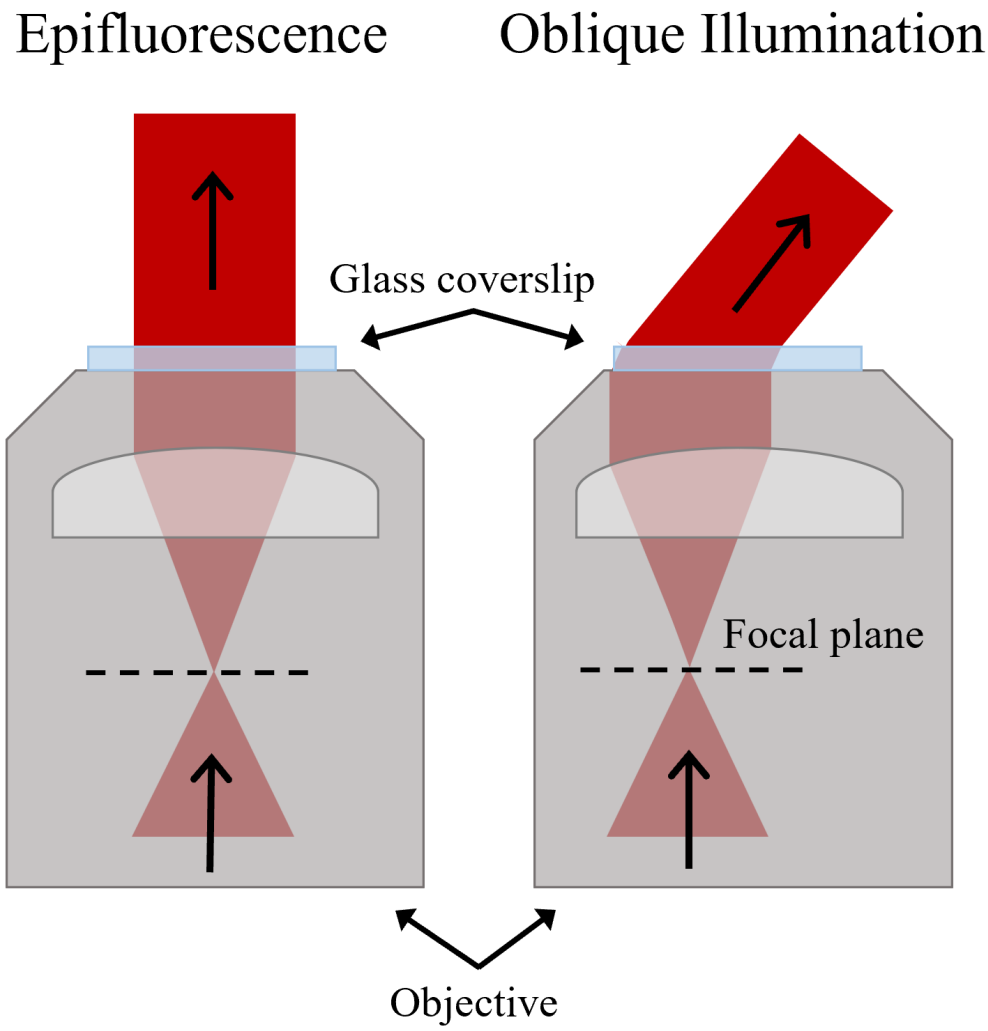


**Figure 1.3:** Diagram showing the principles of epifluorescent and oblique variations of TIRF microscopy, from left to right, respectively (adapted from [4]).

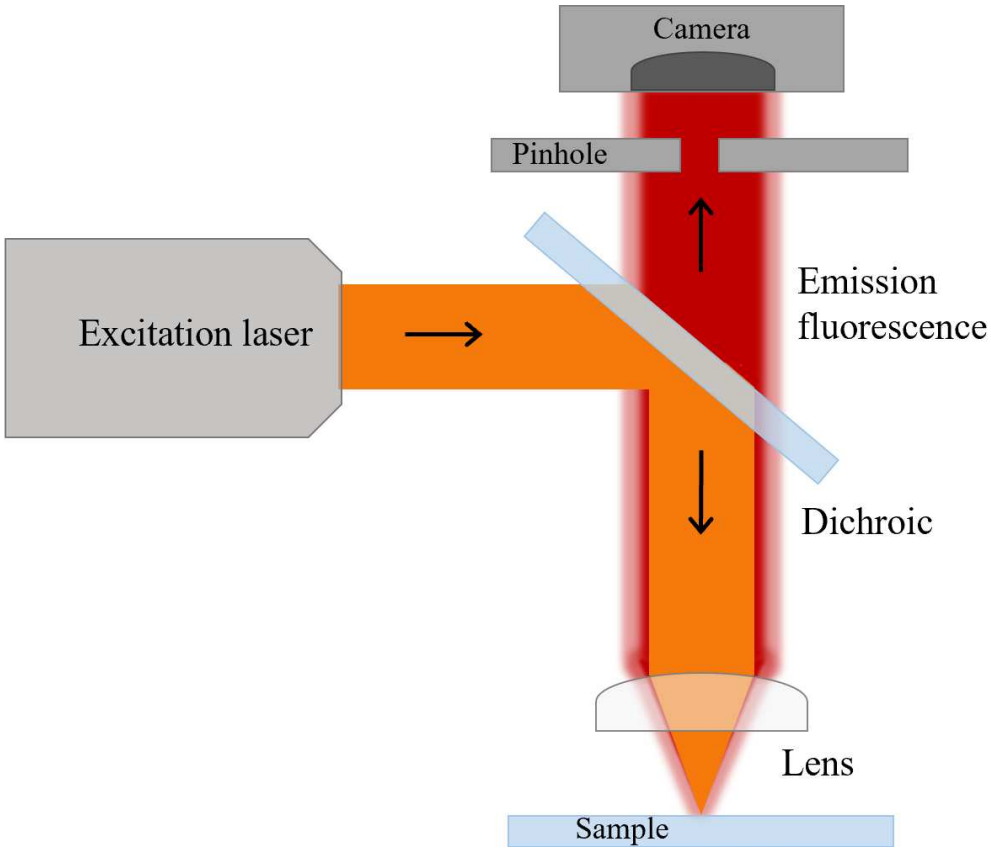


**Figure 1.4:** Diagram showing the principle of confocal fluorescence microscopy (adapted from [5]).

# Chapter 2

# Single-particle Tracking of mRNA Molecules

## 2.1 Introduction

Messenger (m) RNA plays a vital role in the process of converting genetically coded information to newly synthesized proteins, which are responsible for a plethora of cellular and bodily processes. DNA is converted into mRNA in the nucleus of a cell via a process called transcription. mRNA molecules then exit the nucleus before undergoing translation, or protein synthesis. Protein synthesis takes place in ribosomes, wherein mRNA molecules become bound for a period of time, while their base pairs are effectively parsed and rendered into a corresponding sequence of amino acids [41].

The experiments discussed in this chapter involve SPT of mRNA molecules and the myosin IIA protein they code for in live HeLa cells. HeLa cells are an adherent, adenocarcinoma cell of the cervix taken from Henrietta Lacks, who passed away in 1951. HeLa cells are easy to culture, growing rapidly, and were the first ever human cell line [42].

Non-muscle myosin IIA and its associated mRNA sequence is encoded by the *MYH9* gene. Class II non-muscle myosin proteins are prolifically expressed in eukaryotic cells and are involved in many processes such as adhesion, cytokinesis, cell shape and more [43]

The HeLa cells used for imaging in the following experiments have been genetically engineered via stable plasmid transfections such that they utilize an MS2-MCP system. Engineering of this cell line was done by Dr. O'Neil Wiggan at Colorado State University. Each mRNA sequence includes 24 MS2 stem loops with associated MCPs, with a halo tag enzyme (Figure 2.1). The basis of this labeling system was developed and used in living yeast by Bertrand et al., 1998 [44].

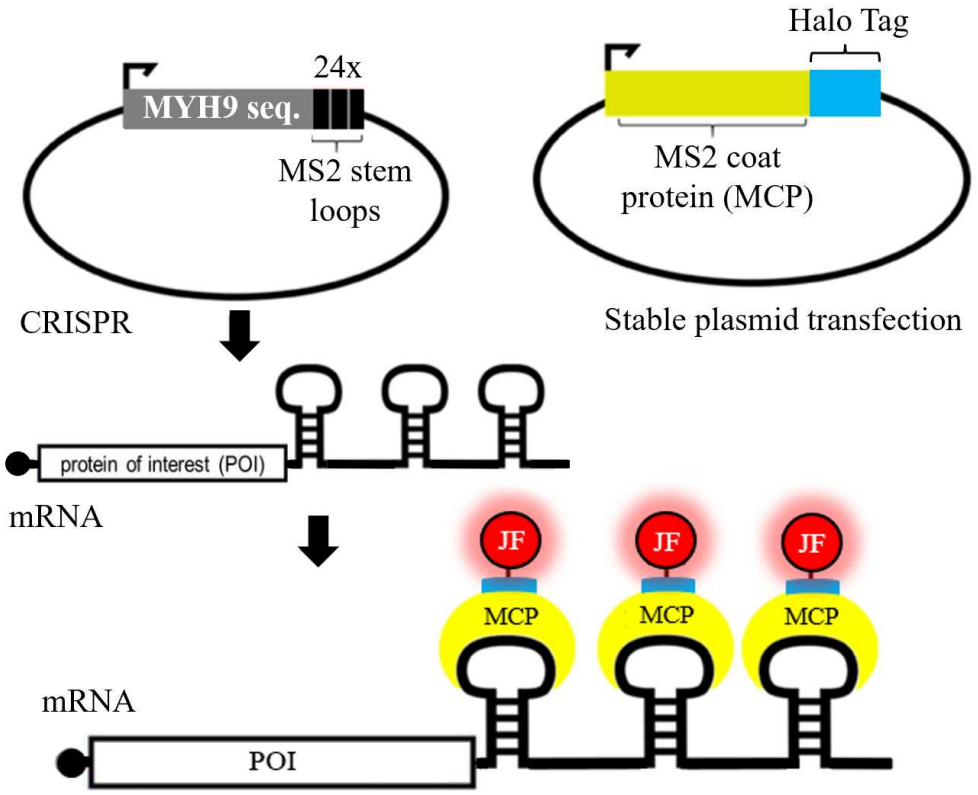


**Figure 2.1:** Schematic showing the MS2-MCP labeling system for mRNA with Janelia Fluor 646-Halo ligand. Figure adapted from George et al., 2018 [6].

The cells are incubated with a Janeila Fluor (JF) 646 / Halo ligand conjugate, resulting in 24 JF646 fluorophores per mRNA molecule [15, 45–47]. All of the trajectory analyses were done using MATLAB scripts that were written by Dr. Diego Krapf at Colorado State University.

We find that in the cytoplasm of HeLa cells, mRNA molecules are subdiffusive, and exhibit ergodicity breaking with statistics that depend on observation time. Additionally, we find that these mRNA molecules switch stochastically between two mobility states that differ by an order of magnitude in MSD.

## 2.2 Materials & Methods

### 2.2.1 Labeling of mRNA

These experiments have made use of a genetically engineered HeLa cell line, created by Drs. O'Neil Wiggan and Tim Stasevich, in which an MS2-MCP system is stably expressed. MS2 loops were engineered via CRISPR, and the corresponding MCP (with a Halo ligand) was stably transfected via a plasmid. [46, 47]. A more detailed protocol for these methods can be found in appendix A. 200 $\mu$L of cells were seeded in a 35 mm$^2$ Delta-T imaging dish approximately 24 hours before imaging and incubated at 37°C and 5.5% $CO_2$. Cells were imaged in 1 mL of cell media [1]. For TIRF microscopy, imaging dishes were kept on a heating stage at 37°C. When using the confocal microscope, cells were kept in a 37°C heated metal chamber at 5% $CO_2$.

### 2.2.2 Instrumentation & Imaging

Movies were obtained using either a confocal microscope with an imaging rate of 1.44 fps and four focal planes of 0.5 $\mu$m each or a TIRF microscope (oblique illumination) with an imaging rate of 10 fps and a single focal plane. On the day of imaging, cells were incubated with a 2 $\mu$M working concentration of JF646-Halo ligand for 15 minutes at 37°C and 5.5% $CO_2$.

While being imaged, cells were placed on a heating stage at 37°C. A more detailed list of imaging parameters are outlined in appendix C.9. TIRF movies spanned a timeframe of 2.5 minutes with a total of 1500 total frames.

### 2.2.3 Trajectory Analysis

mRNA trajectories were obtained using the TrackMate plugin in Fiji (ImageJ). TrackMate parameters varied for each movie, but in general, for data obtained with the TIRF microscope (1 pixel = 0.13 $\mu$m), a rolling ball radius background subtraction was performed with values ranging from ∼7-50. Next, a Gaussian Blur filter was applied with values ranging from 1.2-2.0. The

[1] See B.1

particle diameter was set as 3 pixels, and the quality threshold ranged anywhere from $\sim$10-350. The DoG detector was used for particles with diameters less than 5 pixels, otherwise, the LoG detector was used. The linking max distance, gap-closing max distance, and gap closing max frame were set to 4 pixels, 3 pixels, and 2 frames, respectively. Trajectories were filtered for greater than a range of $\sim$5-15 spots on track. Trajectories were exported as an XML file.

mRNA trajectories were converted from XML files to tables of XY coordinates before being concatenated and analyzed using custom MATLAB software written by Dr. Diego Krapf. For confocal data analysis, the maximum intensity projection from all four planes (2 $\mu$m total) was used.

For segmentation of trajectories, MATLAB scripts that utilized the convex hull method [7] were used to separate trajectories into two mobility states deemed "free" and "confined". For TIRF data, a window size of 6 points and threshold of 0.37 was used to determine the segmentation of the two states. For confocal data, parameters included a window size of 4 points and a threshold of 0.42. Another MATLAB script was used to remove the first confined part of every trajectory, before perfoming further analysis.

## 2.3 Results $\&$ Discussion

For confocal data, mRNA trajectories with minimum lengths of 44 and 89 seconds were analyzed, with corresponding trajectory amounts of 248 and 103, respectively. Trajectories obtained on the confocal microscope utilized four imaging planes of 0.5 $\mu$m each for a total depth of 2 $\mu$m, taking the maximum intensity projection from all four planes. For TIRF data, mRNA trajectories with minimum lengths of 6.4, 12.8 and 25.6 seconds were analyzed, with corresponding trajectory amounts of 5,820, 2,446 and 998, respectively. The majority of data analysis and discussion will refer to TIRF data due to the more statistically significant numbers of trajectories.

Figure 2.2 shows both a brightfield and fluorescence snapshot from one movie obtained with our TIRF microscope. Figure 2.3 shows some corresponding trajectories obtained after tracking with TrackMate.

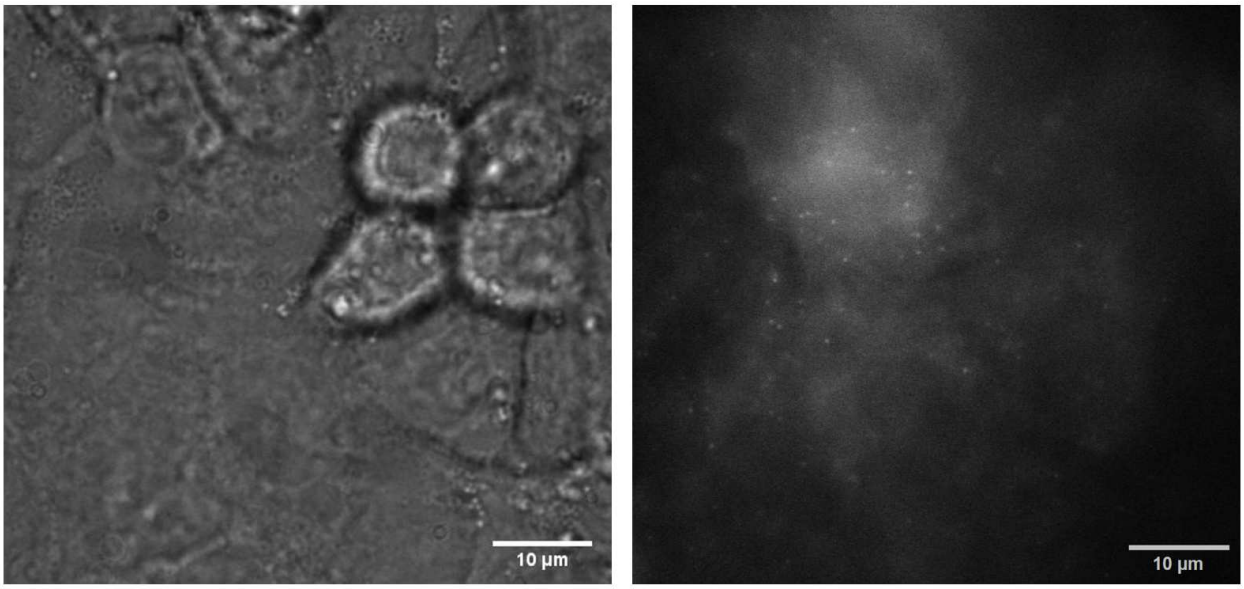


**Figure 2.2:** (left) Brightfield image from a movie of mRNA obtained from our TIRF microscope. (Right) Same region of interest (ROI) as brightfield, but showing the first frame of fluorescence (bright dots are JF-646 fluorophores corresponding to mRNA molecules).

One of the simplest analyses that can be done here is looking at a distribution of spatial displacements, both across many different trajectories (absolute displacements), and also within individual trajectories via normalizing the displacements to their standard deviation. The first fit we used for analyzing displacements are the Gaussian distribution, which for one dimension is given as

$$p\left(x\right) = \frac{1}{\sigma\sqrt{2\pi}} e^{\frac{-(x-\mu)^2}{2\sigma^2}} \tag{2.1}$$

where $\mu$ is the mean and $\sigma^2$ is the variance. The Gaussian distribution is bell-shaped with a peak at the mean, and is popular and interesting because of the central limit theorem [48]. The second fit we used was a classic Laplace distribution [49]

$$p\left(x\right) = \frac{1}{2} e^{-|x|} \tag{2.2}$$

The distributions of absolute displacements for TIRF trajectories with minimum lengths of 6.4 s and 25.6 s both fit an exponential (Laplace) distribution, indicating heterogeneity among trajecto-

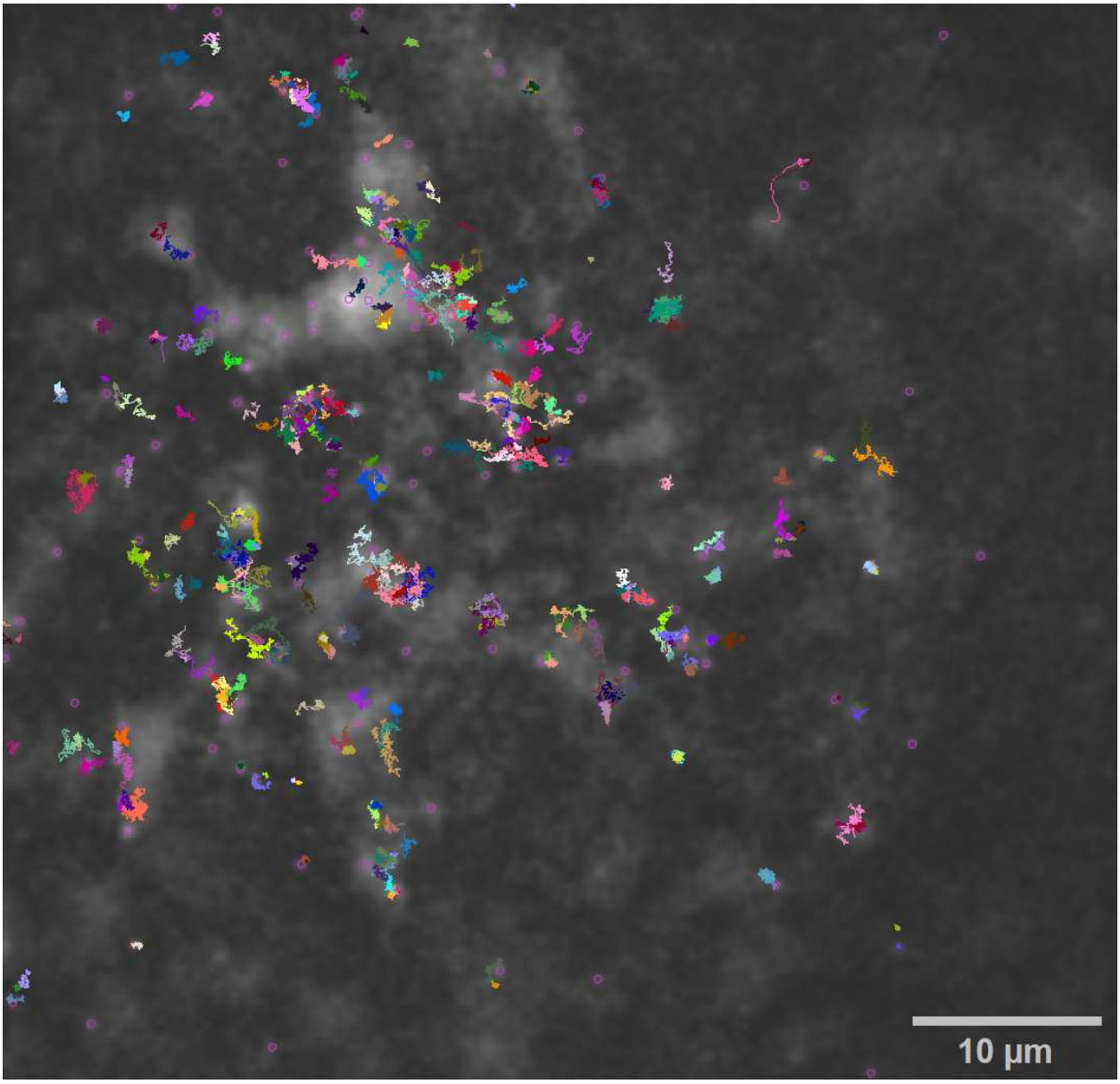


**Figure 2.3:** mRNA trajectories corresponding to the movie which is depicted in Figure 2.2. Trajectories were obtained via TrackMate and are colored by track ID (i.e. each trajectory has a different color).

ries. In other words, there is a broad spectrum of spatial jumps across different trajectories in the cell(s) (Figure 2.4).

Distributions of normalized displacements for trajectories with minimum lengths of 6.4 s and 25.6 s appear to be more homogeneous for smaller displacements (near zero), whereas the fit becomes more exponential for larger displacements. This indicates heterogeneity within individual trajectories that exhibit relatively large displacements; another way of thinking about this is that individual mRNA trajectories are switching between multiple modes of motion (Figure 2.5).

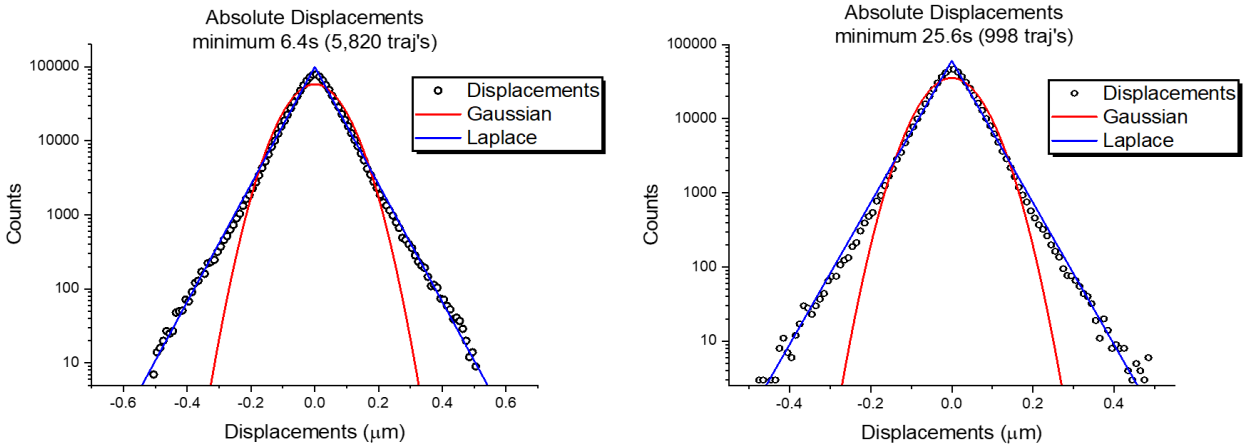


**Figure 2.4:** Absolute displacements of mRNA trajectories for minimum trajectory lengths of 6.4 s (5,820 trajectories) and 25.6 s (998 trajectories) fitted with Gaussian and Laplace curves.

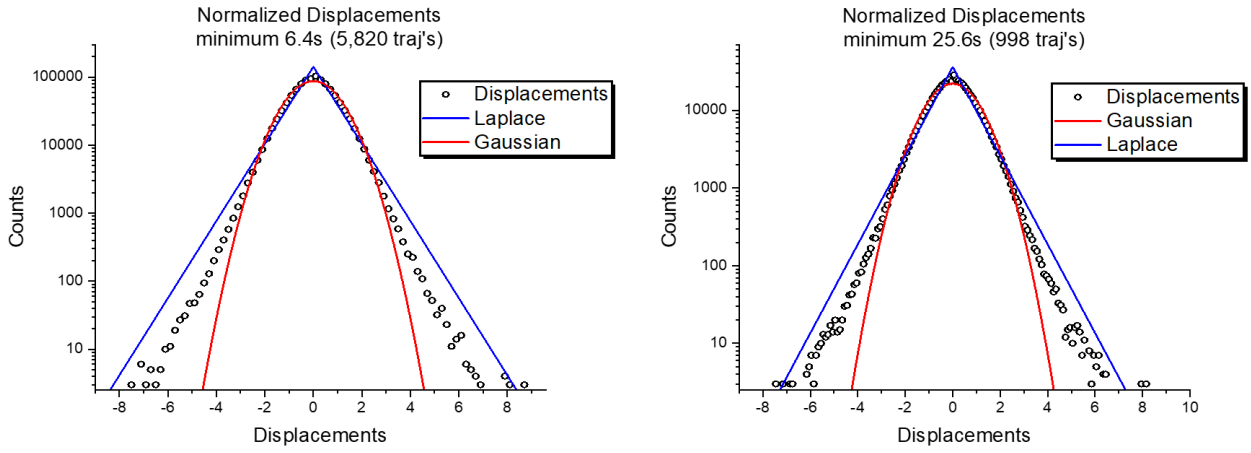


**Figure 2.5:** mRNA trajectory displacements normalized to their standard deviations for minimum trajectory lengths of 6.4 s (5,820 trajectories) and 25.6 s (998 trajectories) fitted with Gaussian and Laplace curves.

Since we have evidence of more than one mode of motion, trajectories were segmented into two mobility states using the convex hull method. The convex hull method utilizes a scanning window of points along the trajectory, and assigns a corresponding diameter to each cluster of points [7] (Figure 2.6).

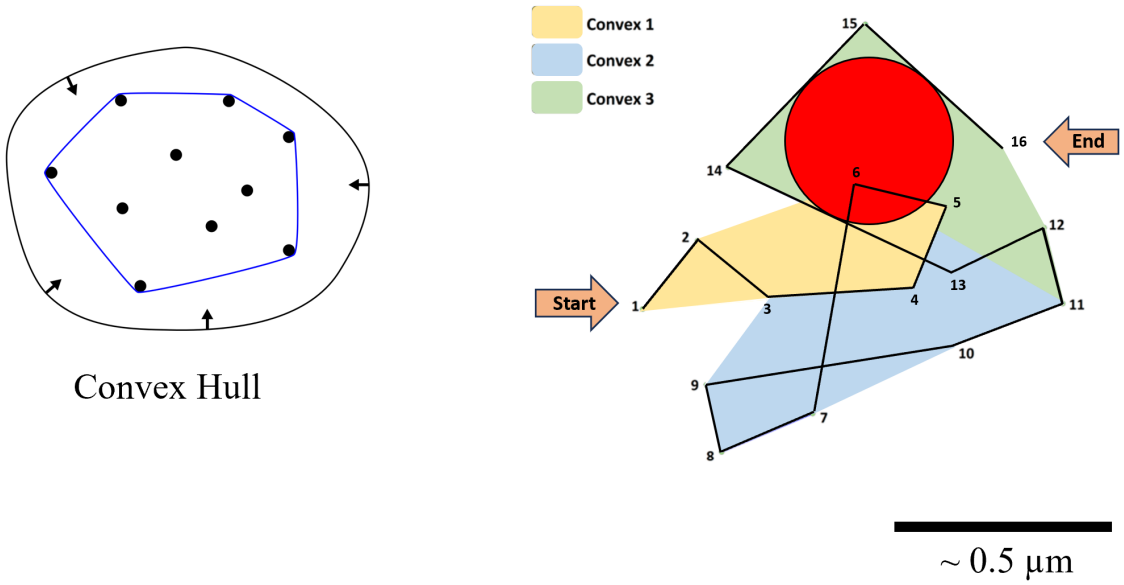


**Figure 2.6:** Illustrations of convex hull method [7] with a window size of 6 points (right).

The parameters required to perform segmentation are a window size of points and a threshold (arbitrary relative value) that corresponds to the diameters. The idea is that we should see well defined separation in diameters or overall mobility throughout trajectories, and use that corresponding threshold to segment the mobility states. This threshold was found via a somewhat painstaking process of comparing many different thresholds and window sizes, and cross-checking the results with the trajectories seen in movies to determine what parameters appeared most appropriate. After performing segmentation, two clear mobility states were found and deemed "free" and "confined" in relation to the threshold used in the convex hull, that is, the "free" state represents trajectory segments greater than the chosen threshold, and the "confined" state represents segments less than the chosen threshold. An example of the convex hull output can be seen in Figure 2.7, where the free state is shown in blue, and the confined state is shown in red. The left plot shows the arbitrary

convex hull measurement (diameter) along the trajectory, and the right plot shows the resulting segmentation as a function of position in x (Figure 2.7).

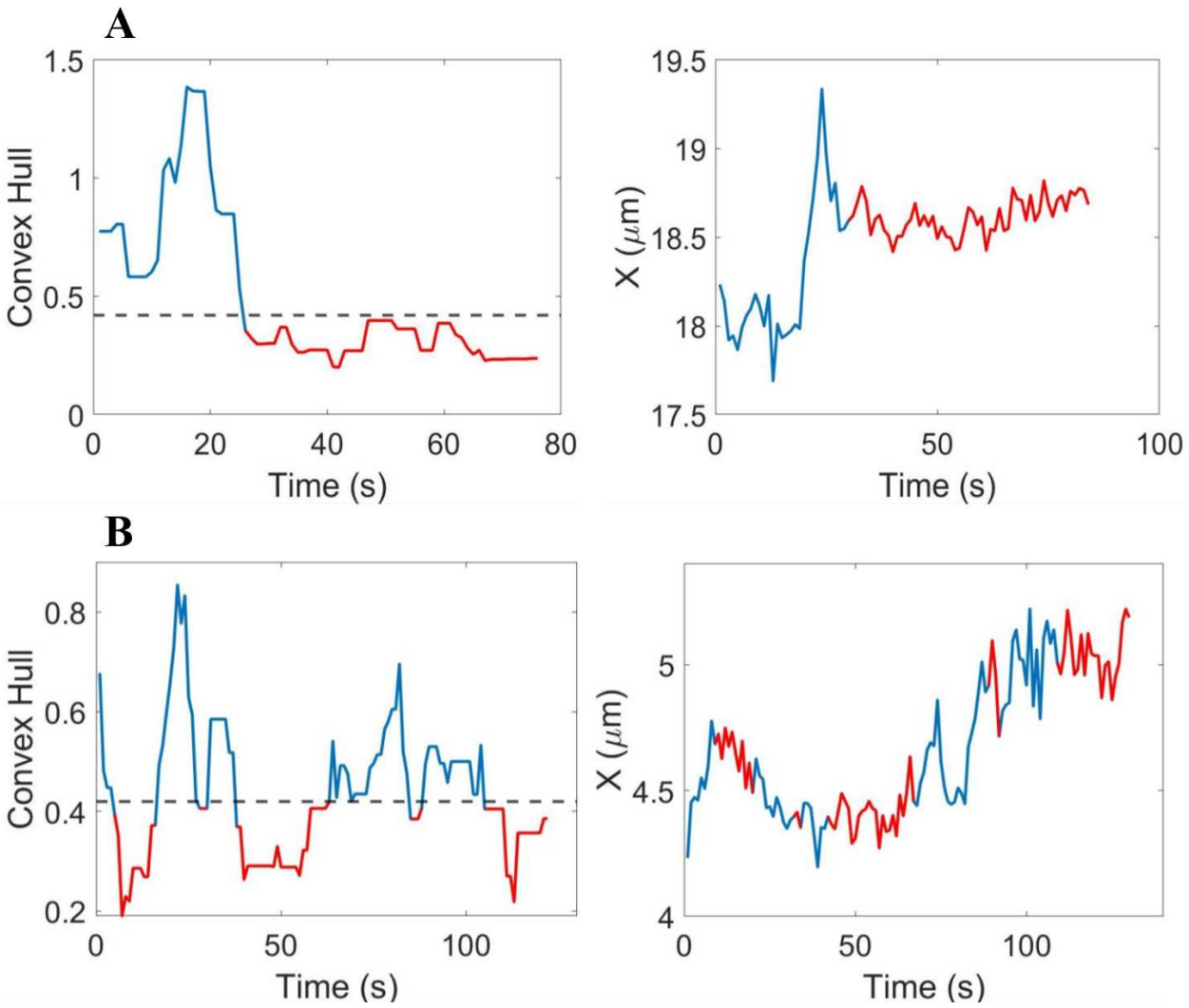


**Figure 2.7:** Two examples of plots obtained from convex hull code (left). This data was obtained with a confocal microscope imaging four focal planes for a total depth of 2 $\mu$m, taking the maximum intensity projection from all four planes. Parameters for the convex hull include a window size of 4 frames and a threshold of 0.42, indicated by a dashed line in the convex hull plots. Sections colored blue denote parts of the trajectory above the threshold (free state), and red are below the threshold (confined state). Corresponding plots of X displacements (right) similarly colored according to free and confined states.

Convex hull parameters used for maximum projection data from the confocal microscope were a window size of 4 points and a threshold of 0.42, whereas parameters used for TIRF data were a window size of 6 points and a threshold of 0.37. Parameters differ according to camera pixel

size and frame rate, or average jump between frames. An example of the resulting segmented trajectories from Figure 2.7 are shown in Figure 2.8, again showing the free state in blue and the confined state in red.

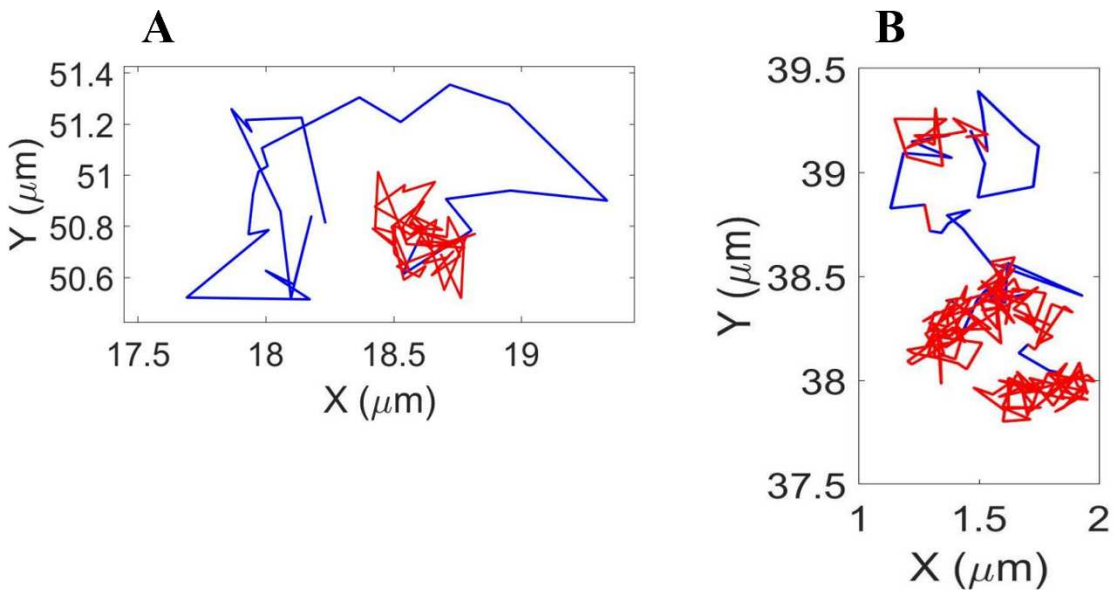


**Figure 2.8:** Resulting segmented trajectories corresponding to plots in Figure 2.7 (A and B, respectively).

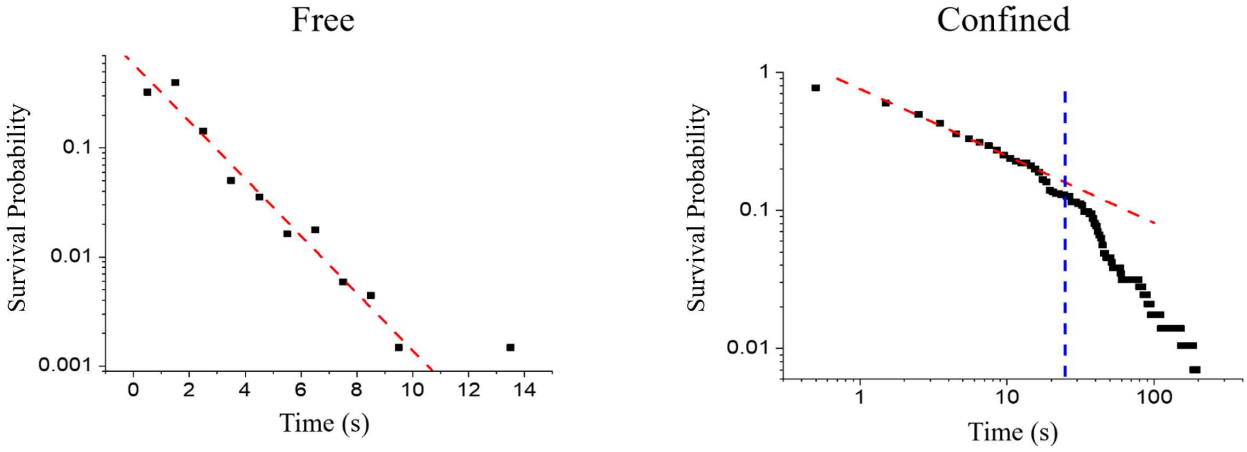


**Figure 2.9:** Sojourn (waiting) times for the free (left) and confined (right) states. The free and confined states show exponential and power-law distributions, respectively.

After trajectories have been segmented according to different mobility states, one can plot the Sojourn (waiting) times to see a comparison of the average time spent in each state. For mRNA, the Sojourn times exhibited exponential and power-law distributions in the free and confined states, respectively (Figure 2.9). Effectively, this means that molecules tend to exit the free state much faster than the confined state, in which they have the capability of staying or being trapped for much longer periods of time.

Since the free state exhibits an exponential (uncorrelated) distribution of waiting times, trajectories were trimmed such that they always start from a free state. This was done by simply removing the first confined state from each trajectory. An example of this result is shown in Figure 2.10.

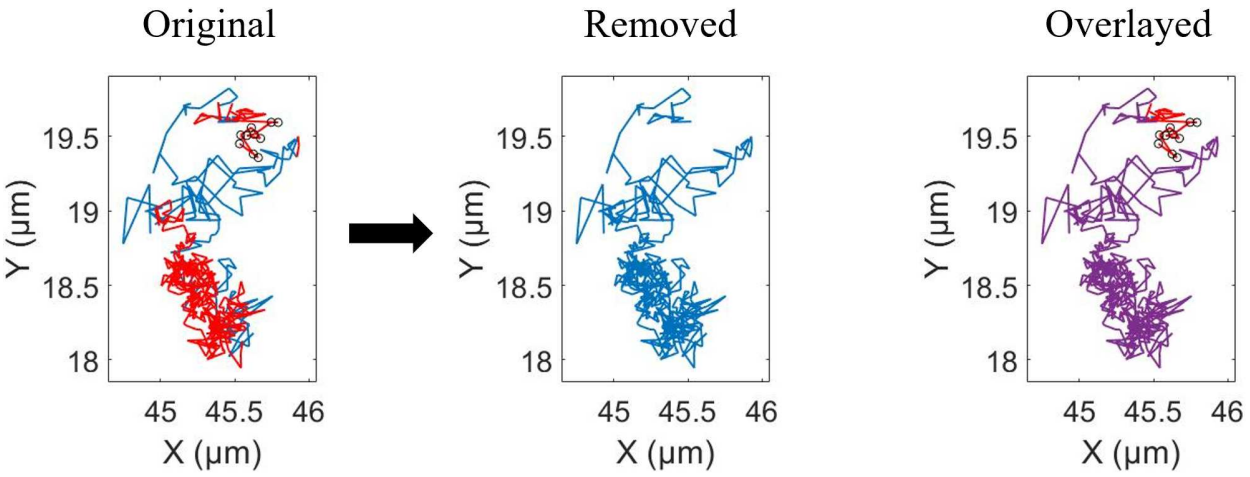


**Figure 2.10:** Figure showing the results of removing the first confined segment of a trajectory (done using a MATLAB code (see appendix E.4)). The left plot shows the full segmented trajectory, with the first 10 points marked with black circles. It is evident that the first part of this trajectory is confined, given the red color. The middle plot shows the resulting trajectory after this first confinement has been removed (note that this trajectory is not displayed with segmentation, it is only showing the truncation of the beginning confined section). Finally, the right plot shows an overlay of the left and middle plots.

The majority of mRNA molecules exhibit anomalous diffusion, which can be seen in Figure 2.11 (left) as MSDs that tend to scale non-linearly with time (slope $\neq 1$). Furthermore, we observe a breaking of ergodicity, which can also be seen in Figure 2.11 (right) as a discrepancy between the

ensemble and time averaged MSDs (i.e., the plots of TA-MSDs do not coincide across an ensemble of 5,820 trajectories).

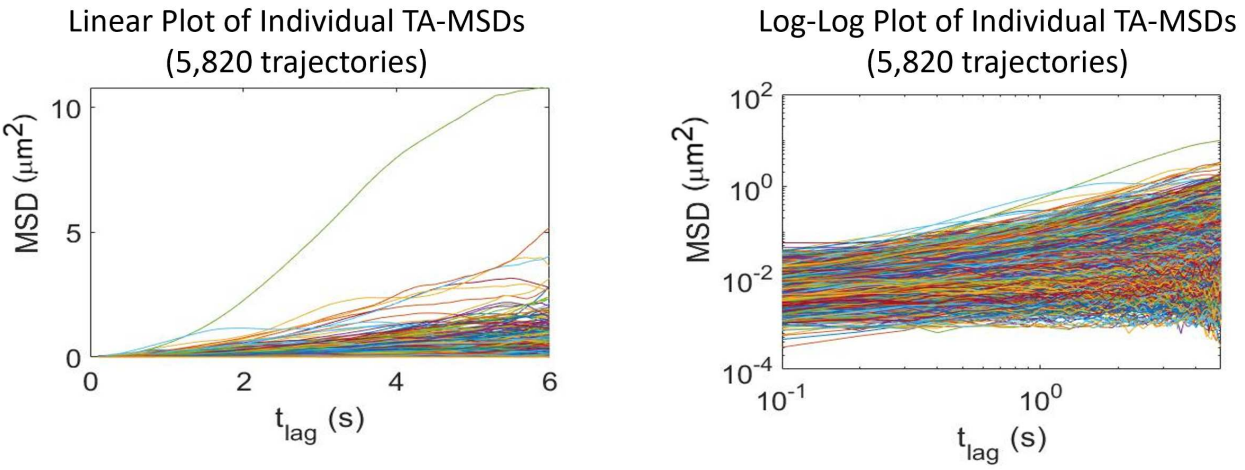


**Figure 2.11:** Linear (left) and log-log (right) plots of TA-MSDs from 5,820 individual mRNA trajectories with minimum lengths of 6.4 s.

ET-MSDs of mRNA trajectories with minimum lengths of 6.4, 12.8 and 25.6 seconds obtained from our TIRF microscope (oblique illumination) are shown in Figure 2.12 with anomalous exponents of 0.85, 0.81 and 0.78, respectively. This illustrates that the dominant type of anomalous diffusion is subdiffusive, as all three minimum trajectory lengths have anomalous exponents $< 1$ when taking the ET-MSD and correcting for localization error. From Figure 2.12, there appears to be a trend of decreasing anomalous exponent for increasing minimum trajectory length. This inverse relationship could be due to a bias in the automated tracking software to keep longer trajectories that have lower overall motion (i.e. trajectories with higher MSDs tend to be lost by the software more quickly).

Figure 2.13 depicts the ET-MSDs for both the free and confined states individually after segmentation. Both states differed in MSD by roughly one order of magnitude, which is indication that our segmentation worked well.

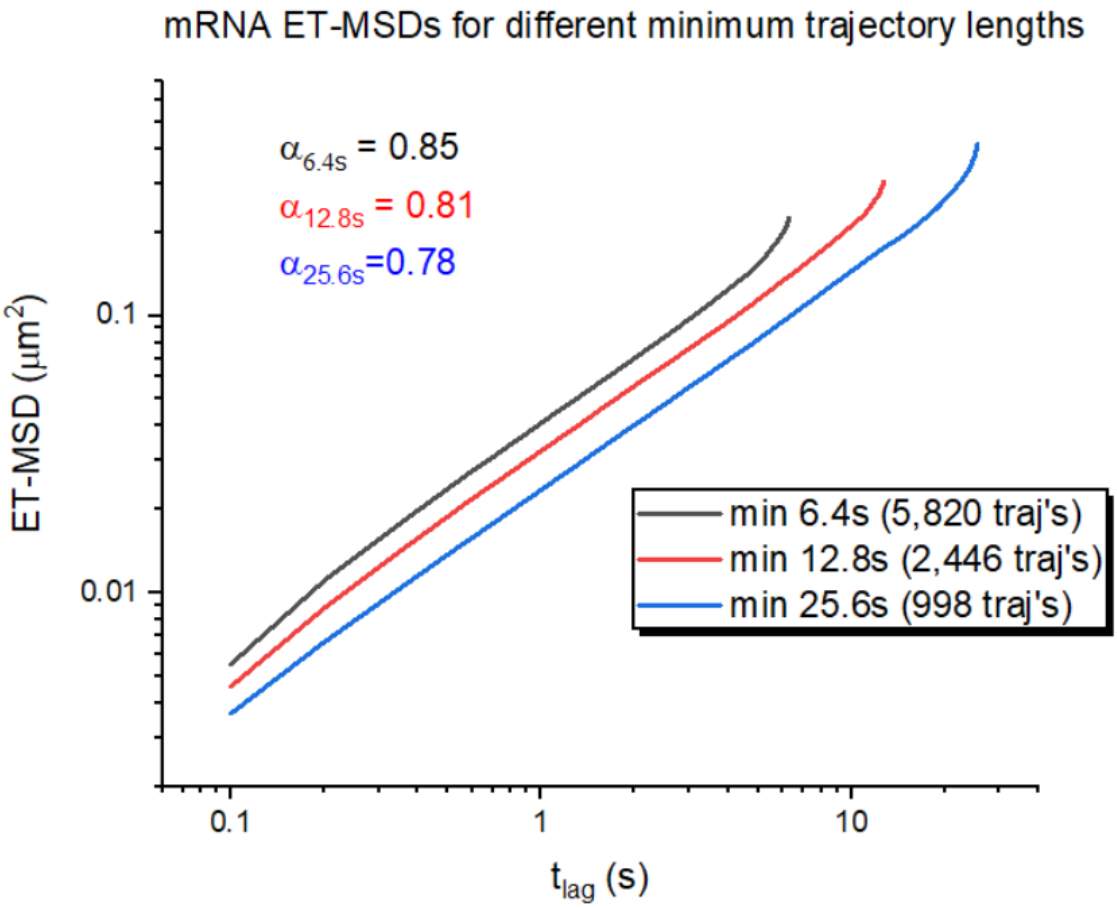


**Figure 2.12:** ET-MSDs for mRNA trajectories with minimum lengths of 6.4 s (5,820 trajectories), 12.8 s (2,446 trajectories) and 25.6 s (998 trajectories). All trajectories were obtained using a TIRF microscope (oblique illumination).

Trajectories obtained from both the confocal (Figures 2.14 and 2.15) and TIRF (Figure 2.16) microscopes were found to exhibit aging, specifically, both the ET-MSD and PSD show a decrease for a corresponding increase in observation time.

Recalling the Sojourn times (Figure 2.9), since the free state waiting times are significantly more transient than the confined state, we thought it would be interesting to examine the locations of the few trajectories that have relatively long lasting free states. These trajectories were uncommon, and we selected 9 trajectories that stayed in the free state for at least 27 seconds. It turns out that roughly 78% of these trajectories (7 out of 9) were found qualitatively to be located near the periphery of cells (Figure 2.17).

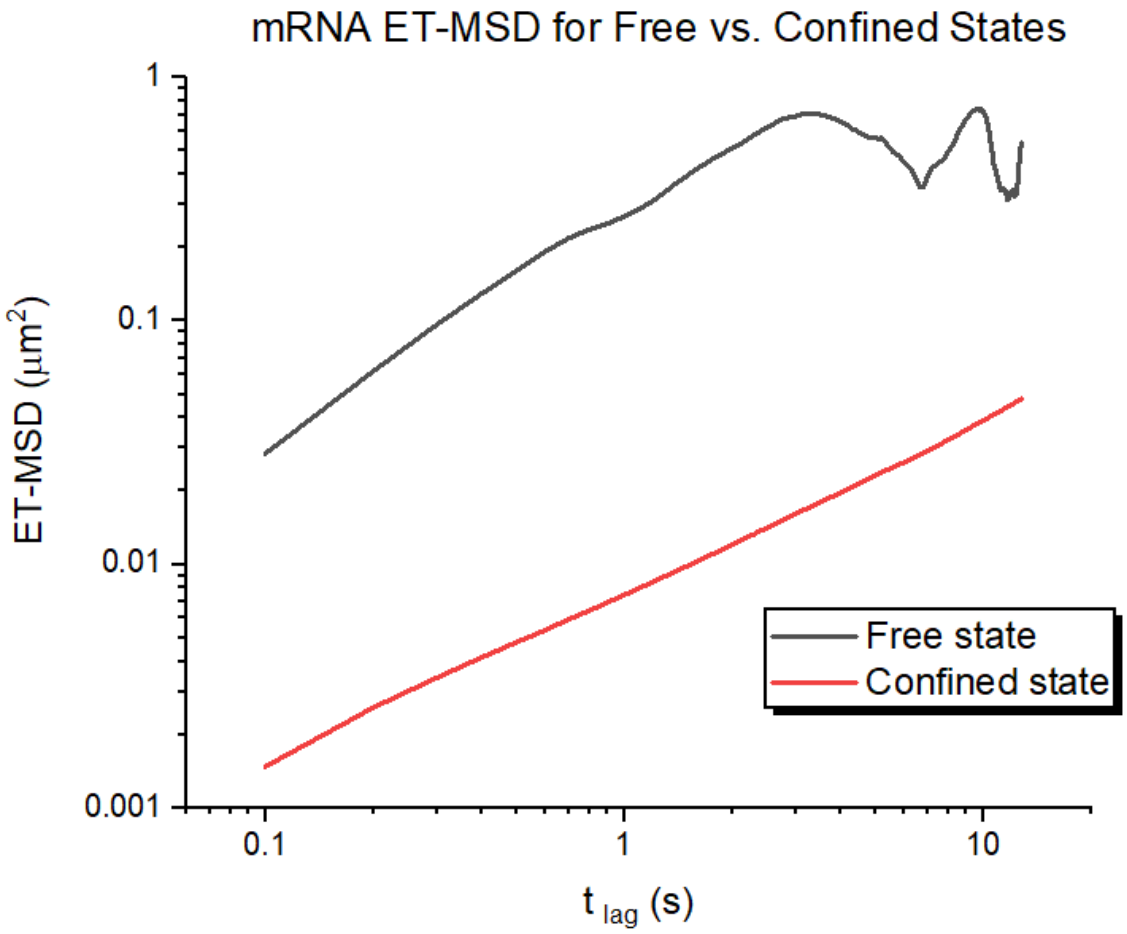


**Figure 2.13:** ET-MSD of mRNA trajectories with minimum lengths of 12.8 s (2,446 trajectories) in both the free (black) and confined (red) state.

The observation that mRNA molecules with long lasting free states tend to be located near the edge of the cell (and thus, farther away from ribosomes and the ER), combined with the observed stochastic switching between mobility states that differ significantly in their respective MSDs have led us to the hypothesis that confined states may be representative of mRNA molecules undergoing translation. Since mRNA molecules become bound to ribosomes during translation, it may be that the confinement we observe is indication that the molecule has become trapped in translation by a ribosome. Given that many ribosomes may be bound to the ER and located more densly near the nuclear envelope (depending on the stages of the cell cycle) [50], mRNA molecules near the cell periphery may be able to move more freely for longer periods of time if there are not as many ribosomes present. This hypothesis will be investigated in the next chapter.

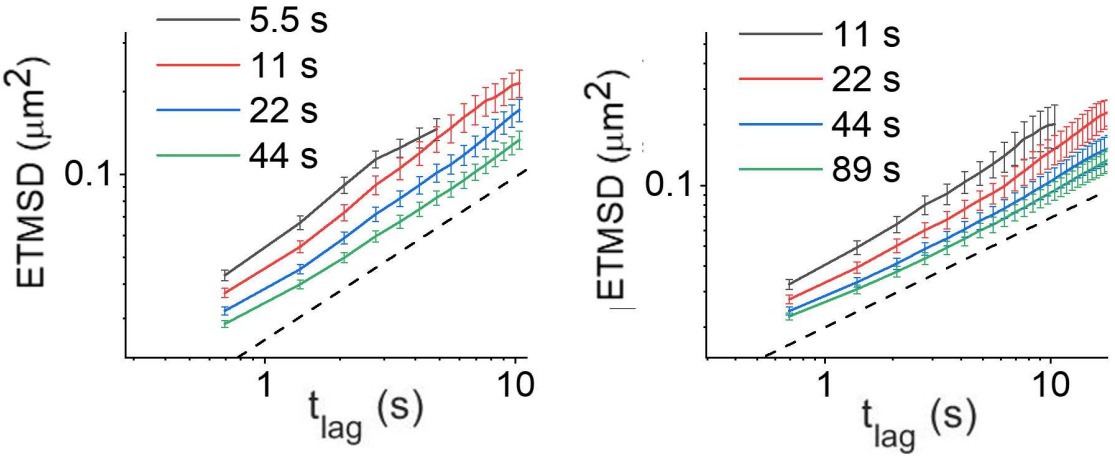


**Figure 2.14:** Confocal data showing aging (specifically, a decrease in the ET-MSD for an increase in observation time) in the ET-MSD for mRNA trajectories with minimum lengths of 44 s (left: 248 trajectories) and 89 s (right: 103 trajectories). Realization times used for the left plot were 5.5 s, 11 s, 22 s and 44 s. Realization times used for the right plot were 11 s, 22 s, 44 s and 89 s.

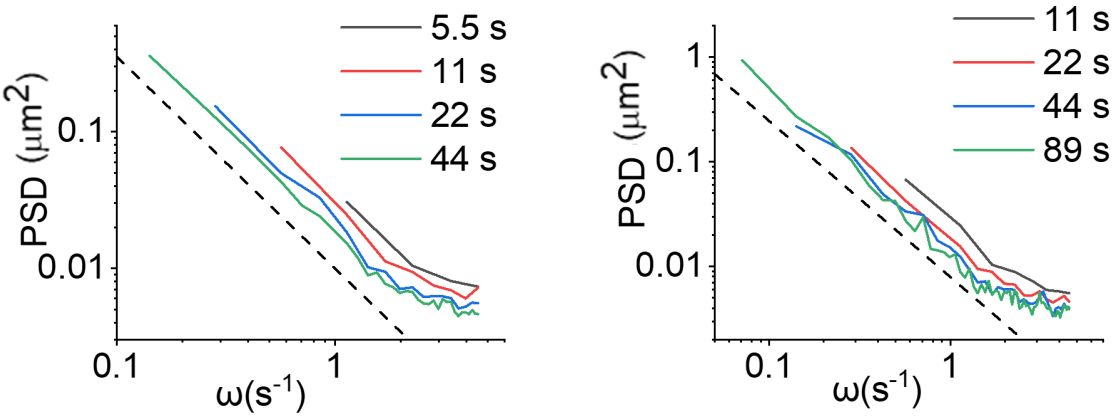


**Figure 2.15:** Confocal data showing aging (specifically, a decrease in PSD for an increase in observation time) in the PSD for mRNA trajectories with minimum lengths of 44 s (left: 248 trajectories) and 89 s (right: 103 trajectories). Realization times used for the left plot were 5.5 s, 11 s, 22 s and 44 s. Realization times used for the right plot were 11 s, 22 s, 44 s and 89 s.

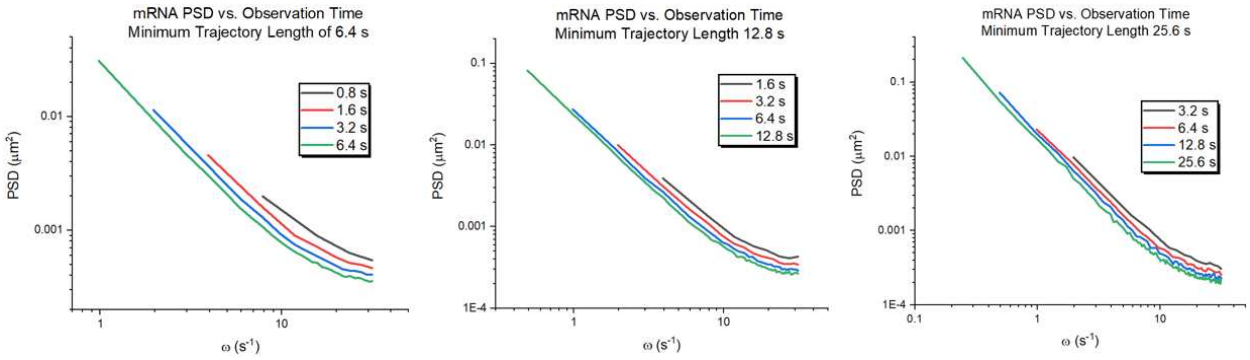


**Figure 2.16:** TIRF data showing aging (specifically, a decrease in PSD for an increase in observation time) in the PSD for mRNA trajectories with minimum lengths of 6.4 s (left: 5,820 trajectories), 12.8 s (center: 2,446 trajectories) and 25.6 s (right: 998 trajectories).

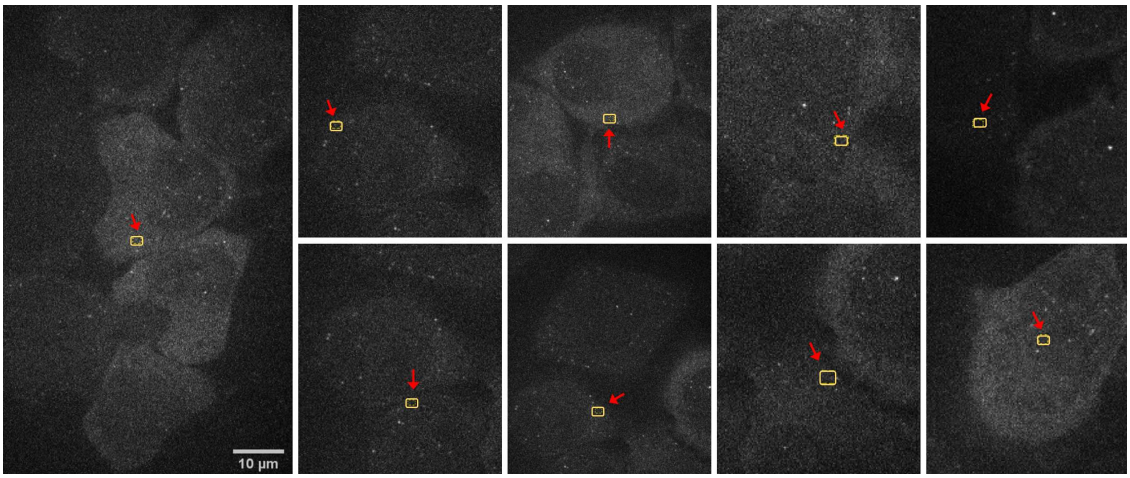


**Figure 2.17:** Qualitative observation of 9 trajectories, all exhibiting free state waiting times greater than 27 seconds. 7 of 9 trajectories (78%) are observed to be in close proximity to the periphery of their cell.

# Chapter 3

# mRNA Dynamics in Response to Disruption of Intracellular Structures & Translation

## 3.1 Introduction

Intracellular structures like the cytoskeleton (composed of filiments and tubules) and organelles like the endoplasmic reticulum (ER) contribute to the heterogeneous environment of a cell, and thus can dictate how proteins and molecules diffuse intracellularly [11, 51, 52]. Experiments have been done that demonstrate changes in the diffusivity of particles in response to disruption of intracellular structures [11, 53, 54].

As discussed previously, translation is the conversion of mRNA into proteins via ribosomes [41]. As mentiond at the end of chpater 2, we hypothesize that previously observed "confined" mobility states may be attributed to mRNA molecules that are undergoing translation. The first experiments discussed in this chapter investigate the effects of the disruption of microtubules and the ER on the dynamics of mRNA. Later experiments in this chapter investigate the effects of interfering with translation (specifically, using the drugs puromycin and cycloheximide to release mRNA from ribosomes and lock mRNA in ribosomes, respectively) on the dynamics of mRNA molecules determined in the previous chapter. We find that disruption of neither microtubules nor the ER significantly alter the average MSD of mRNA molecules in the cytoplasm of HeLa cells compared to control trajectories. We also find that interfering with translation using both puromycin and cycloheximide do not significantly alter the MSD of mRNA molecules compared to control trajectories.

## 3.2 Materials & Methods

### 3.2.1 Disruption of Microtubules, ER and Translation

HeLa cells were treated with nocodazole, which is a drug known to disrupt microtubules. For disruption of microtubules, cells were subjected to a 30 $\mu$M concentration of nocodazole and incubated on ice for 10 minutes before being imaged. For disruption of the ER, cells were treated with a 15 $\mu\mathrm{g/mL}$ concentration of filipin and incubated at room temperature for 30 minutes before imaging. For locking mRNA in ribosomes, cells were treated with a 0.5 mM concentration of cycloheximide and incubated at 37°C for 10 minutes before imaging. For disruption of translation, cells were treated with a 92 $\mu$M concentration of puromycin and incubated at 37°C for 10 minutes before imaging. Detailed protocols for all of these processes can be found in appendices C.4-7. All imaging experiments were done at 37°C.

### 3.2.2 Instrumentation & Imaging

All of these imaging experiments were performed using oblique illumination with a TIRF microscope and a single imaging plane. Movies were taken for a duration of 2.5 minutes at 10 fps (1500 frames).

### 3.2.3 Trajectory Analysis

mRNA trajectories were obtained using the TrackMate plugin in Fiji (ImageJ). TrackMate parameters varied for each movie, but in general, a rolling ball radius background subtraction was performed with values ranging from ∼7-50. Next, a Gaussian Blur filter was applied with values ranging from 1.2-2.0. The particle diameter was set as 3 pixels, and the quality threshold ranged anywhere from ∼10-350. The DoG detector was used for particles with diameters less than 5 pixels, otherwise, the LoG detector was used. The linking max distance, gap-closing max distance, and gap closing max frame were set to 4 pixels, 3 pixels, and 2 frames, respectively. Trajectories

were filtered for greater than a range of ∼5-15 spots on track. Trajectories were exported as an XML file.

mRNA trajectories were converted from XML files to tables of XY coordinates before being concatenated and analyzed using custom MATLAB software. For segmentation of trajectories, MATLAB scripts that utilized the convex hull method [7] were used to separate trajectories into two mobility states deemed "free" and "confined". A window size of 6 and threshold of 0.37 was used to determine the segmentation of the two states. Another MATLAB script was used to remove the first confined part of every trajectory, before further analysis.

## 3.3 Results & Discussion

We observed aging in mRNA molecules similar to control experiments (i.e. a decrease in MSD for a corresponding increase in observation time) in DMSO, nocodazole and filipin treated cells (Figure 3.1).

When comparing the control trajectories to DMSO, nocodazole and filipin treated cells for minimum trajectory lengths of 6.4 s, 12.8 s and 25.6 s, we observed no significant changes in the average ET-MSD. The average ET-MSD decreased very slightly after disruption of the ER for all three minimum lengths, with a more significant decrease for minimum trajectory lengths of 12.8 s and 25.6 s compared to 6.4 s (Figure 3.2).

We observed a slight increase in the ET-MSD of mRNA trajectories in cells treated with both puromycin and cycloheximide, albeit very small and statistically insignificant (Figure 3.3).

Similarly to the MSDs, we did not observe a significant change in waiting times for both the free and confined states after the treatment of both puromycin and cycloheximide. The waiting times for the free state show virtually no change after treatment with puromycin, and a very slight, insignificant increase for the confined state. We also observed a very slight decrease in waiting times for both the free and confined states after treatment with cycloheximide (Figures 3.4 and 3.5).

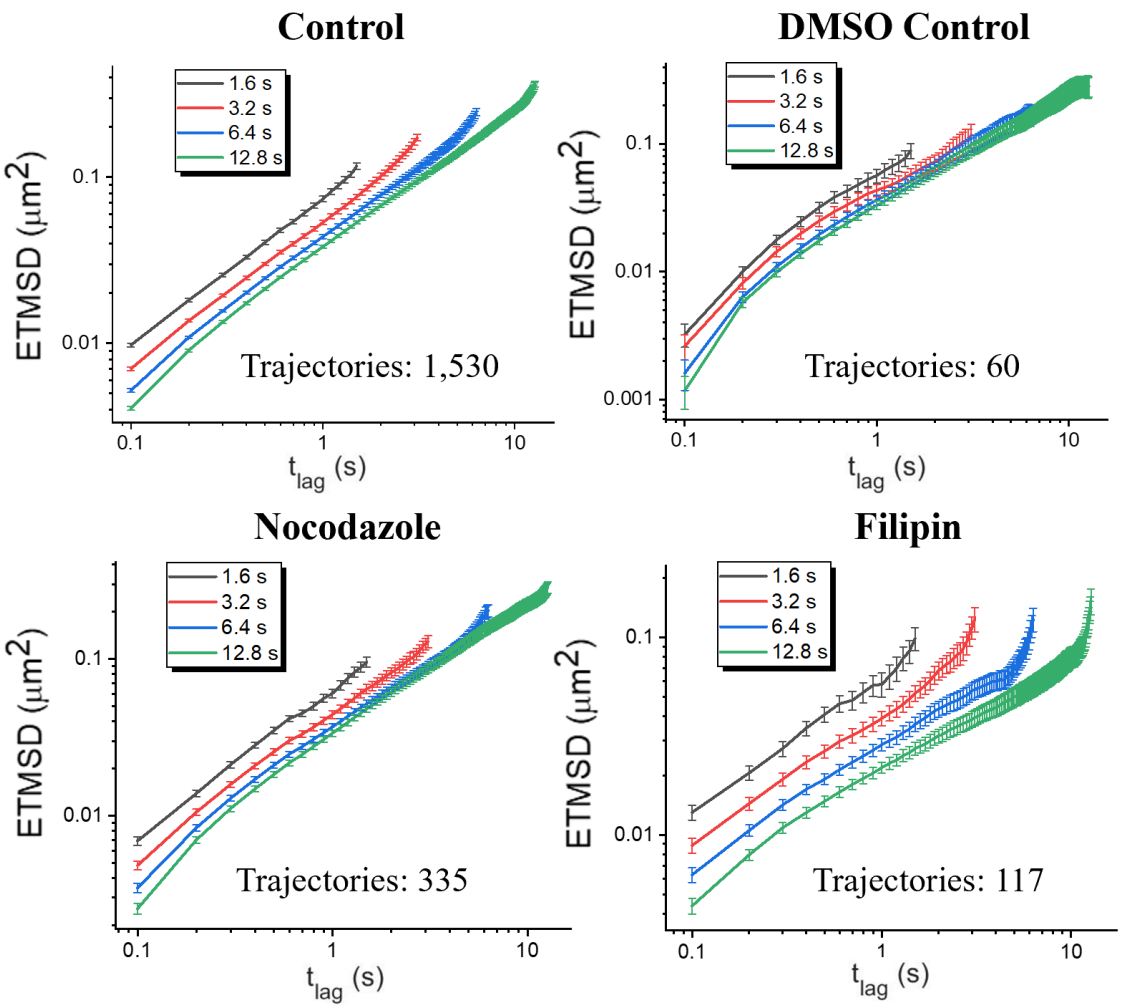


**Figure 3.1:** Plots showing aging (specifically, a decrease in average ET-MSD for an increase in observation time) in the ET-MSD for mRNA trajectories with minimum lengths of 12.8 s for control (no treatment), DMSO (control), nocodazole and filipin treated cells. Realization times used for the left plot were 1.6 s, 3.2 s, 6.4 s and 12.8 s.

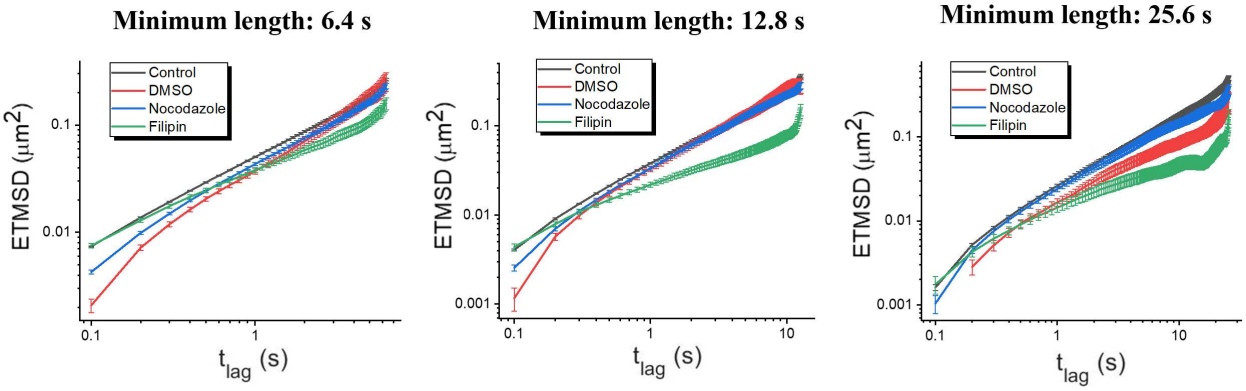


**Figure 3.2:** Plots comparing the ET-MSD for mRNA trajectories with minimum lengths of 6.4 s, 12.8 s and 25.6 s for control (no treatment), DMSO (control), nocodazole and filipin treated cells.

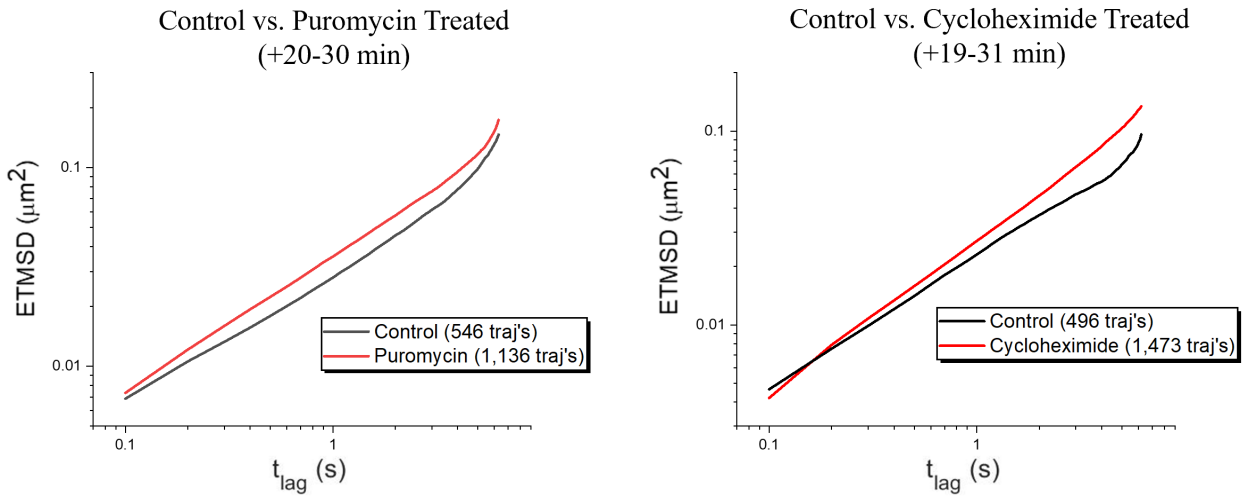


**Figure 3.3:** (left) Plot comparing the ET-MSD for mRNA trajectories for control (no treatment) and puromycin (imaged 20-30 min after treatment) treated cells. (right) Plot comparing the ET-MSD for mRNA trajectories for control (no treatment) and cycloheximide (imaged 19-31 min after treatment) treated cells.

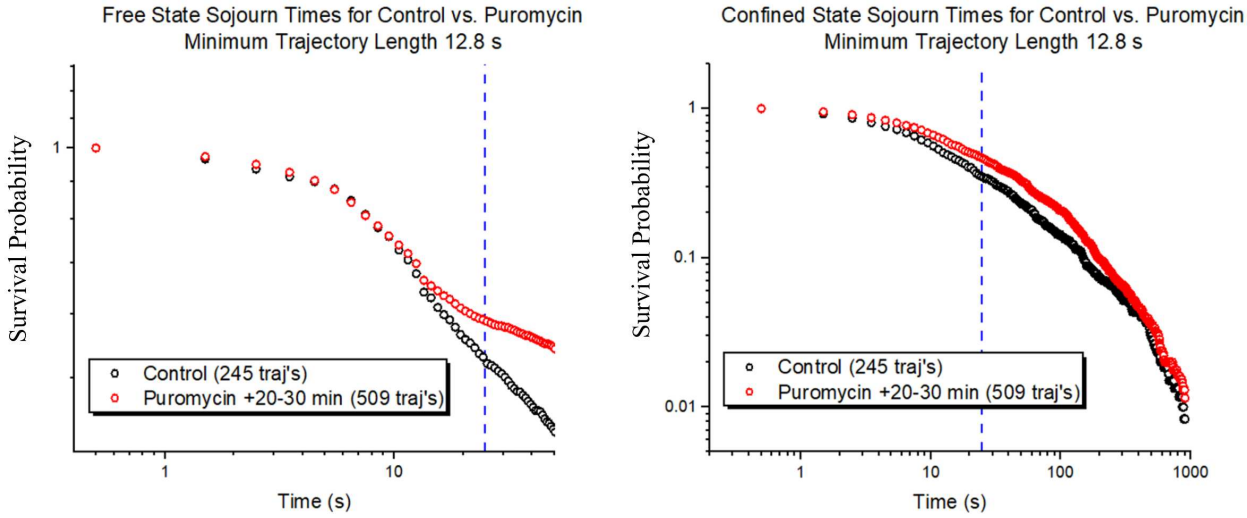


**Figure 3.4:** (left) Plot comparing the Sojourn times for mRNA trajectories in the free state for control (no treatment) and puromycin (imaged 20-30 min after treatment) treated cells. (right) Plot comparing the Sojourn times for mRNA trajectories in the confined state for control (no treatment) and puromycin (imaged 20-30 min after treatment) treated cells.

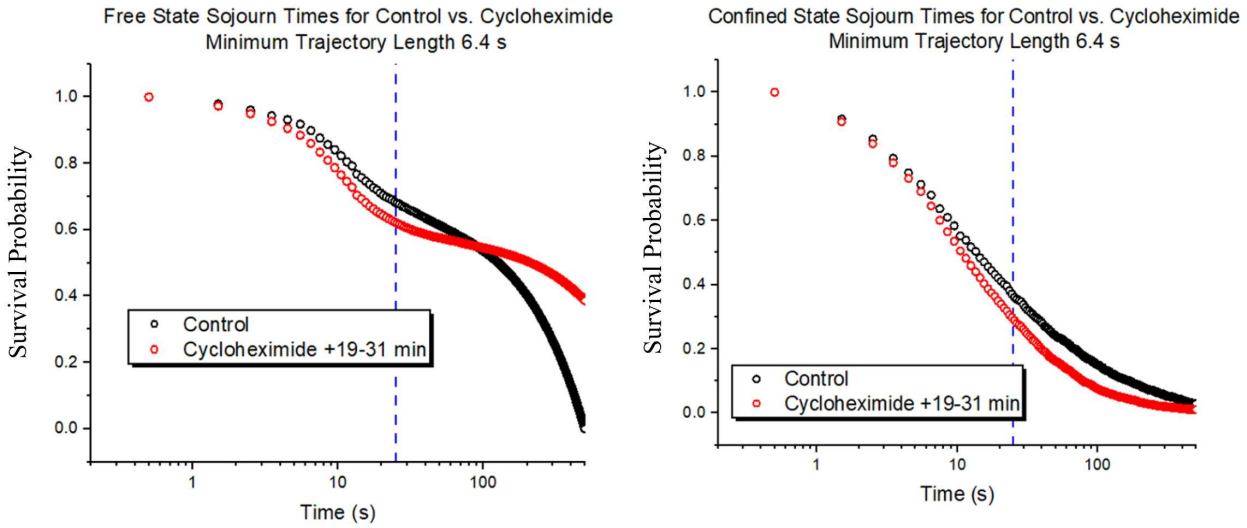


**Figure 3.5:** (left) Plot comparing the Sojourn times for mRNA trajectories in the free state for control (no treatment) and cycloheximide (imaged 19-31 min after treatment) treated cells. (right) Plot comparing the Sojourn times for mRNA trajectories in the confined state for control (no treatment) and cycloheximide (imaged 19-31 min after treatment) treated cells.

Regarding the disruption of microtubules and the ER, it is a bit surprising to see such insignificant changes in dynamics, but the amount of data collected pales in comparison to our previous control experiments. It may also be that the dynamics and statistics we observe are due to structures, escort proteins, and/or local environments that have nothing to do with microtubules or the ER.

The hypothesis that the confined states observed in Chapter 2 represent active translation suggests that treatment with puromycin might result in either a higher average MSD and/or an increase in waiting times for the free state, since mRNA molecules would no longer be bound by ribosomes. Conversely, it suggests that after treatment with cycloheximide, we might observe a decrease in the average MSD and an increase in waiting times for the confined state, since mRNA molecules are unable to escape ribosomes. However, neither of these observations came to fruition. It could be that the statistics we observe in terms of MSD and waiting times are not associated with ribosomes and translation. Cycloheximide may not change anything, since RNA molecules that would already be bound to ribosomes would simply stay bound after treatment, although you might expect confined waiting times to increase. It could also be that treatment with these drugs was ineffec-

tive, although this is unlikely, as we followed previously established and tested protocols. Another explanation could be that there is simply not enough data to result in significant results when compared with control experiments.

# Chapter 4

# Single Particle Tracking of miRNA Molecules

## 4.1 Introduction

miRNAs are single stranded, non-coding RNA guide molecules that are heavily involved in regulation of gene expression for a diverse set of cellular processes [55]. One function of miRNAs is to bind to and in some cases degrade their target mRNA as a form of post-transcriptional gene regulation [55]. In this chapter, we present some preliminary data of the diffusivity of miRNA in the cytoplasm of HeLa cells, just as chapters 2 and 3 did for mRNA.

## 4.2 Materials & Methods

Cell culture methods follow those outlined in chapters 2 and 3. The following procedure was developed and performed by Snehal Patil. miRNAs were introduced via bead loading, before labeling them with the same MS2-MCP method as mRNA. Imaging experiments were done just as they were for mRNA, using oblique illumination via a TIRF microscope. More detailed protocols for bead loading can be found in Appendix C.8. The miRNA used targets the *MYH9* gene.

## 4.3 Trajectory Analysis

The methods for trajectory analysis follow those outlined in chapters 2 and 3.

## 4.4 Results & Discussion

Similar to mRNA, distributions of absolute displacements follow exponential distributions, indicating a broad spectrum of diffusivity among trajectories. When displacements were normalized to their standard deviation, again, smaller displacements fit a more Gaussian distribution, whereas larger displacements appear more heterogeneous, suggesting that there are several modes of motion within trajectories (Figure 4.1).

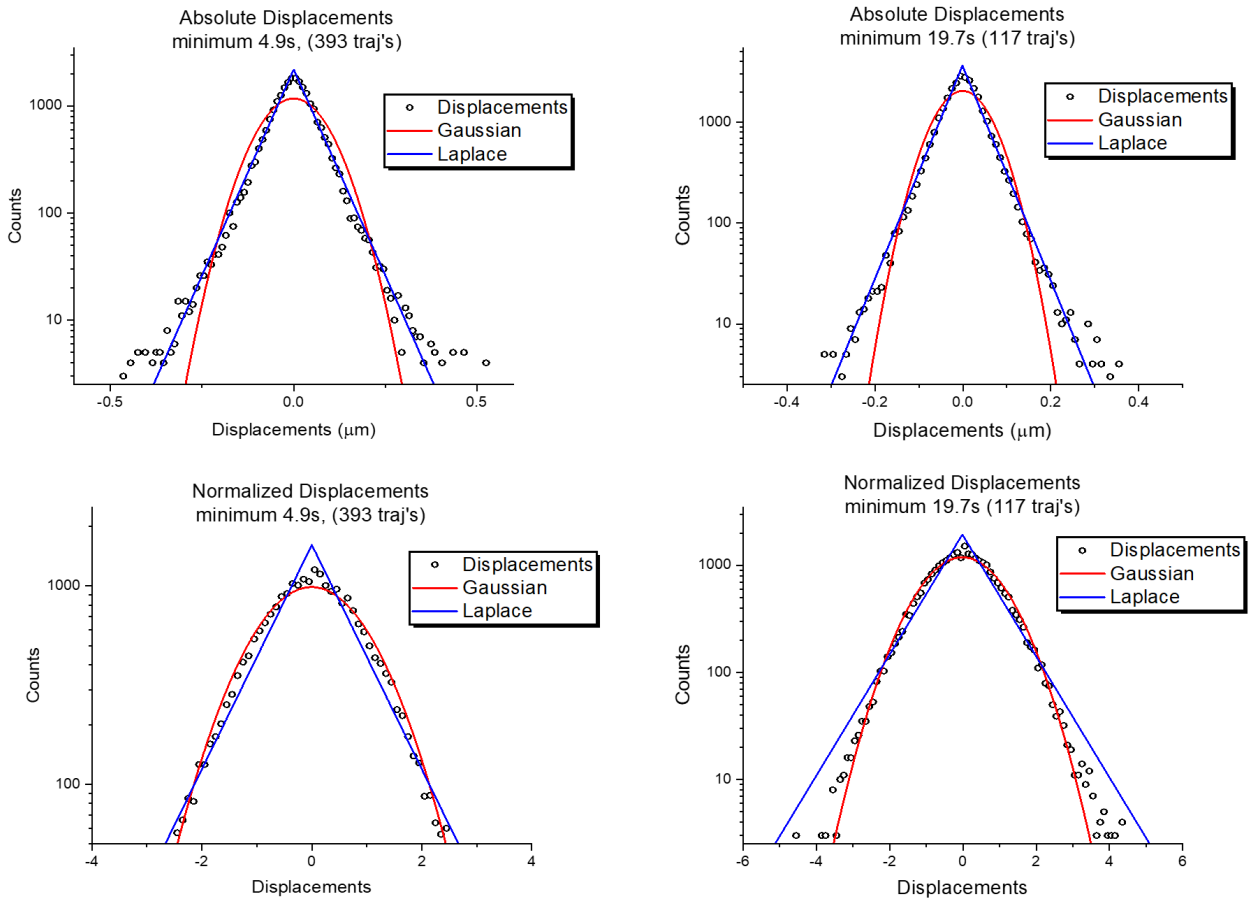


**Figure 4.1:** Plots showing the distributions of absolute and normalized displacements for minimum trajectory lenths of 4.9 s (left: 393 trajectories) and 19.7 s (right: 117 trajectories).

Figure 4.2 shows the ET-MSD for miRNA trajectories with minimum lengths of 4.9 s and 9.9 s. Trajectories with minimum lengths of 4.9 s had an anomalous exponent $\alpha = 1.08$, and trajectories with minimum lengths of 9.9 s had an anomalous exponent $\alpha = 1.43$. Thus, these miRNA molecules are exhibiting superdiffusion on average. However, as shown in Figure 4.3, there is a broad distribution of anomalous exponents. Clearly, the presence of larger anomalous exponents dominates when taking the ET-MSD and correcting for localization error.

miRNAs have the potential to form clusters, so we hypothesized that there may be a correlation between the intensity of miRNA molecules and their corresponding diffusivities (i.e., molecules with higher intensities may represent clusters, and thus have different dynamics). Figure 4.4 compares the average intensity with the diffusion coefficients $K_\alpha$ and anomalous exponents $\alpha$ in one dimension for individual miRNA trajectories from one movie. No significant correlation between

average molecule intensity and either $K_\alpha$ or $\alpha$ was observed, but this analysis was done for a very small amount of data.

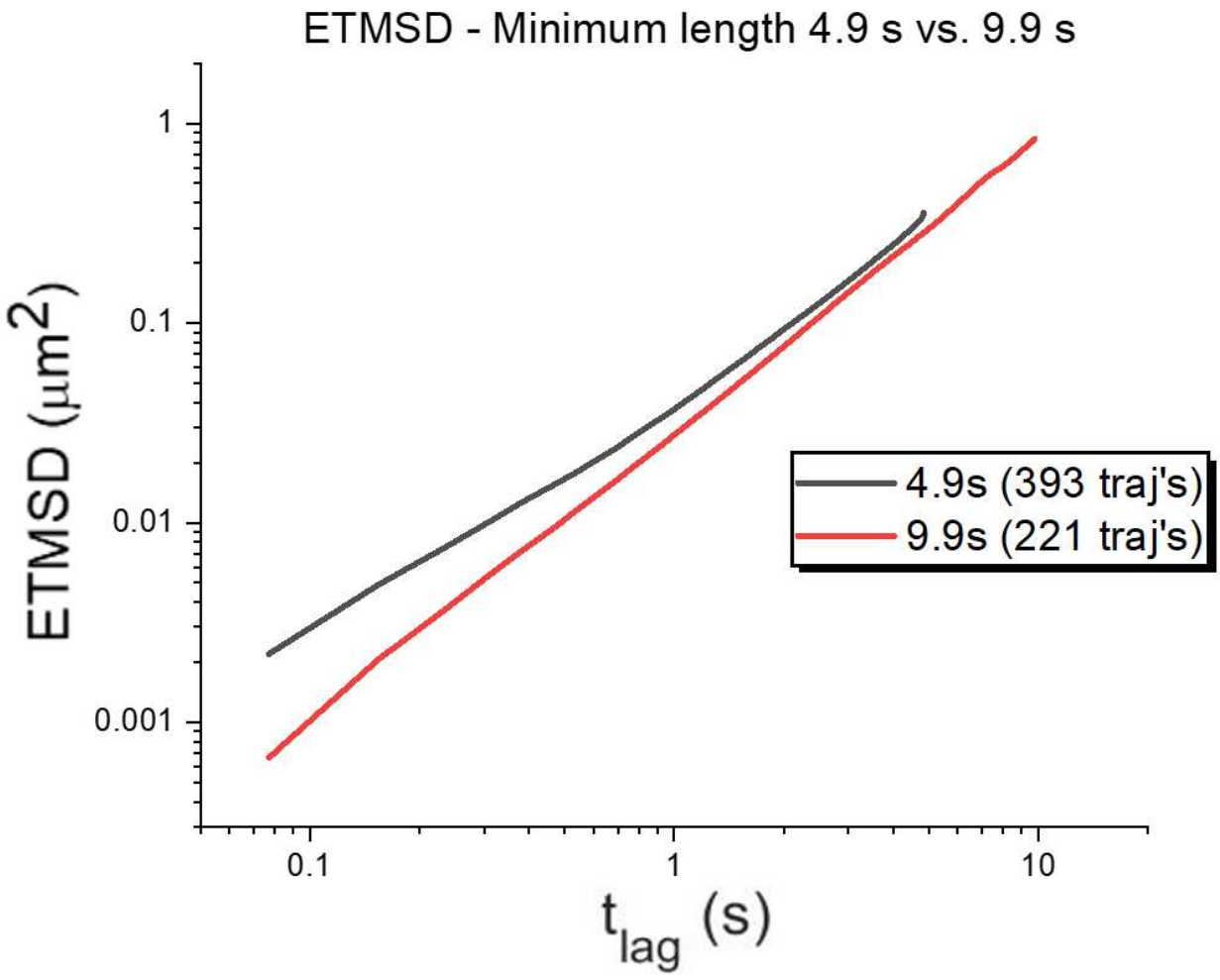


**Figure 4.2:** Plot showing the ET-MSDs of miRNA trajectories with minimum lengths of 4.9 s (393 trajectories) and 9.9 s (221 trajectories).

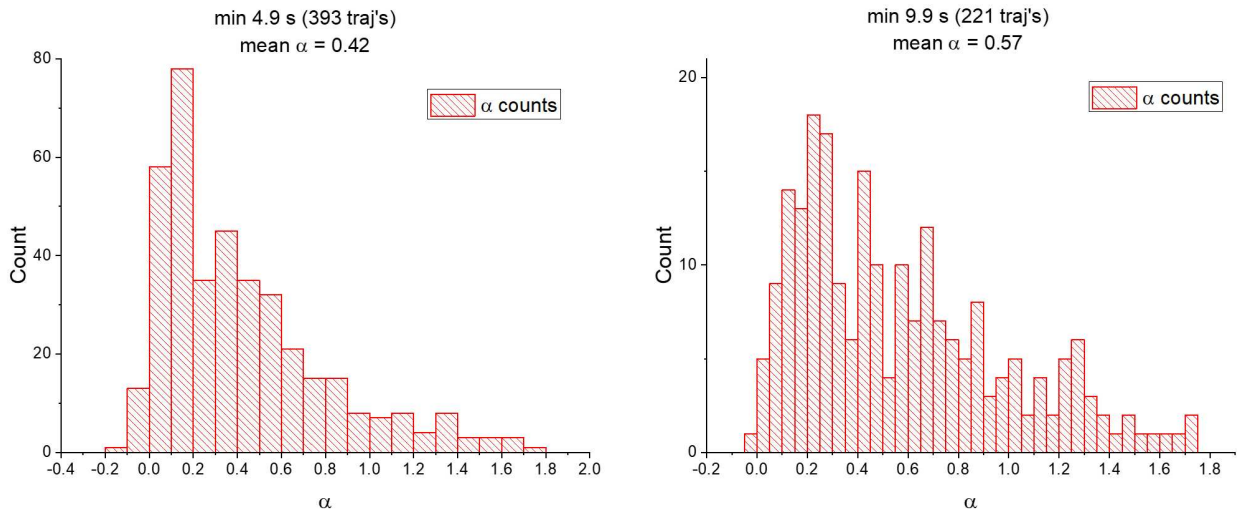


**Figure 4.3:** Plots showing the distributions of anomalous exponents for minimum trajectory lengths of 4.9 s (393 trajectories) and 9.9 s (221 trajectories).

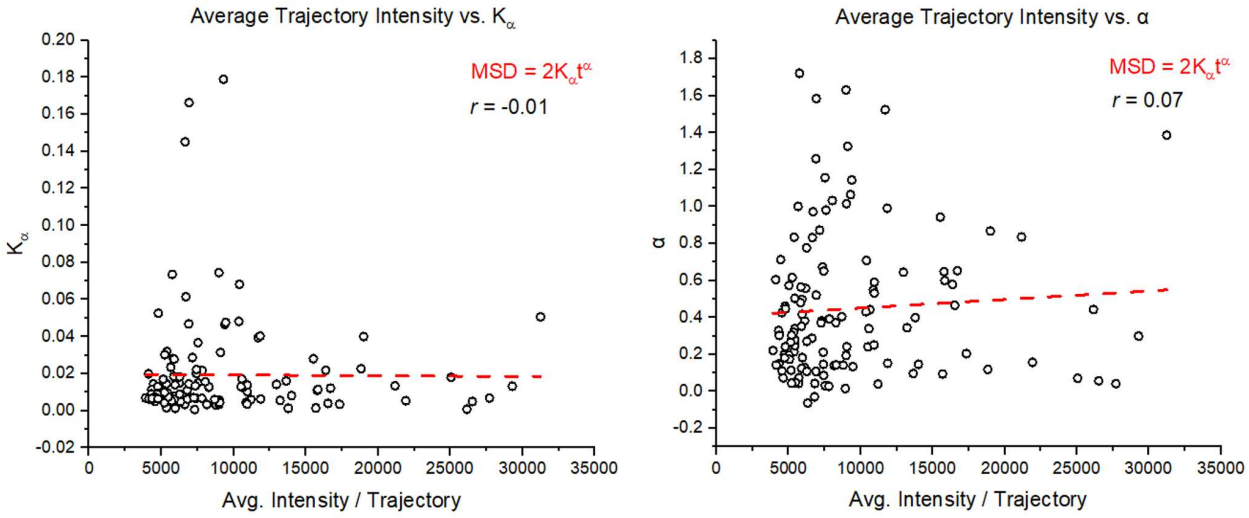


**Figure 4.4:** Plots showing the average mRNA molecule intensity versus the diffusion coefficient $K_\alpha$ (left) and anomalous exponents $\alpha$ (right) for a single movie. We find no correlation between average intensity and both $K_\alpha$ and $\alpha$. Pearson correlation coefficients ($r$) for the left and right plots were -0.01 and 0.07, respectively.

# Chapter 5

# Conclusions & Future Aims

In this thesis, SPT was used to obtain 2D (XY) trajectories of mRNA and miRNA molecules in the cytoplasm of live HeLa cells using both confocal and TIRF (oblique illumination) microscopy techniques. We found that mRNA molecules exhibit subdiffusion, ergodicity breaking, and have statistics that depend on observation time (i.e. aging). Molecules switch stochastically between two mobility states - differing by roughly one order of magnitude in their MSD - which is likely the cause of the aging behavior we observe. We termed each mobility state as "free" and "confined" according to their MSD. The free state exhibits an exponential distribution (uncorrelated) of waiting times, being much more transient than the confined state. The confined state, however, exhibits a power-law distribution of waiting times.

We found that treating cells with drugs which disrupt intracellular structures such as microtubules and the ER did not have a significant effect on the dynamics of mRNA molecules, although it could tentatively be said that disruption of the ER lowers the MSD of mRNA, although more data is preferable to confirm this. Similarly, interfering with translation by both releasing mRNA from ribosomes and locking them inside of ribosomes does not seem to have a significant effect on mRNA dynamics. Future experiments include disruption of the intermediate filament vimentin and actin.

We found that miRNA trajectories also exhibit heterogeneity in their absolute and normalized displacements, as well as a broad spectrum of anomalous exponents, indicating there could be multiple modes of motion in individual miRNA trajectories. We are currently working on separating the modes of motion for miRNA as was done with the convex hull method for mRNA in Chapter 2. The anomalous exponent for the ET-MSD of miRNA ranges from normal diffusion to superdiffusive, depending on the minimum trajectory length analyzed. Future work will involve separating these modes of motion as we did with mRNA using the convex hull method. Additional future experiments will include quantifying the number of mRNA molecules present in cells be-

fore and after introducing miRNA to the cells, as well as examining the effects of miRNA on both transcription and translation sites.

# Bibliography


[1] Jean Yves Tinevez, Nick Perry, Johannes Schindelin, Genevieve M. Hoopes, Gregory D. Reynolds, Emmanuel Laplantine, Sebastian Y. Bednarek, Spencer L. Shorte, and Kevin W. Eliceiri. TrackMate: An open and extensible platform for single-particle tracking. *Methods*, 115(2017):80–90, 2017.

[2] Jeff W. Lichtman and José Angel Conchello. Fluorescence microscopy. *Nature Methods*, 2(12):910–919, 2005.

[3] Bart Geverts, Martin E. Van Royen, and Adriaan B. Houtsmuller. *Analysis of biomolecular dynamics by frap and computer simulation*, volume 1251. 2014.

[4] Adrien Mau, Karoline Friedl, Christophe Leterrier, Nicolas Bourg, and Sandrine Lévêque-Fort. Fast scanned widefield scheme provides tunable and uniform illumination for optimized SMLM on large fields of view. *bioRxiv*, 2(d):2020.05.08.083774, 2020.

[5] Adaobi Nwaneshiudu, Christiane Kuschal, Fernanda H. Sakamoto, R. Rox Anderson, Kathryn Schwarzenberger, and Roger C. Young. Introduction to confocal microscopy. *Journal of Investigative Dermatology*, 132(12):1–5, 2012.

[6] Logan George, Fred E Indig, Kotb Abdelmohsen, and Myriam Gorospe. Intracellular RNA-tracking methods. 2018.

[7] Yann Lanoiselée and Denis S. Grebenkov. Unraveling intermittent features in single-particle trajectories by a local convex hull method. *Phys. Rev. E*, 96:022144, Aug 2017.

[8] Tati Suhartati. No title. (May):106, 2013.

[9] R Allen and Norman J Chonacky. Biological diffusion processes, 1975.

[10] Paul S Agutter and Denys N Wheatley. Diffusion theory in biology: A relic of mechanistic materialism, 2000.

[11] Adal Sabri, Xinran Xu, Diego Krapf, and Matthias Weiss. Elucidating the origin of heterogeneous anomalous diffusion in the cytoplasm of mammalian cells. *Phys. Rev. Lett.*, 125:058101, Jul 2020.

[12] Aubrey V. Weigel, Blair Simon, Michael M. Tamkun, and Diego Krapf. Ergodic and nonergodic processes coexist in the plasma membrane as observed by single-molecule tracking. *Proceedings of the National Academy of Sciences of the United States of America*, 108(16):6438–6443, 2011.

[13] Marco Grimaldo, Hender Lopez, Christian Beck, Felix Roosen-Runge, Martine Moulin, Juliette M. Devos, Valerie Laux, Michael Härtlein, Stefano Da Vela, Ralf Schweins, Alessandro Mariani, Fajun Zhang, Jean Louis Barrat, Martin Oettel, V. Trevor Forsyth, Tilo Seydel, and Frank Schreiber. Protein short-time diffusion in a naturally crowded environment. *Journal of Physical Chemistry Letters*, 10:1709–1715, 4 2019.

[14] Diego Krapf, Grace Campagnola, Kanti Nepal, and Olve B. Peersen. Strange kinetics of bulk-mediated diffusion on lipid bilayers. *Physical Chemistry Chemical Physics*, 18:12633–12641, 2016.

[15] Tatsuya Morisaki and Timothy J Stasevich. Single-Molecule imaging of mRNA interactions with stress granules. *Methods Mol Biol*, 2428:349–360, 2022.

[16] Titus Lucretius and William Ellery Leonard. *Of The Nature of Things*, volume II. 7 2008.

[17] Peter Mörters and Yuval Peres. Brownian motion, 2010.

[18] Helmut Mehrer and Nicolaas A Stolwijk. Heroes and highlights in the history of diffusion the open-access journal for the basic principles of diffusion theory, experiment and application, 2009.

[19] Diego Krapf. Chapter five - mechanisms underlying anomalous diffusion in the plasma membrane. In Anne K. Kenworthy, editor, *Lipid Domains*, volume 75 of *Current Topics in Membranes*, pages 167–207. Academic Press, 2015.

[20] Aleksander Weron, Krzysztof Burnecki, Elizabeth J Akin, Laura Solé, Michał Balcerek, Michael M Tamkun, and Diego Krapf. Ergodicity breaking on the neuronal surface emerges from random switching between diffusive states. *Scientific Reports*, 7(1):5404, July 2017.

[21] Carlo Manzo, Juan A. Torreno-Pina, Pietro Massignan, Gerald J. Lapeyre, Maciej Lewenstein, and Maria F. Garcia Parajo. Weak ergodicity breaking of receptor motion in living cells stemming from random diffusivity. *Phys. Rev. X*, 5:011021, Feb 2015.

[22] Ohad Vilk, Erez Aghion, Tal Avgar, Carsten Beta, Oliver Nagel, Adal Sabri, Raphael Sarfati, Daniel K. Schwartz, Matthias Weiss, Diego Krapf, Ran Nathan, Ralf Metzler, and Michael Assaf. Unravelling the origins of anomalous diffusion: From molecules to migrating storks. *Physical Review Research*, 4(3):1–30, 2022.

[23] Stas Burov, Jae Hyung Jeon, Ralf Metzler, and Eli Barkai. Single particle tracking in systems showing anomalous diffusion: The role of weak ergodicity breaking. *Physical Chemistry Chemical Physics*, 13(5):1800–1812, 2011.

[24] Zachary R Fox, Eli Barkai, and Diego Krapf. Aging power spectrum of membrane protein transport and other subordinated random walks. *Nature communications*, 12(1):1–9, 2021.

[25] Diego Krapf, Enzo Marinari, Ralf Metzler, Gleb Oshanin, Xinran Xu, and Alessio Squarcini. Power spectral density of a single brownian trajectory: what one can and cannot learn from it. *New Journal of Physics*, 20(2):023029, 2018.

[26] Diego Krapf. Nonergodicity in nanoscale electrodes. *Physical Chemistry Chemical Physics*, 15(2):459–465, 2013.

[27] FN Hooge, TGM Kleinpenning, and Lode KJ Vandamme. Experimental studies on 1/f noise. *Reports on progress in Physics*, 44(5):479, 1981.

[28] Matthew Pelton, David G Grier, and Philippe Guyot-Sionnest. Characterizing quantum-dot blinking using noise power spectra. *Applied physics letters*, 85(5):819–821, 2004.

[29] Richard F Voss. Evolution of long-range fractal correlations and 1/f noise in dna base sequences. *Physical review letters*, 68(25):3805, 1992.

[30] Anne Sornette and Didier Sornette. Self-organized criticality and earthquakes. *EPL (Europhysics Letters)*, 9(3):197, 1989.

[31] Plamen Ch Ivanov, Luis A Nunes Amaral, Ary L Goldberger, Shlomo Havlin, Michael G Rosenblum, H Eugene Stanley, and Zbigniew R Struzik. From 1/f noise to multifractal cascades in heartbeat dynamics. *Chaos: An Interdisciplinary Journal of Nonlinear Science*, 11(3):641–652, 2001.

[32] N Leibovich, A Dechant, E Lutz, and E Barkai. Aging wiener-khinchin theorem and critical exponents of 1/f $\beta$ noise. *Physical Review E*, 94(5):052130, 2016.

[33] Andreas Dechant and Eric Lutz. Wiener-khinchin theorem for nonstationary scale-invariant processes. *Physical review letters*, 115(8):080603, 2015.

[34] A. Khintchine. Korrelationstheorie der stationären stochastischen Prozesse. *Mathematische Annalen*, 109(1):604–615, 1934.

[35] N. Leibovich and E. Barkai. Aging wiener-khinchin theorem. *Phys. Rev. Lett.*, 115:080602, Aug 2015.

[36] Jedrzej Szymanski and Matthias Weiss. Elucidating the origin of anomalous diffusion in crowded fluids. *Physical Review Letters*, 103(3):1–4, 2009.

[37] Andrey G. Cherstvy, Aleksei V. Chechkin, and Ralf Metzler. Anomalous diffusion and ergodicity breaking in heterogeneous diffusion processes. *New Journal of Physics*, 15, 2013.

[38] Pekka Hänninen. Light microscopy: Beyond the diffraction limit. *Nature*, 419(6909):802, 2002.

[39] Pekka Hänninen. Light microscopy: Beyond the diffraction limit. *Nature*, 419(6909):802, 2002.

[40] Editorial: Beyond the diffraction limit. *Nature Photonics*, 3(7):361, 2009.

[41] Cooper GM. *The Cell: A Molecular Approach*. Sinauer Associates, Sunderland, MA, 2000.

[42] Brendan P Lucey, Walter A Nelson-Rees, Grover M Hutchins, and Henrietta. Historical Perspective Henrietta Lacks, HeLa Cells, and Cell Culture Contamination. *Arch Pathol Lab Med—Vol HeLa Cells and Cell Culture Contamination—Lucey et al*, 133, 2009.

[43] Alessandro Pecci, Xuefei Ma, Anna Savoia, and Robert S. Adelstein. MYH9: Structure, functions and role of non-muscle myosin IIA in human disease. *Gene*, 664(April):152–167, 2018.

[44] Edouard Bertrand, Pascal Chartrand, Matthias Schaefer, Shailesh M. Shenoy, Robert H. Singer, and Roy M. Long. Localization of ASH1 mRNA particles in living yeast. *Molecular Cell*, 2(4):437–445, 1998.

[45] Evelina Tutucci, Maria Vera, Jeetayu Biswas, Jennifer Garcia, Roy Parker, and Robert H Singer. An improved MS2 system for accurate reporting of the mRNA life cycle. *Nat Methods*, 15(1):81–89, November 2017.

[46] Tatsuya Morisaki, Kenneth Lyon, Keith F. DeLuca, Jennifer G. DeLuca, Brian P. English, Zhengjian Zhang, Luke D. Lavis, Jonathan B. Grimm, Sarada Viswanathan, Loren L. Looger, Timothee Lionnet, and Timothy J. Stasevich. Real-time quantification of single RNA translation dynamics in living cells. *Science*, 352(6292):1425–1429, 2016.

[47] Arif Wicaksana and Tahar Rachman. No title no title no title. *Angewandte Chemie International Edition, 6(11), 951–952.*, 3(1):10–27, 2018.

[48] Dale Reed. Gaussian distribution. *Printed Circuit Fabrication*, 15(5):64–66, 1992.

[49] Krzysztof Podgorski Samuel Kotz, Tomasz Kozubowski. *The Laplace Distribution and Generalizations: A Revisit with Applications to Communications, Economics, Engineering, and Finance*. 2001.

[50] Yuan Jhih Tsai, Hsing I. Lee, and Alan Lin. Ribosome distribution in HeLa cells during the cell cycle. *PLoS ONE*, 7(3), 2012.

[51] J. J. Blum, G. Lawler, M. Reed, and I. Shin. Effect of cytoskeletal geometry on intracellular diffusion. *Biophysical Journal*, 56(5):995–1005, 1989.

[52] Thomas J. Lampo, Stella Stylianidou, Mikael P. Backlund, Paul A. Wiggins, and Andrew J. Spakowitz. Cytoplasmic RNA-Protein Particles Exhibit Non-Gaussian Subdiffusive Behavior. *Biophysical Journal*, 112(3):532–542, 2017.

[53] V. A. Saks, E. Vasil'eva, Yu O. Belikova, A. V. Kuznetsov, S. Lyapina, L. Petrova, and N. A. Perov. Retarded diffusion of ADP in cardiomyocytes: possible role of mitochondrial outer membrane and creatine kinase in cellular regulation of oxidative phosphorylation. *BBA - Bioenergetics*, 1144(2):134–148, 1993.

[54] Iva Marija Tolić-Nørrelykke, Emilia Laura Munteanu, Genevieve Thon, Lene Oddershede, and Kirstine Berg-Sørensen. Anomalous diffusion in living yeast cells. *Physical Review Letters*, 93(7):1–4, 2004.

[55] Ayla Valinezhad Orang, Reza Safaralizadeh, and Mina Kazemzadeh-Bavili. Mechanisms of miRNA-mediated gene regulation from common downregulation to mRNA-specific upregulation. *International Journal of Genomics*, 2014(June 2013), 2014.

[56] O'Neil Wiggan, Jennifer G. Deluca, Timothy J. Stasevich, and James R. Bamburg. Lamin A/C deficiency enables increased myosin-II bipolar filament ensembles that promote divergent actomyosin network anomalies through self-organization. *Molecular Biology of the Cell*, 31(21):2363–2378, 2020.

[57] Manuel Stemmer, Thomas Thumberger, Maria Del Sol Keyer, Joachim Wittbrodt, and Juan L. Mateo. CCTop: An intuitive, flexible and reliable CRISPR/Cas9 target prediction tool. *PLoS ONE*, 10(4):1–11, 2015.

[58] Le Cong, F Ann Ran, David Cox, Shuailiang Lin, Robert Barretto, Patrick D Hsu, Xuebing Wu, Wenyan Jiang, and Luciano a Marraffini. Cong, L., Ran, F. A., Cox, D., Lin, S., Barretto, R., Habib, N., ... Zhang, F. (2013). Multiplex Genome Engineering Using CRISPR/Cas Systems. Science (New York, N.Y.). *Science (New York, N.Y.)*, 339(6121):819–823, 2013.

[59] Daniel E. Bauer, Matthew C. Canver, and Stuart H. Orkin. Generation of genomic deletions in mammalian cell lines via CRISPR/Cas9. *Journal of Visualized Experiments*, (95):1–9, 2015.

[60] Toyoaki Natsume, Tomomi Kiyomitsu, Yumiko Saga, and Masato T. Kanemaki. Rapid Protein Depletion in Human Cells by Auxin-Inducible Degron Tagging with Short Homology Donors. *Cell Reports*, 15(1):210–218, 2016.

[61] Saverus. No Title. *Jurnal Kajian Pendidikan Ekonomi dan Ilmu Ekonomi*, 2(1):1–19, 2019.

[62] Sahara. Submitted By :. *Academia.Edu*, 4:1–189, 2022.

# Appendix A

# Engineering of HeLa Cells

Protocol for stable transfection of HeLa Cells (Adapted from [56]):

This procedure was developed and performed by Drs. O'Neil Wiggan and Tim Stasevich. Single-guide RNAs (sgRNAs) targeting N- and C-terminal coding exons of the *MYH9* gene were designed using CCTop [57]. sgRNAs were cloned into the plasmid pX330-U6-ChimericBB-CBh-hSpCas9 (Addgene plasmid 42230 [58, 59]). Homology-directed repair donor plasmids were generated using a combination of gene synthesized DNA sequences ($\sim$ 225-base-pair homology arms) and either mAID-mCherry2 derived from plasmid pMK292 (Addgene plasmid 72830) for C-terminal tagging or sfGFP for N-terminal tagging [60]. Cells were transfected with plasmids for sgRNA and donor repair using Lipofectamine 2000. Following neomycin selection, mCherry-positive cells were confirmed for proper recombination by genomic DNA PCR genotyping [59], and by visual evaluation of expected mCherry-protein cellular distribution through fluorescence microscopy. Confirmed mCherry-expressing cells were subjected to another round of CRISPR editing with plasmids for N-terminal sfGFP tagging. Dual GFP/mCherry-positive cells were isolated via fluorescence-activated cell sorting and characterized as described earlier.

# Appendix B

# Cell Culture

## B.1 Protocol for Preparing Cell Culture Media

This protocol describes the methods for preparing media for cell culture. As with all cell culture related protocols, all work should be performed inside the biosafety cabinet and proper aseptic technique practiced. [2]

| Material | Volume (mL) | Vendor | Product No. |
|---|---|---|---|
| FBS | 50 | Atlas Biologicals | EF-0500-A |
| DMEM (with phenol red) | 500 | Thermo Fisher Scientific | SH3002201 |
| 100X Antibiotic (Streptomycin/Penicillin) | 5 | N/A | N/A |
| Sterile glass bottle | 500 | Life Science | CT-229717 |
| Bottle top filter | N/A | N/A | N/A |

1. Heat shock 50 ml Aliquot of FBS. Let the FBS sit in water bath at 37°C for 1 hour after being thawed.

2. Thaw antibiotic. Do not let thawed antibiotic remain unfrozen for an extended amount of time.

3. Once FBS is thawed and heat shocked, add to DMEM.

4. Pass DMEM + FBS + antibiotic solution through a bottle top filter into a sterile glass bottle 108.

   (a) Filter DMEM first, then add antibiotic. Add FBS at the end.

[2] Adapted from [61].

(b) For Imaging, perform this protocol with colorless MEM media instead of DMEM (with phenol red).

5. Label bottle with description, initials and date.

6. Store media in fridge.

## B.2 Protocol for Splitting Cells

This protocol describes the methods for splitting/passing HeLa cells in order to maintain healthy cells and levels of confluence. [3]

General Notes

- The hood should always be maintained as contaminant-free as possible. Spray and/or wipe gloves and materials before going under the hood.
- Try not to reach over materials, especially ones that are open or exposed.
- When using disposable pipettes from wrappers: try and peel the wrapper halfway down and keep it to one side to dispose of the pipette in it later to help against contamination.
- You can always turn pipettes when placing them in the dispenser so you can easily see the numbers.
- Always make sure to warm all solutions in water bath at 37$\circ$C before beginning the procedure.

[3] Adapted from [8, 61]

| Material | Volume (mL) | Vendor | Product No. |
|---|---|---|---|
| Cell Culture Media [4] | Varies | N/A | N/A |
| Trypsin | Varies | Thermo Fisher Scientific | 25200114 |
| Serilogical pipettes | 10 | CellTreat | CT-229421 |
| Centrifuge tubes | 10 | N/A | N/A |
| 75 $cm^2$ tissue culture flasks | N/A | CellTreat | CT-229341 |
| 35 mm Delta T culture dish | N/A | Biotechs | N/A |

1. A dish with confluent cells should be ready to split before running this protocol.
2. Label new dishes with initials, date, cell type and amount of cells.
   (a) NOTE: If splitting more than one type of cell (e.g. Myosin-labeled and non-Myosin-labeled), label centrifuge tubes to distinguish (step 11).
3. UV all the culture dishes that cells will be split into for 5-30 min in the biosafety cabinet.
4. Add 10 ml cell culture media from protocol "Preparing Cell Media" to each new 100 mm dish.
5. If live cell imaging is needed, also add 1 ml culture media into 35 mm Delta T dishes.
6. Place all dishes in the incubator until ready.
7. Check confluency of cells in each dish for deciding amount to seed in step 13.
8. Aspirate media from dish with confluent cells.
9. Pipette 4 ml of Trypsin into the dish, and put it back to the incubator for about 3 min.
10. Once cells have lifted from bottom of dish, gentle tap the dish to help with cell lifting.
11. Add another 6 ml culture media into the dish.

12. Centrifuge at 200g speed for 2 min.

13. Aspirate the supernatant and resuspend the cell pellet with 1 ml culture media.

14. Pipette 0.5-1 mL (whatever amount is appropriate, i.e. if 90-100% confluent, use 0.5 mL, else use 1 mL) of cells into each new dish, then put them back in the incubator.

## B.3 Protocol for Freezing Cells

Materials:

| Material | Volume (mL) | Vendor | Product No. |
|---|---|---|---|
| Cell Culture Media [5] | Varies | N/A | N/A |
| FBS | 4.5 | Atlas Biologicals | EF-0500-A |
| DMSO | 0.5 | N/A | N/A |
| Trypsin | Varies | Thermo Fisher Scientific | 25200114 |
| Serilogical pipettes | 10 | CellTreat | CT-229421 |
| Centrifuge tubes | 10 | N/A | N/A |

This protocol describes the methods for freezing cells for the purpose of storing for later use.

1. Prepare 5 ml freezing medium, containing 90% FBS and 10% DMSO.

2. Thaw FBS at room temperature.

3. Prepare three 1.5 ml sterile centrifuge tubes.

4. Either use cell scrapers or Trypsin (same method as in protocol "Splitting HeLa cells") to remove cells from the culture dish surface. Then pipette them all into the 10 ml centrifuge tube.

5. Centrifuge at 200g speed for 2 min.

6. Aspirate the supernatant and resuspend the cell pellets with 3 ml of freezing medium as mentioned above.

7. Split into three centrifuge tubes, then store at -80°C.

# Appendix C

# Imaging & Pharmacological Treatment of Cells

## C.1 Protocol for Laser Alignment

This imaging set-up uses a TIRF microscope. The laser and microscope has to be aligned before every experiment to obtain good quality images[6].

1. LASER: The laser emits light of wavelength 641.5 nm.

2. SHUTTER: This can be operated manually or through NIS elements software. An ND filter can be placed while aligning to reduce the intensity of light, but it must be placed at an angle such that the reflected beam does not travel back into the laser cavity.

3. MOVABLE MIRROR PAIRS: On the table, place the first mirror such that the laser beam reflects off its center and the mirror is angled at 45 degrees to its stand. Use an aperture for this alignment. Now place the second mirror such that the beam hits the center of the mirror and is also laterally and vertically aligned at all points between the two mirrors. Use a tall stand with a sticky note to check the alignment. If you notice that the beam is shifting, move the second mirror to a better location and use the knobs on the first mirror for fine adjustments.

4. TELESCOPE: Once the beam is aligned until the telescope, laser beam should be centered at the first telescopic lens. Use pertures to ensure that the beam is centered and that it maintains the same height and lateral position. Also check for reflections and make sure they align with the laser beam on the lens. Place the second lens of the telescope such that the distance between the lenses is the sum of their focal lengths. For alignment, use the knobs on the xyz stand that the second lens is mounted on. The beam emerging from the

[6]Adapted from [62]

telescope should be collimated. If the beam appears to be shrinking, the lenses are too far and if the beam expands, the lenses are too close together. Once the beam is collimated and is aligned laterally and vertically, move to the next step.

5. ALIGNING MIRRORS: To allow multiple lasers to illuminate the microscope, the laser follows the same path from the set of dichroics to the microscope as shown in Fig E.2.

6. This protocol will refer to this section of shared path as the "main line". The alignment microscope allows this shared path by aligning the beam along the main line. The first aligning mirror should be placed such that it is at 45-degree angle to its stand and the beam is centered. The beam should be collimated and aligned at all points between the mirror and the second telescopic lens. If not, go back to section 4. The second mirror should have the beam centered and follow the alignment and collimation conditions. Use the knobs on the first mirror to make any fine adjustments.

7. DICHROIC: The dichroic passes only a specific wavelength. The beam should be centered at the dichroic as well.

Due to drifts, the laser alignment may vary, especially at the main line and should be re-adjusted before imaging.

1. Remove the first steering mirror and the two telescopic lenses of the second telescope before aligning the laser through the main line.

2. There are two apertures in the main line. The steering mirror diagonal to the aperture is used to align the beam through it, that is, the aligning mirror on the right side of the table (next to the first telescope) is used for near aperture and the aligning mirror on the left side (before the dichroic) aligns the laser beam at the far aperture. If you see that the alignment gets only worse after a few iterations, switch the aligning mirrors- mirror on the left for near and the one on the right for far. Use the right aligning mirror to center the beam at the near aperture. This will move the beam farther from the far aperture. Center the beam at the far aperture

using the left aligning mirror. That will cause the beam to go off-center at near aperture. Adjust the aligning mirrors in this manner until the beam is centered at both the apertures.

3. SECOND TELESCOPE- Place the telescopic lenses such that the laser beam is centered at them both, aligned at all points between them and the lenses are at a distance equal to the sum of their focal lengths. Check for collimation and adjust the length of the telescope accordingly.

4. Once the beam appears to be collimated and aligned throughout the table, place the first steering mirror back such that the beam is centered on it. Remove the focusing lens from its stand and proceed to the next step.

## C.2 Protocol for Aligning TIRF Microscope

This protocol begins with the assumption that the telescope is already aligned. This should be checked before each imaging session and before starting this protocol. If more than one beam is being used for illumination further care will need to be taken to ensure that the beams are not only aligned for TIRF imaging, but also co-aligned to each other. [7]

Materials:

| Material | Vendor | Product No. |
|---|---|---|
| SM1 Tube | N/A | N/A |
| Apertures (4x) | N/A | N/A |
| Adaptor with external RMS threads and internal SM1 threads | N/A | N/A |
| Cross-hair (usually drawn on a sheet of paper) | N/A | N/A |

1. Remove focusing lens from path. [8]

[7] Adapted from [8]

[8] The logic in this method is to first align the beam with the SM1 tubes so that it is entering the microscope parallel to the table and exiting the microscope perpendicularly. The crosshair on the ceiling marks this. Between steps 3 and

2. Place an aperture on the second lens of the telescope and close it so that the beam is small as it enters the microscope. Use the steering mirrors S1 and S2 and align with the SM1 tube. The beam should have an aperture before the two steering mirrors and be aligned such that it goes through the bottom and top iris of the tube and onto the ceiling. Use S1 to center the beam with the bottom aperture closed and S2 to center the beam through the top aperture.

3. Center the crosshair on the ceiling to the aligned beam as a marker for later steps. Do not touch the steering mirrors until after the focusing lens is in place.

4. Replace the tube with the objective. If using the objective heater you can put this on the objective now as well (and turn on the objective heater power supply).

5. Put the focusing lens back into the micrometer holder.

6. Adjust the lens so that the beam passes through the center. Use an aperture on the focusing lens and telescope (to reduce the size of the beam) to help find center more easily.

7. Make sure that the reflection of the beam off the focusing lens aligns to the original beam on mirror S2.

8. Once aligned tighten the focusing lens in place.

9. Using only the micrometer (do not use the steering mirrors at this point!) adjust the focusing lens so that beam on the ceiling is going through the crosshair. This will move the beam off center from the lens. This will be adjusted next.

10. Using S1 re-center the beam onto the focusing lens (close both the aperture on the telescope lens and the focusing lens to do this).

11. Open the apertures and re-center the spot on the ceiling using S2.

---

6 the biggest change made to the system is adding the focusing lens. Thus, to ensure alignment the beam needs to be adjusted so that it is aligned back to the crosshair using only focusing lens. After this only small adjustments are made with the mirrors to perfect the alignment.

12. Repeat steps 10 and 11 until the beam is going through the center of the focusing lens and aligned to the crosshair on the ceiling. 13. Once aligned, remove all apertures (so as not to clip the beam) and if using the heated stage place this on the microscope as well2 but do not turn on until a dish is in place. The system is reading for imaging.

13. Once aligned, remove all apertures (so as not to clip the beam) and if using the heated stage place this on the microscope as well [9] but do not turn on until a dish is in place. The system is reading for imaging.

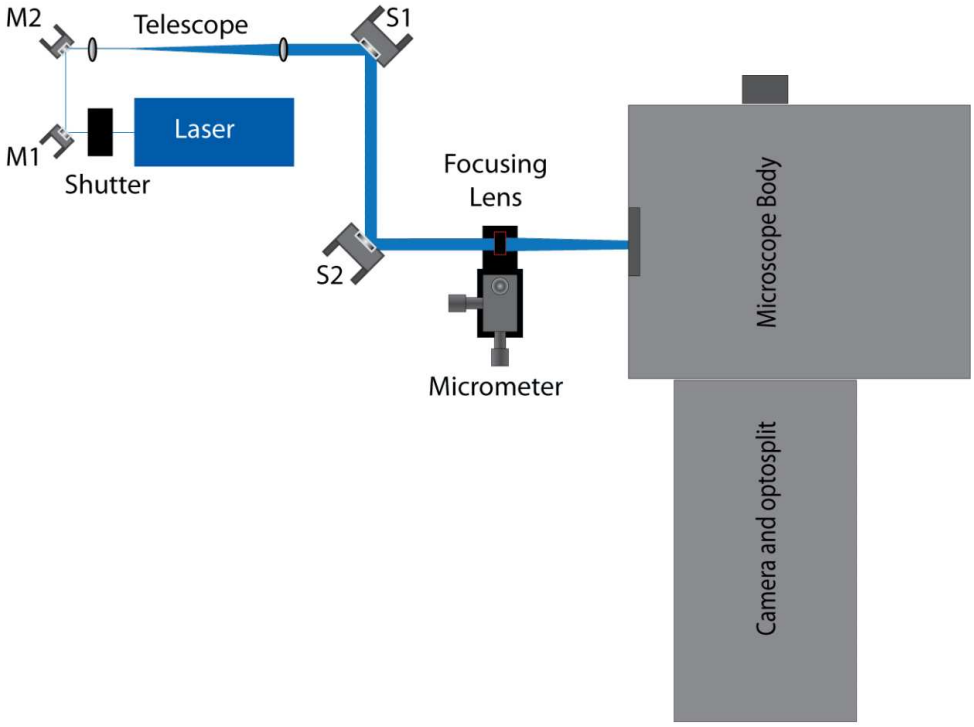


**Figure C.1:** Schematic of TIRF microscope, lasers, optics, and camera. [8].

## C.3 Protocol for Labeling and Imaging mRNA

Preparation & Storage Janelia Fluor (JF) 646 Stock Solution:

[9]The objective heater may be turned on immediately. It take time to warm up the objective so it is better to give the heater 30 minutes or more. The stage heater however provides instantaneous heat. The stage heater should never be turned on without a dish in place.

1. Janelia Fluor (JF) 646 HaloTag ligand should be resuspended in DMSO to create a 200 $\mu$M stock solution. Stock solution should be aliquoted into single use tubes of 1 $\mu$L each to avoid destabilization of ligand from repeated thawing and refreezing.

2. Store in -20°C freezer upright and protected from light.

Imaging:

| **Material** | **Volume (mL)** | **Vendor** | **Product No.** |
|---|---|---|---|
| JF646 Stock Solution | 0.5 $\mu$L | Promega | N/A |
| Cell Culture Media [10] | 1.5 per dish | N/A | N/A |
| Imaging Media [11] | 3 per dish | N/A | N/A |
| 35 mm Delta T culture dish | N/A | Biotechs | N/A |

Preparation (day before imaging):

1. Delta culture dish(es) should be kept in a biosafety cabinet and sterilized for 5-30 min in UV before performing the experiment. Please take extreme care to be as clean and sterile as possible.

2. Before splitting cells, add 1 mL of cell media [12] to imaging dish(es) and incubate at 37°C.

3. While splitting cells, add 25 $\mu$L of resuspended cells to each Delta culture dish and incubate overnight at 37°C.

Protocol for Imaging (day of imaging):

1. Make sure stage heater is calibrated and laser(s) and microscope are aligned.

2. Prepare a 1:200 dilution with 1 $\mu$L of JF 646 stock solution (less is better if you need to mitigate auto-fluorescence ($\sim$0.2-0.5 $\mu$L)) and 199 $\mu$L of cell media, creating a 1 $\mu$M concentration of fluorophore.

[12] See B.1

3. Remove 200 $\mu$L of cell media from the culture dish (containing 1 mL of media from the previous day) and add the 200 $\mu$L of JF 646/cell media dilution (from step 2) to the culture dish. This creates a 1:1000 dilution, or a 5X working solution (0.2 $\mu$M) of JF 646. Incubate for 30 min.

4. Aspirate media from the dish and wash 2-3 times with imaging media. [13]

5. Add 1 mL of imaging media to dish. Incubate cells for 20 min before imaging.

## C.4 Protocol for Treating HeLa Cells with Cycloheximide

Cycloheximide is a drug that interferes with translation by locking mRNA in ribosomes.

Preparing & Storing Cycloheximide Stock Solution:

1. Final Stock solution of Cycloheximide: 5 mg/mL in Ethanol.

2. Weigh out 5.0 mg of cycloheximide powder preferably in a fume hood, protected from light.

3. Add 1 mL of ethanol and gently mix.

4. Aliquot cycloheximide/EtOH stock solution (17.77 mM) into thirty-three 30 $\mu$L single use aliquots (150 $\mu\mathrm{g}/\mathrm{mL}$ working concentration).

5. Store in -20°C freezer upright, numbered, and protected from light.

Imaging and Treating with Cycloheximide:

[13] See B.1

| Material | Volume (mL) | Vendor | Product No. |
|---|---|---|---|
| Cycloheximide Stock Solution | 30 $\mu$L | Sigma Aldrich | MKCS2639 |
| JF646 Stock Solution | 0.5 $\mu$L | Promega | N/A |
| Cell Culture Media [14] | 1.5 per dish | N/A | N/A |
| Imaging Media [15] | 3 per dish | N/A | N/A |
| 35 mm Delta T culture dish | N/A | Biotechs | N/A |

Preparation (day before imaging):

1. Delta culture dish(es) should be kept in a biosafety cabinet and sterilized for 5-30 min in UV before performing the experiment. Please take extreme care to be as clean and sterile as possible.

2. Before splitting cells, add 1 mL of cell media [16] to imaging dish(es) and incubate at 37°C.

3. While splitting cells, add 25 $\mu$L of resuspended cells to each Delta culture dish and incubate overnight at 37°C.

Protocol for Imaging (day of imaging):

1. Make sure stage heater is calibrated and laser(s) and microscope are aligned.

2. Prepare a 1:200 dilution with 1 $\mu$L of JF 646 stock solution (less is better if you need to mitigate auto-fluorescence ($\sim$0.2-0.5 $\mu$L)) and 199 $\mu$L of cell media, creating a 1 $\mu$M concentration of fluorophore.

3. Remove 200 $\mu$L of cell media from the culture dish (containing 1 mL of media from the previous day) and add the 200 $\mu$L of JF 646/cell media dilution (from step 2) to the culture dish. This creates a 1:1000 dilution, or a 5X working solution (0.2 $\mu$M) of JF 646. Incubate for 15 min.

[16] See B.1

4. Aspirate media from the dish and wash 2-3x with imaging media. Add 1 mL fresh cell media and incubate for 5 minutes.

5. Replace the media with a mixture of 970 $\mu$L imaging media and 30 $\mu$L of cycloheximide (17.8 mM stock). Working solution becomes 0.522 mM. For control experiments add 30 $\mu$L ethanol without cycloheximide.

6. Incubate for 10 minutes at 37°C before imaging.

## C.5 Protocol for Treating HeLa Cells with Filipin

Filipin III is a drug that disrupts the ER.

Preparing & Storing Filipin Stock Solution:

1. Add 0.2 mL of DMSO directly to 1 mg vial of Filipin III.

2. Aliquot 0.2 mL of 5 mg/mL filipin III/DMSO stock solution into ten 20 uL aliquots.

3. Store in freezer upright, numbered at -20° protected from light.

Imaging and Treating with Filipin:

| **Material** | **Volume (mL)** | **Vendor** | **Product No.** |
|---|---|---|---|
| Filipin Stock Solution | 3 $\mu$L | Sigma Aldrich | N/A |
| JF646 Stock Solution | 0.5 $\mu$L | Promega | N/A |
| Cell Culture Media [17] | 1.5 per dish | N/A | N/A |
| Imaging Media [18] | 3 per dish | N/A | N/A |
| 35 mm Delta T culture dish | N/A | Biotechs | N/A |

Preparation (day before imaging):

1. Delta culture dish(es) should be kept in a biosafety cabinet and sterilized for 5-30 min in UV before performing the experiment. Please take extreme care to be as clean and sterile as possible.

2. Before splitting cells, add 1 mL of cell media [19] to imaging dish(es) and incubate at 37°C.

3. While splitting cells, add 25 $\mu$L of resuspended cells to each Delta culture dish and incubate overnight at 37°C.

Protocol for Imaging (day of imaging):

1. Make sure stage heater is calibrated and laser(s) and microscope are aligned.

2. Prepare a 1:200 dilution with 1 $\mu$L of JF 646 stock solution (less is better if you need to mitigate auto-fluorescence ($\sim$0.2-0.5 $\mu$L)) and 199 $\mu$L of cell media, creating a 1 $\mu$M concentration of fluorophore.

3. Remove 200 $\mu$L of cell media from the culture dish (containing 1 mL of media from the previous day) and add the 200 $\mu$L of JF 646/cell media dilution (from step 2) to the culture dish. This creates a 1:1000 dilution, or a 5X working solution (0.2 $\mu$M) of JF 646. Incubate for 15 min.

4. Aspirate media from the dish and wash 2-3x with imaging media. Add 1 mL fresh cell media and incubate for 5 minutes.

5. Replace the media with a mixture of 997 $\mu$L imaging media and 3 $\mu$L of filipin. Working solution becomes 15 $\mu\mathrm{g}/\mathrm{mL}$. For control experiments add 3 $\mu$L DMSO without filipin.

6. Incubate for 30 minutes at room temperature before imaging.

[19] See B.1

## C.6 Protocol for Treating HeLa Cells with Nocodazole

Nocodazole is a drug that disrupts microtubules.

Preparing & Storing Nocodazole Stock Solution:

Resuspend nocodazole in DMSO creating a 2 mM stock solution. Aliquot and store upright at -20°C.

Imaging and Treating with Nocodazole:

| Material | Volume (mL) | Vendor | Product No. |
|---|---|---|---|
| Nocodazole Stock Solution | 3 $\mu$L | AdipGen | CAS No-31430-18-9 |
| JF646 Stock Solution | 0.5 $\mu$L | Promega | N/A |
| Cell Culture Media [20] | 1.5 per dish | N/A | N/A |
| Imaging Media [21] | 3 per dish | N/A | N/A |
| 35 mm Delta T culture dish | N/A | Biotechs | N/A |

Preparation (day before imaging):

1. Delta culture dish(es) should be kept in a biosafety cabinet and sterilized for 5-30 min in UV before performing the experiment. Please take extreme care to be as clean and sterile as possible.

2. Before splitting cells, add 1 mL of cell media [22] to imaging dish(es) and incubate at 37°C.

3. While splitting cells, add 25 $\mu$L of resuspended cells to each Delta culture dish and incubate overnight at 37°C.

Protocol for Imaging (day of imaging):

1. Make sure stage heater is calibrated and laser(s) and microscope are aligned.

[22] See B.1

2. Prepare a 1:200 dilution with 1 $\mu$L of JF 646 stock solution (less is better if you need to mitigate auto-fluorescence ($\sim$0.2-0.5 $\mu$L)) and 199 $\mu$L of cell media, creating a 1 $\mu$M concentration of fluorophore.

3. Remove 200 $\mu$L of cell media from the culture dish (containing 1 mL of media from the previous day) and add the 200 $\mu$L of JF 646/cell media dilution (from step 2) to the culture dish. This creates a 1:1000 dilution, or a 5X working solution (0.2 $\mu$M) of JF 646. Incubate for 15 min.

4. Aspirate media from the dish and wash 2-3x with imaging media. Add 1 mL fresh cell media and incubate for 5 minutes.

5. Replace the media with a mixture of 985 $\mu$L imaging media and 15 $\mu$L of nocodazole (2 mM stock). Working solution becomes 30 $\mu$M. For control experiments add 15 $\mu$L DMSO without nocodazole.

6. Incubate for 10 minutes on ice.

7. Incubate for 15 minutes at 37°C before imaging.

## C.7 Protocol for Treating HeLa Cells with Puromycin

Puromycin is a drug that releases mRNA from ribosomes.

Preparing & Storing Puromycin Stock Solution:

1. Weigh out 2.0 mg of puromycin powder preferably in a fume hood, protected from light.

2. Add 400 uL of DI water and gently mix (5 mg/mL solubility).

3. Aliquot puromycin/water stock solution (9.18 mM) into forty 10 uL single use aliquots.

4. Store in freezer upright, numbered at -20° protected from light.

Imaging and Treating with Filipin:

| Material | Volume (mL) | Vendor | Product No. |
|---|---|---|---|
| Puromycin Stock Solution | 3 $\mu$L | Sigma Aldrich | 0000186068 |
| JF646 Stock Solution | 0.5 $\mu$L | Promega | N/A |
| Cell Culture Media [23] | 1.5 per dish | N/A | N/A |
| Imaging Media [24] | 3 per dish | N/A | N/A |
| 35 mm Delta T culture dish | N/A | Biotechs | N/A |

Preparation (day before imaging):

1. Delta culture dish(es) should be kept in a biosafety cabinet and sterilized for 5-30 min in UV before performing the experiment. Please take extreme care to be as clean and sterile as possible.

2. Before splitting cells, add 1 mL of cell media [25] to imaging dish(es) and incubate at 37°C.

3. While splitting cells, add 25 $\mu$L of resuspended cells to each Delta culture dish and incubate overnight at 37°C.

Protocol for Imaging (day of imaging):

1. Make sure stage heater is calibrated and laser(s) and microscope are aligned.

2. Prepare a 1:200 dilution with 1 $\mu$L of JF 646 stock solution (less is better if you need to mitigate auto-fluorescence ($\sim$0.2-0.5 $\mu$L)) and 199 $\mu$L of cell media, creating a 1 $\mu$M concentration of fluorophore.

3. Remove 200 $\mu$L of cell media from the culture dish (containing 1 mL of media from the previous day) and add the 200 $\mu$L of JF 646/cell media dilution (from step 2) to the culture

[25] See B.1

dish. This creates a 1:1000 dilution, or a 5X working solution (0.2 $\mu$M) of JF 646. Incubate for 15 min.

4. Aspirate media from the dish and wash 2-3x with imaging media. Add 1 mL fresh cell media and incubate for 5 minutes.

5. Replace the media with a mixture of 900 $\mu$L imaging media and 10 $\mu$L of puromycin (9.18 mM stock). Working solution becomes 91.8 $\mu$M. For control experiments add 10 $\mu$L DI water without puromycin.

6. Incubate for 10 minutes at 37°C before imaging.

## C.8 Protocol for Bead Loading miRNA

Bead loading is a very easy, cost effective and fast method for loading the miRNA molecules into the adherent human cells (for example Hela cells). Glass beads used in this technique are spread on top of the cells which leads to disruption of the cells membrane. This allows for the miRNA molecules to enter the cells and helps in studying single molecule tracking. This procedure was developed and performed by Snehal Patil.

Materials:

Table 1. Reagents and corresponding concentrations for the Bead loading experiment

| Material | Volume (mL) | Vendor | Product No. |
|---|---|---|---|
| Cell Culture Media [26] | 1.5 per dish | N/A | N/A |
| Fluorophore Stock Solution | 0.5 $\mu$L | N/A | N/A |
| 35 mm Delta T culture dish | N/A | Biotechs | N/A |
| Imaging Media [27] | 3 per dish | N/A | N/A |
| miRNA | 1 | N/A | N/A |
| Polypropylene mesh | N/A | N/A | N/A |
| Bead loading apparatus | N/A | N/A | N/A |
| Sodium hydroxide (2M) | 25 | Fisher Scientific | N/A |
| Glass beads | 5 g | Sigma | N/A |
| Silica gel | 1 kg | ACROS organics | N/A |
| Petri dish (100 mm*20 mm) | N/A | Celltreat | N/A |
| 35 mm petri dish | N/A | Mat Tek Corporation | N/A |

B. Protocol

1. Cleaning of glass beads:

   (a) Take 50 ml of conical tube and add 25 ml of sodium hydroxide (2M NaOH) in the conical tube. Measure 5 g of glass beads and add in conical tube containing NaOH. Mix the glass beads and NaOH by using shaker or rotor for 2 hrs.

   (b) Remove the NaOH keeping the beads. If there are beads in the suspension then centrifuge for 1000g, 1min at room temperature.

   (c) Beads should be washed with autoclaved milliQ water until the pH is neutral. Remove the wash water every time after use.

   (d) Again wash the beads with 100

(e) Spread the washed beads on the sterile petri dish (10 cm) and keeping the petri dish open in the safety hood overnight to air dry the glass beads. After drying the beads should be dry and there should be no clumps present.

(f) UV-Sterilize the dried glass beads in safety hood for 15 mins.

2. Bead loader apparatus:

   (a) UV-Sterilize the apparatus for 15 mins. Add the beads to the apparatus and seal the apparatus.

   (b) Store the apparatus in the dry, sealed container which is desiccated with the dry silica gel. If the beads are wet or they are clumped then dry the beads again, sterilize the apparatus and replace the beads with the fresh beads.

3. Preparation of cells:

   (a) The Hela cells are cultured on the 35 mm glass-bottom chamber and should have 80

   (b) Incubate at 37°C for 15 mins in the CO2 culture incubator.

      i. Note: The cells should be attached to the surface otherwise they may peel off during experiment.

4. Bead loading of cells:

   (a) Note: If needed, wash the cells with phosphate buffer saline (PBS) and then add 2ml of medium. Incubate for 30 mins.

5. Prepare solution of 1 $\mu$L miRNA (0.2 $\mu$M stock) and 3$\mu$L of PBS for a working concentration of 50 nM.

6. Mix the solution thoroughly and the rest of the procedure is carried in the safety hood.

7. Remove the media from the cells and keep it aside in the tube.

(a) Note: Care should be taken not to touch the tip of pipette to the glass, this may result in the peeling off the cells from the substrate.

8. Add the bead loading solution in the center of the glass bottom chamber. Also add the layer of glass beds over the cells.

9. Hold the apparatus with two fingers and tap (generally for Hela cells the tapping should be done eight times).

10. Gently add the DMEM media and remove any of the floating beads present. Again, add the DMEM media and incubate for 2 hrs in the incubator.

11. Create 1:200 (final concentration 1 mM) dilution of aliquoted fluorophore HaloTag Ligand in 37°C DMEM. This will form 5X working stock solution.

12. Remove 200 µl DMEM from the culture dish and add 200 µl diluted HaloTag to the culture dish.

13. Incubate at 37°C for 15 mins in the CO2 culture incubator.

14. Aspirate media and again add 1 ml 37°C DMEM. Incubate for 5 min at 37°C in the CO2 incubator.

15. Replace the DMEM (1ml) media with the MEM (1ml) media.

16. Wash the cells three times with imaging media to remove any beads or loading components present in the solution.

17. Transfer to the microscope and capture images immediately.

## C.9 Protocol for Cleaning Delta T Imaging Dishes

This protocol explains the method used to clean already-used imaging dishes. This ensures that the dishes are both sterile for the cells and the glass is clean so as not to add any background

fluorescence while imaging. [28]

Materials:

| Material | Vendor | Product No. |
|---|---|---|
| $ddH_2O$ | N/A | N/A |
| Soft bristle tooth brush | N/A | N/A |
| 10% Bleach + 10% Alconox solution (made with $ddH_20$) | N/A | N/A |
| Isopropyl Alcohol | N/A | N/A |
| Compressed $N_2$ | N/A | N/A |

1. Use a 10% Bleach + 10% Alconox with $ddH_2O$ solution to clean dishes with a soft bristle tooth brush.
   (a) Be sure that there is no residue left in bottom 'rim' of dishes.
2. Rinse thoroughly with $ddH_2O$.
3. Wash last amount of $ddH_2O$ away with Isopropyl Alcohol and dry with compressed $N_2$.
   (a) Be sure not to leave any water spots on glass surface.
   (b) If there are oil smudges still present on glass bottom after drying with N2use a cotton swab and Isopropyl Alcohol to scrub the bottom of the dish. Then repeat step 3.
4. If dishes are being used immediately for transfecting/imaging place in biosafety cabinet and UV for 5 min.

[28] Adapted from [8]

# Appendix D

# Tracking with TrackMate [1]

NOTE: Record all parameters used (background subtract, Gaussian blur, diameter, threshold, linking/gap distances).

1. Loading data
    (a) If .moe-tiff file, Import > Bio-formats > select file > OK
    (b) Drag and drop file into ImageJ
    (c) View stack with Hyperstack
    (d) If working with max projection data (multiple planes):
        i. Select “virtual stack” > De-select “convert to RGB”
    (e) Image > Duplicate
        i. Select “duplicate stack”
    (f) If > 1 channel (color), Image > split channels
2. Background Subtract (only do this if you believe it helps)
    (a) Method 1 (best)
        i. Process > Subtract Background for rolling-ball-radius method
    (b) Method 2:
        i. Draw a square outside of cells
        ii. Analyze > Measure (or Ctrl+M)
        iii. Click off of square
        iv. Process > Math > Subtract measured value

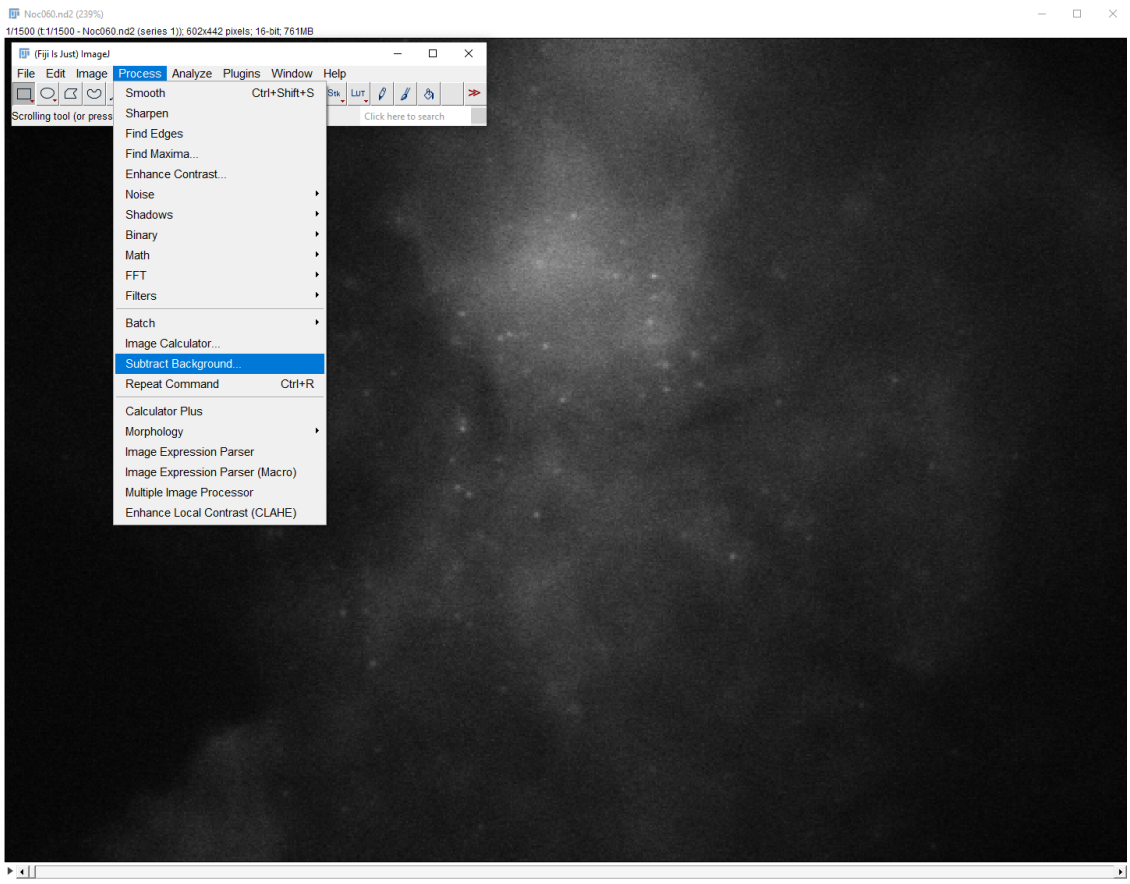


**Figure D.1:** Rolling ball background subtraction.

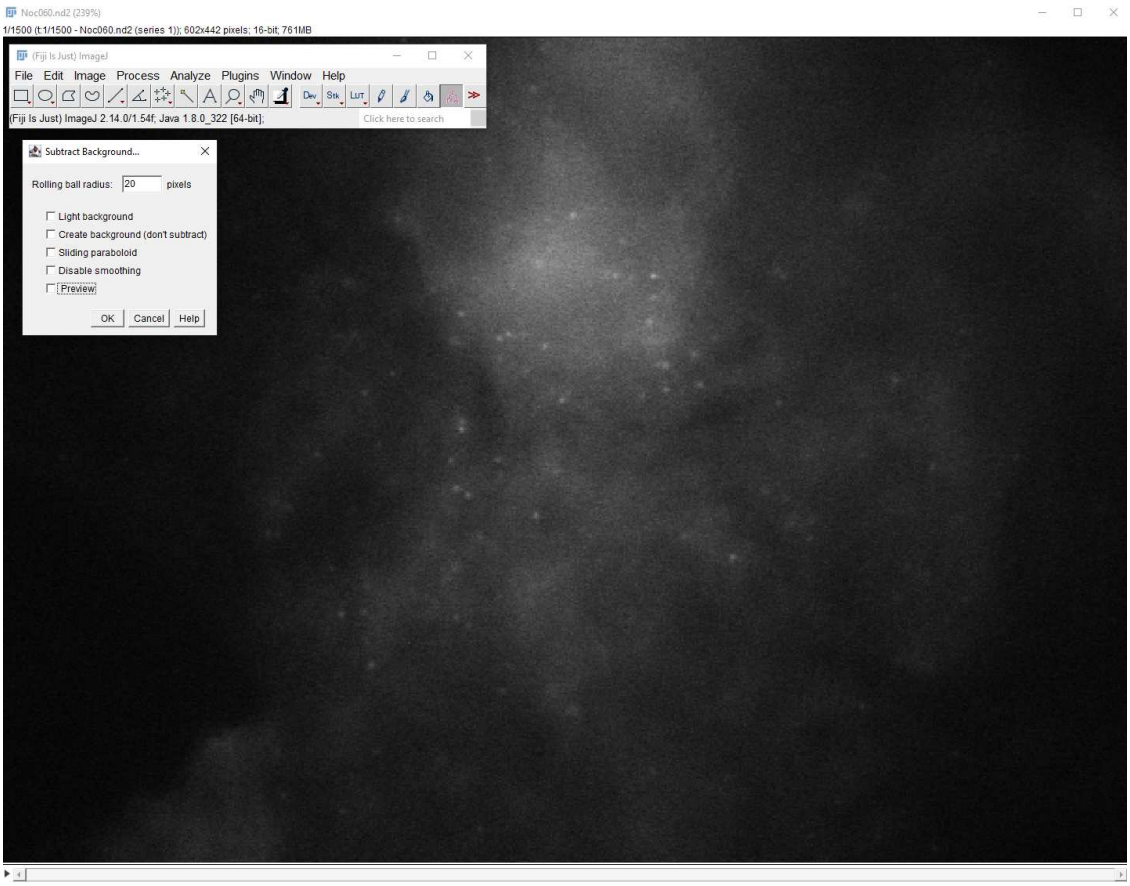


**Figure D.2:** Rolling ball background subtraction.

(c) Ctrl + Shift + C > adjust to your liking

3. Process > filter > Gaussian blur

   (a) Lowest value that achieves circular particles (zoom in to see better) – usually 1.2-1.5

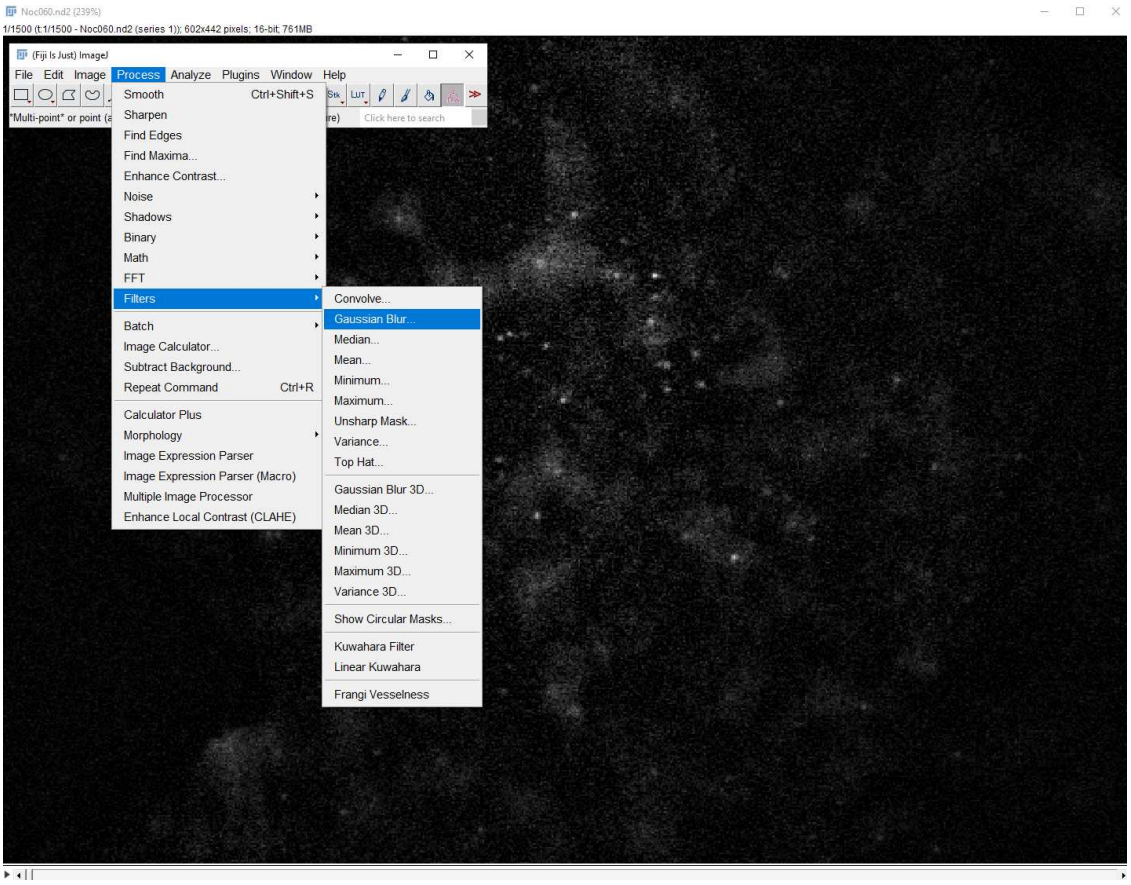


**Figure D.3:** Gaussian blur filter.

   (b) Ctrl + Shift + C > adjust to your liking

      i. Click 'Auto' → Adjust 'Maximum' all the way up → Change brightness and contrast accordingly (lowering contrast helps to show more particles)

4. If there are cells with high autofluorescence (i.e., there are cells that appear much better than others), simply draw around good cells, enclosing them. Click inside to limit tracking to this area.

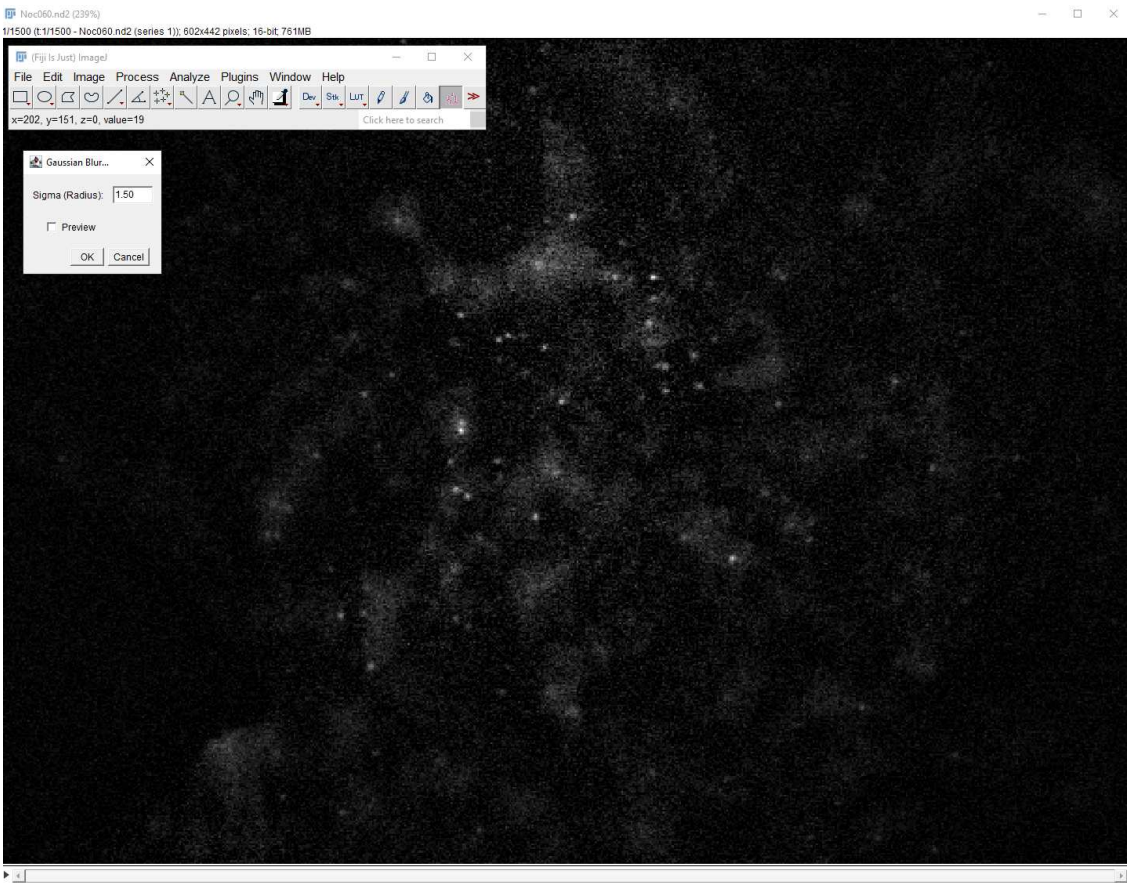


**Figure D.4:** Gaussian blur filter.

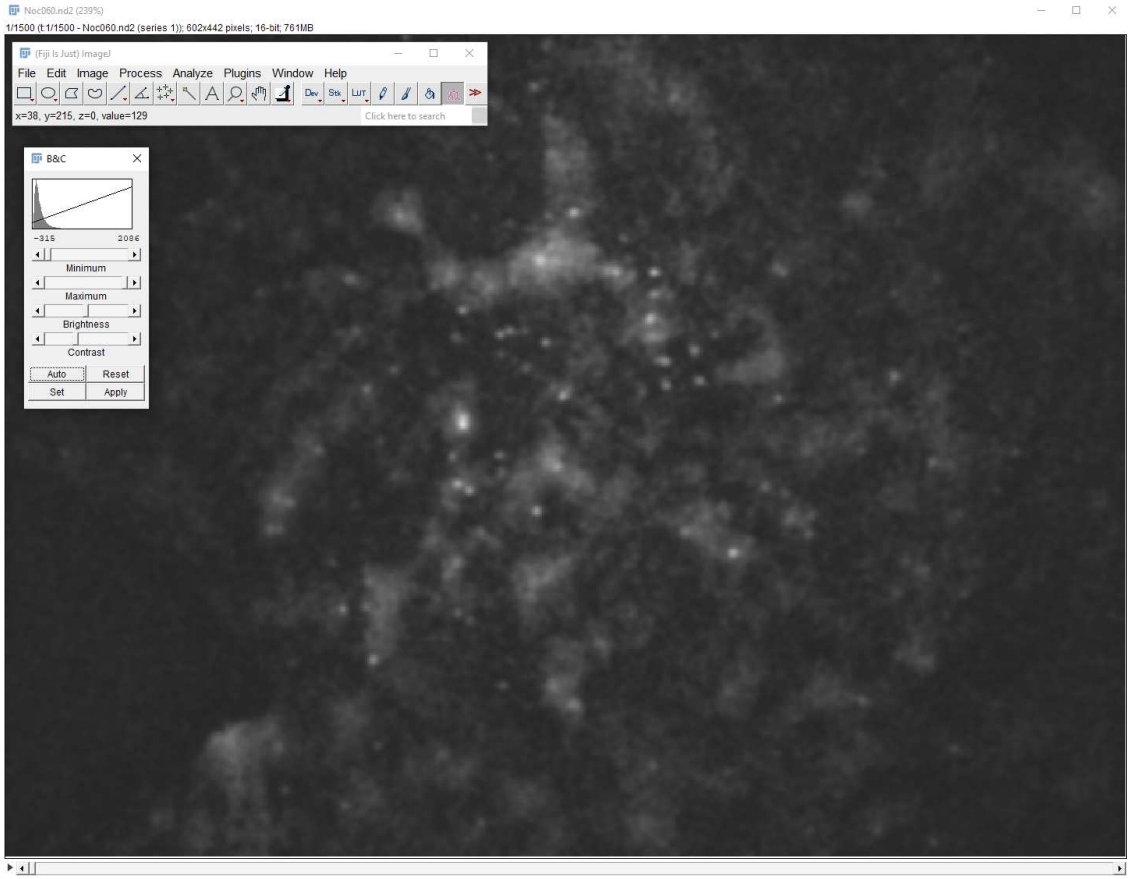


**Figure D.5:** Image contrast adjustment.

(a) DO NOT “clear” outside

5. Plugins > Tracking > TrackMate

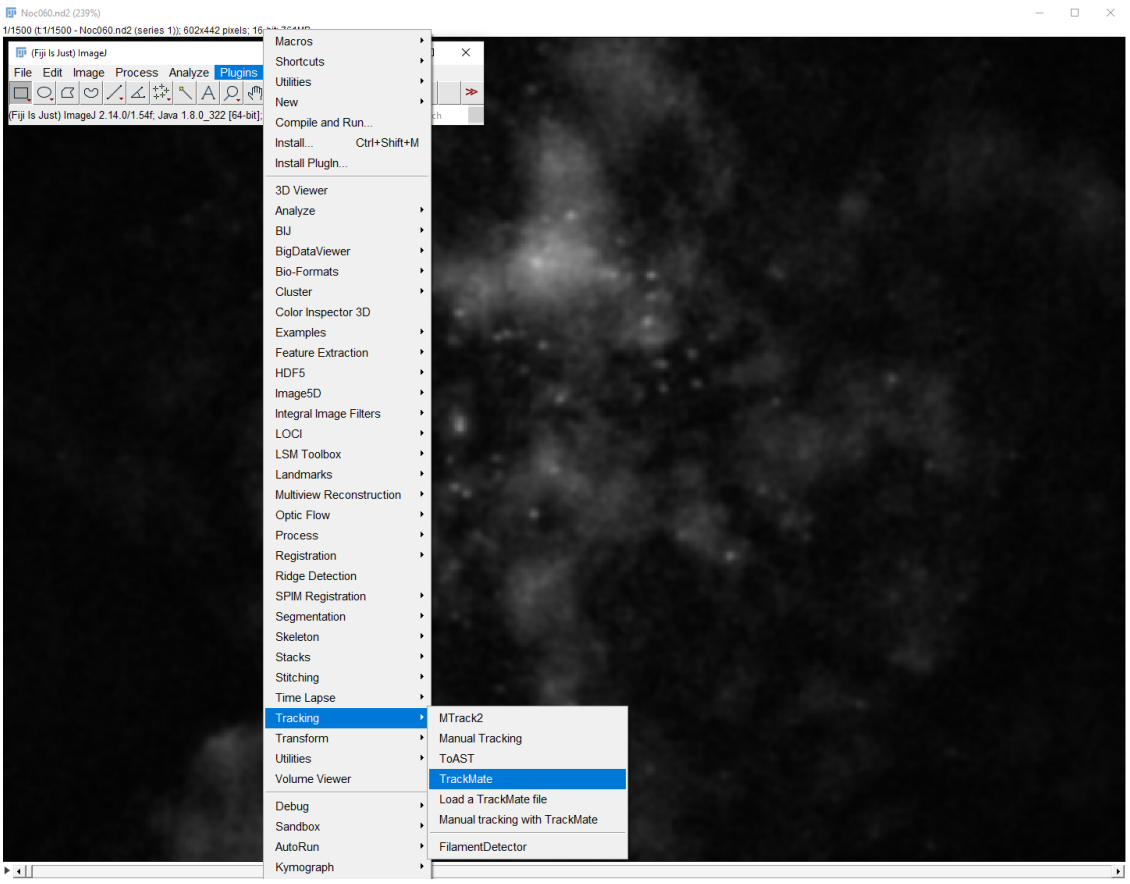


**Figure D.6:** TrackMate plugin selection.

(a) Click Yes to swap Z and T

6. Detector: LoG / use DoG if particle diameter is below 5 pixels

7. Set Diameter / Threshold

(a) (TIRF microscope) 1 pixel = 0.130 um (1 um = 7.7 pixels)

(b) Don’t detect anything that isn’t clear to you by eye

(c) Select “pre-process with median filter” and “sub-pixel localization”, preview until satisfied

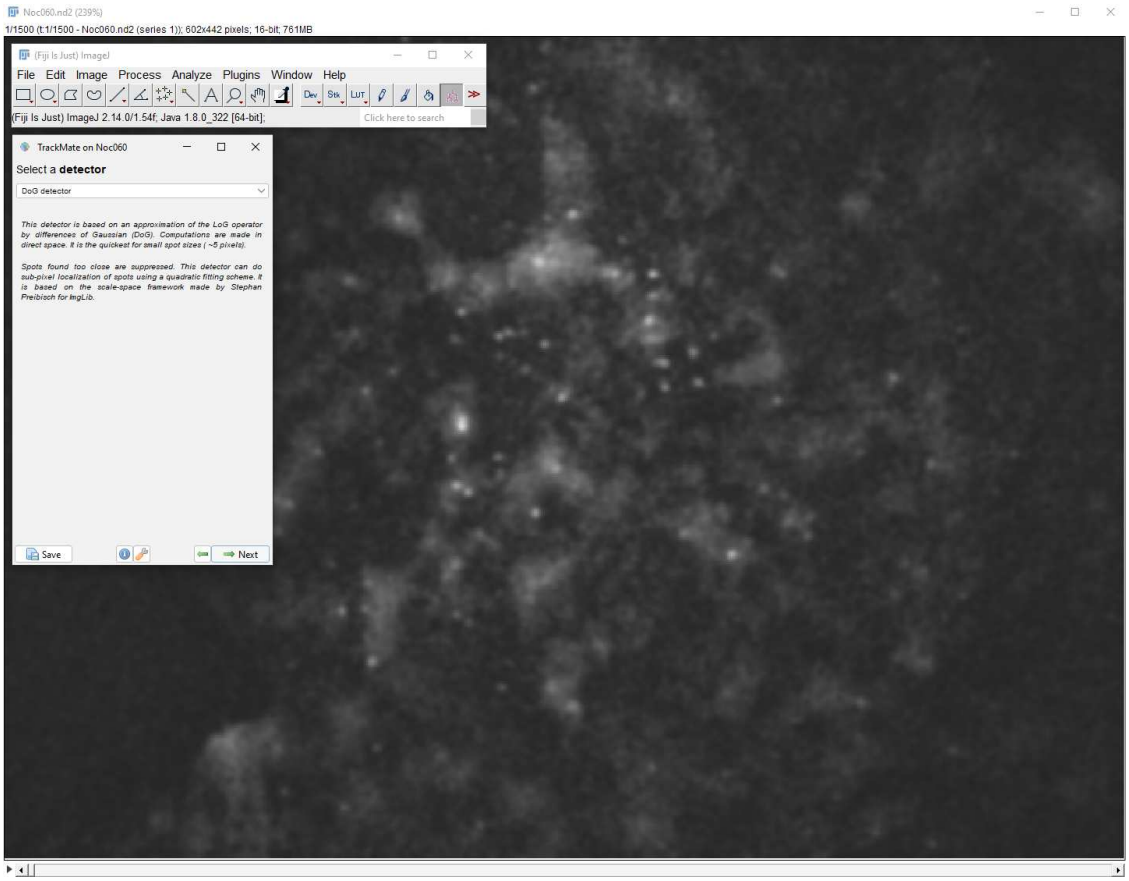


**Figure D.7:** Detector selection.

i. If you have segregated cells per step 4, there may be false positive particles along the edge of the area you've drawn. You can de-select "pre-process with median filter" to help with this. Usually the rest will get filtered out in step 10a.

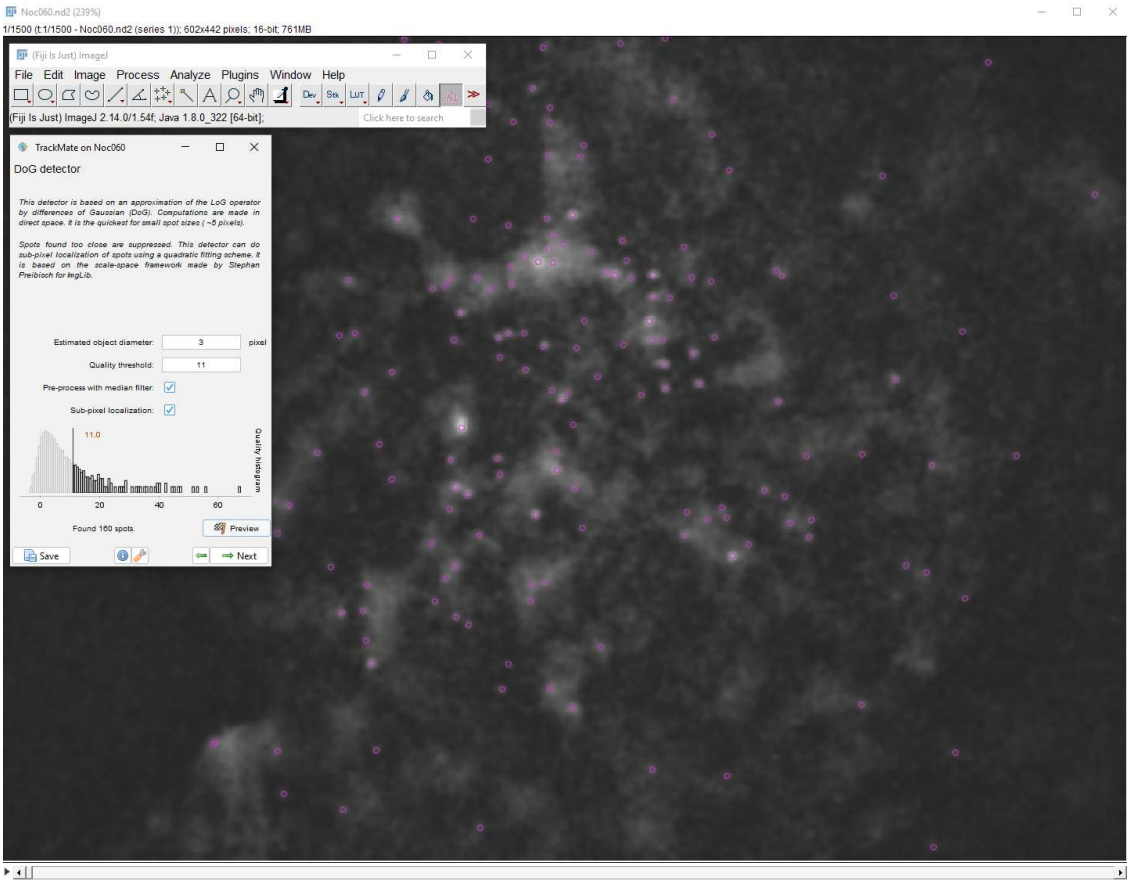


**Figure D.8:** Particle detection.

8. Initial Thresholding

   (a) Drag all the way to the left

9. Simple LAP tracker

10. Trajectory parameters

    (a) Linking max distance: $\sim$ 1um / $\sim$ 4 pixels

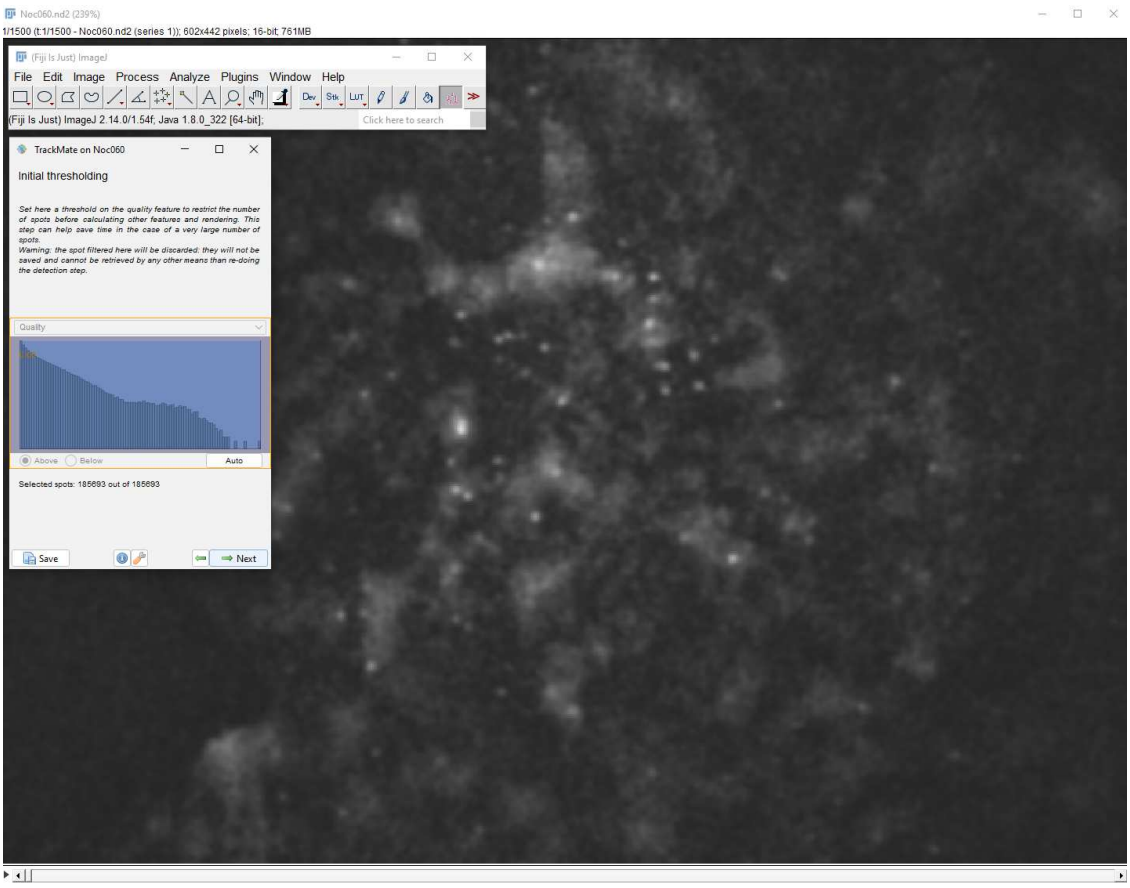


**Figure D.9:** Initial thresholding.

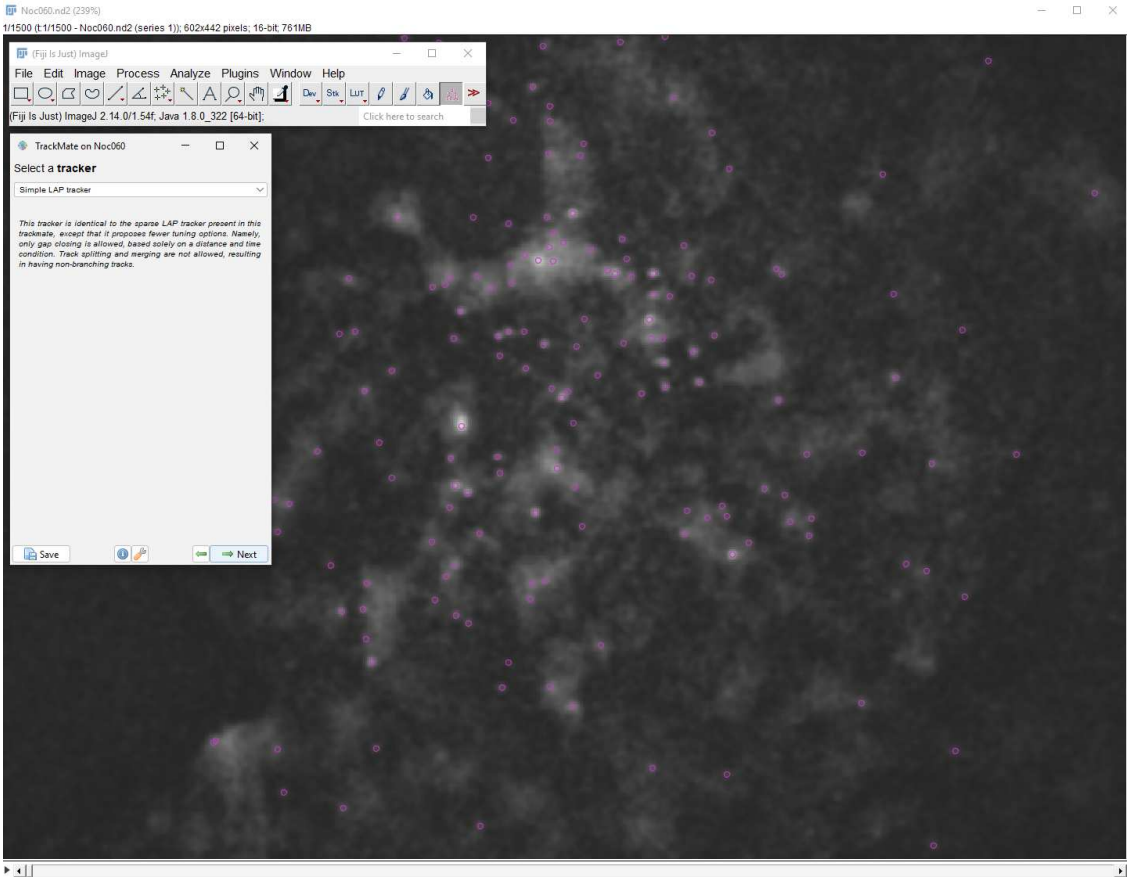


**Figure D.10:** Simple LAP tracker selection.

(b) Gap-closing max distance: $\sim$ 1um / $\sim$ 3 pixels

(c) Gap closing max frame: 0-3 (2 is good)

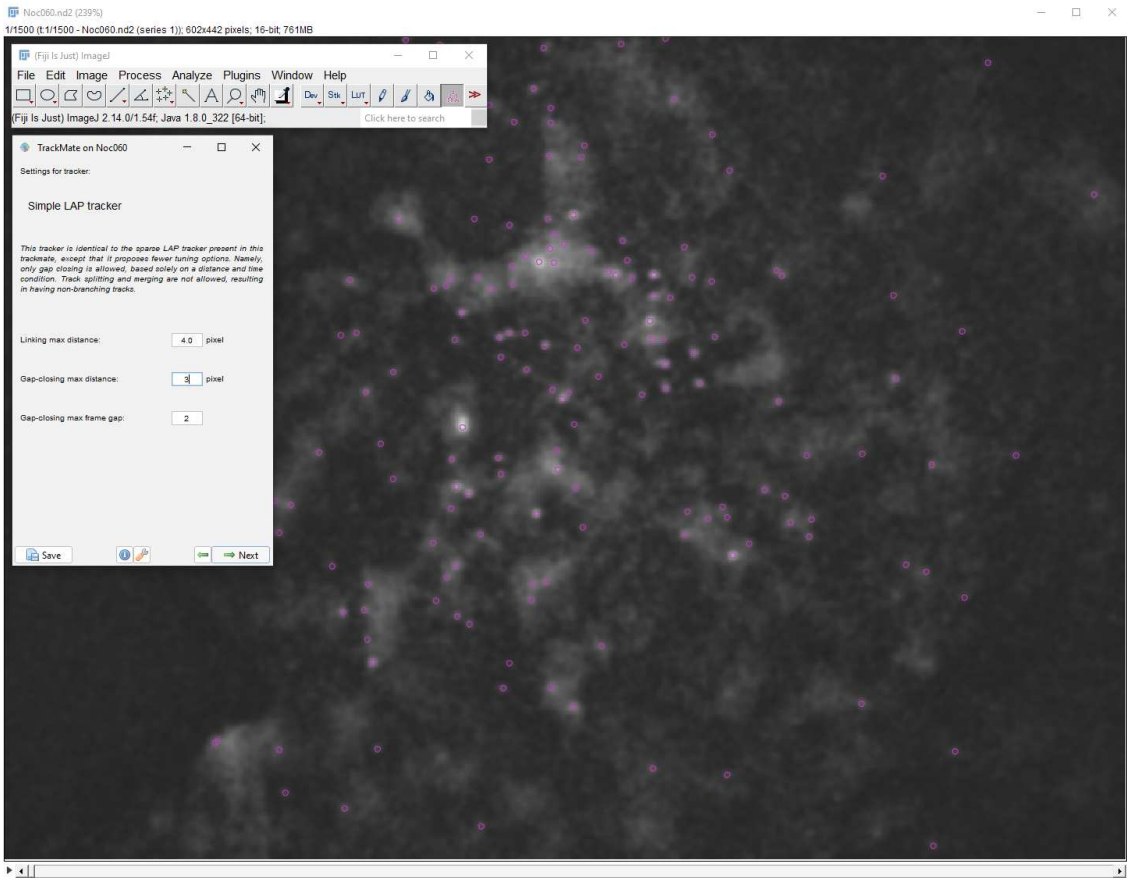


**Figure D.11:** Parameter selections.

11. Next, set filters on tracks

    (a) Set “Number of spots on tracks” > 5-15 to filter out very short trajectories

    (b) Check trajectories by eye. If they look wrong, go back and change parameters. Do this until trajectories look good to you.

12. Analysis > save track statistics

13. To obtain table of intensities:

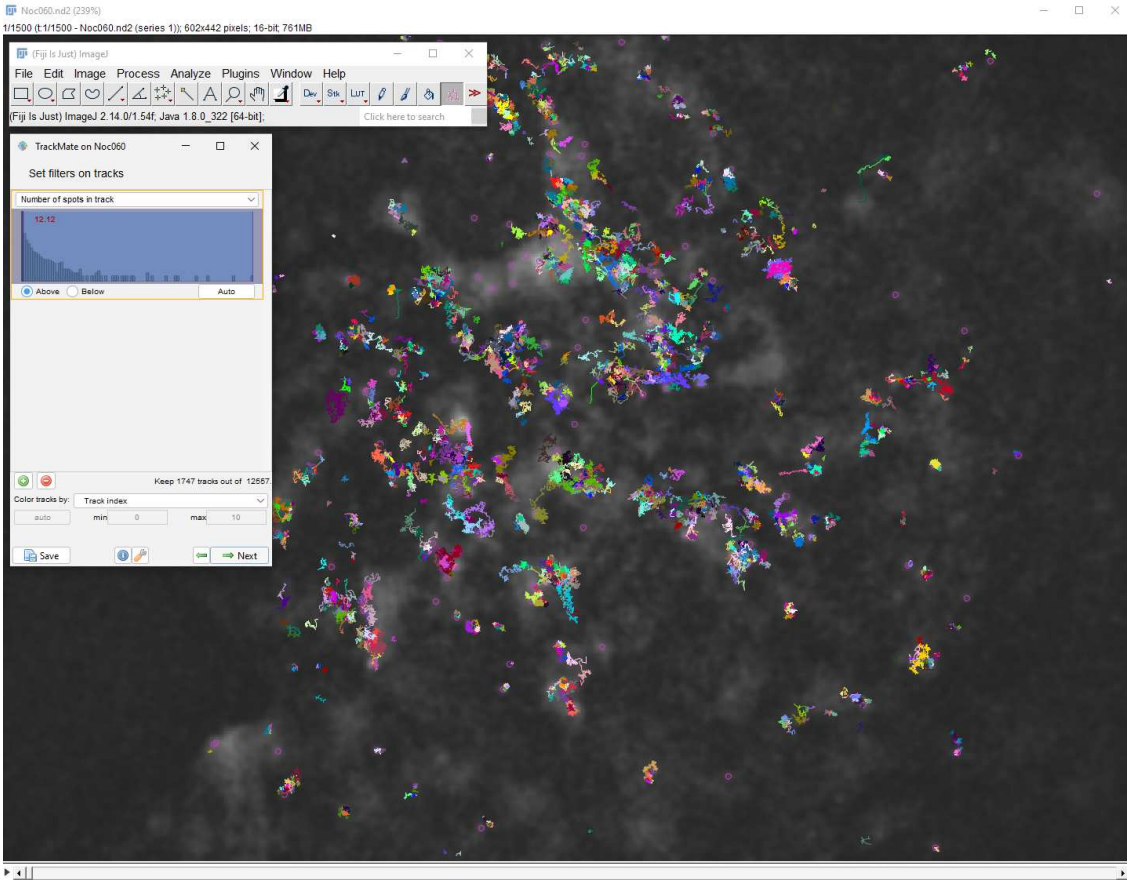


**Figure D.12:** Filtering for spots on track.

(a) Display Options > color spots by sum intensity ch1

(b) Select "Tracks" to open Spots table

(c) Export to CSV

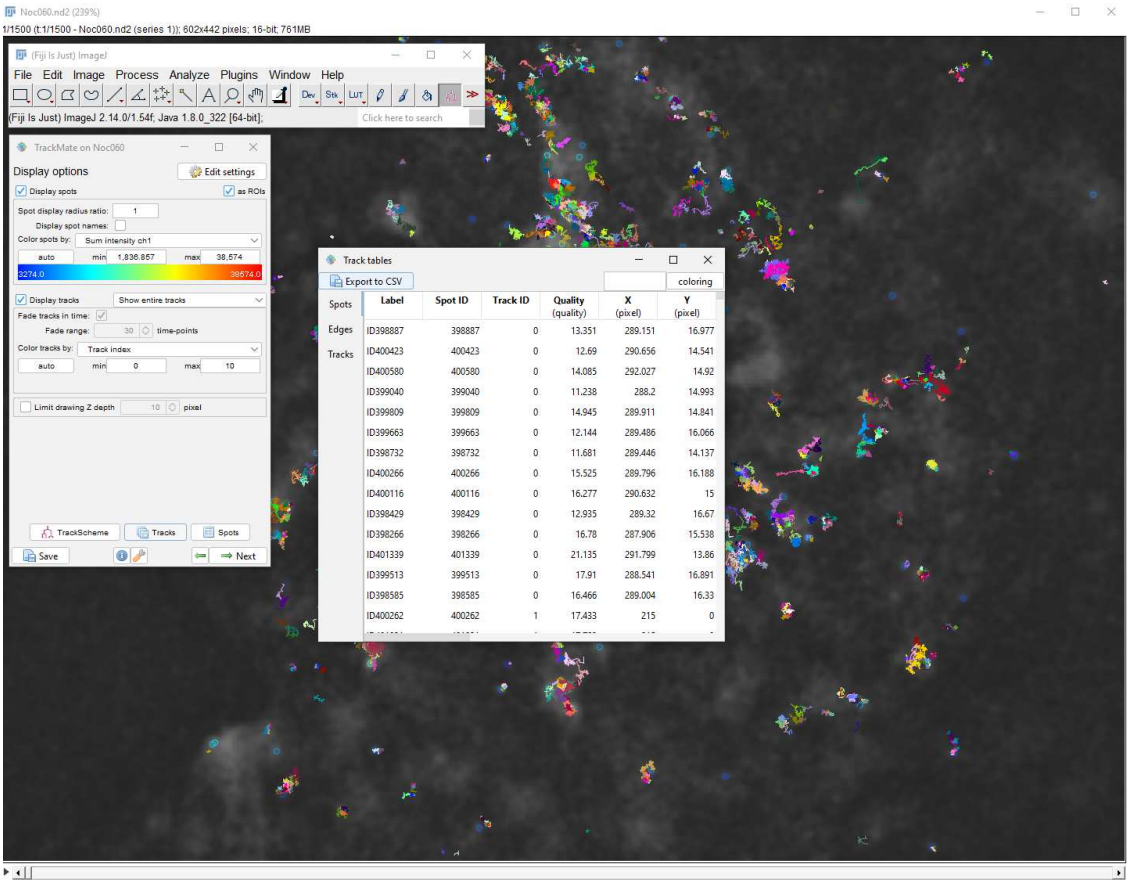


**Figure D.13:** Obtaining a CSV table of sum intensities per spot.

14. Export tracks to XML file

(a) Set Feature for X axis = T

(b) Set Feature for Y axis = X

(c) Add second feature for Y axis = Y

(d) Select an action > Export tracks to XML file

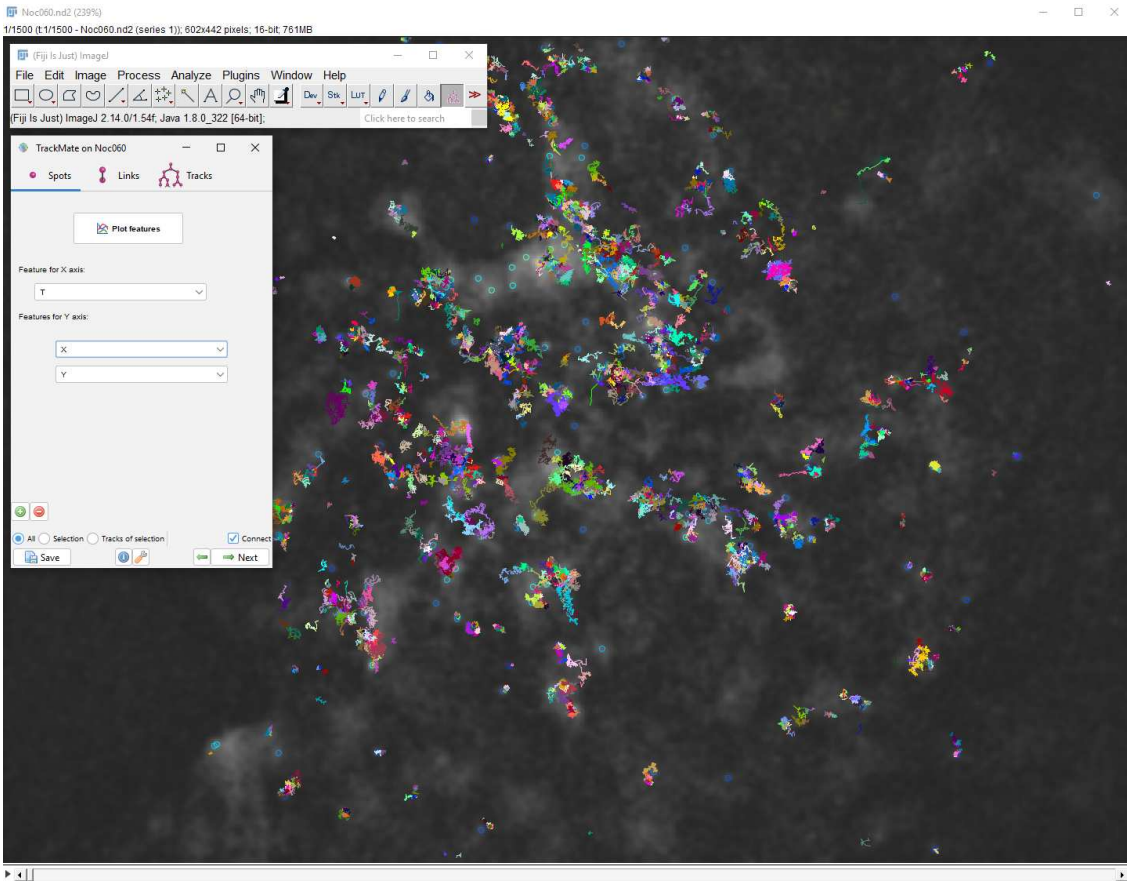


**Figure D.14:** Setting features for resulting XML file.

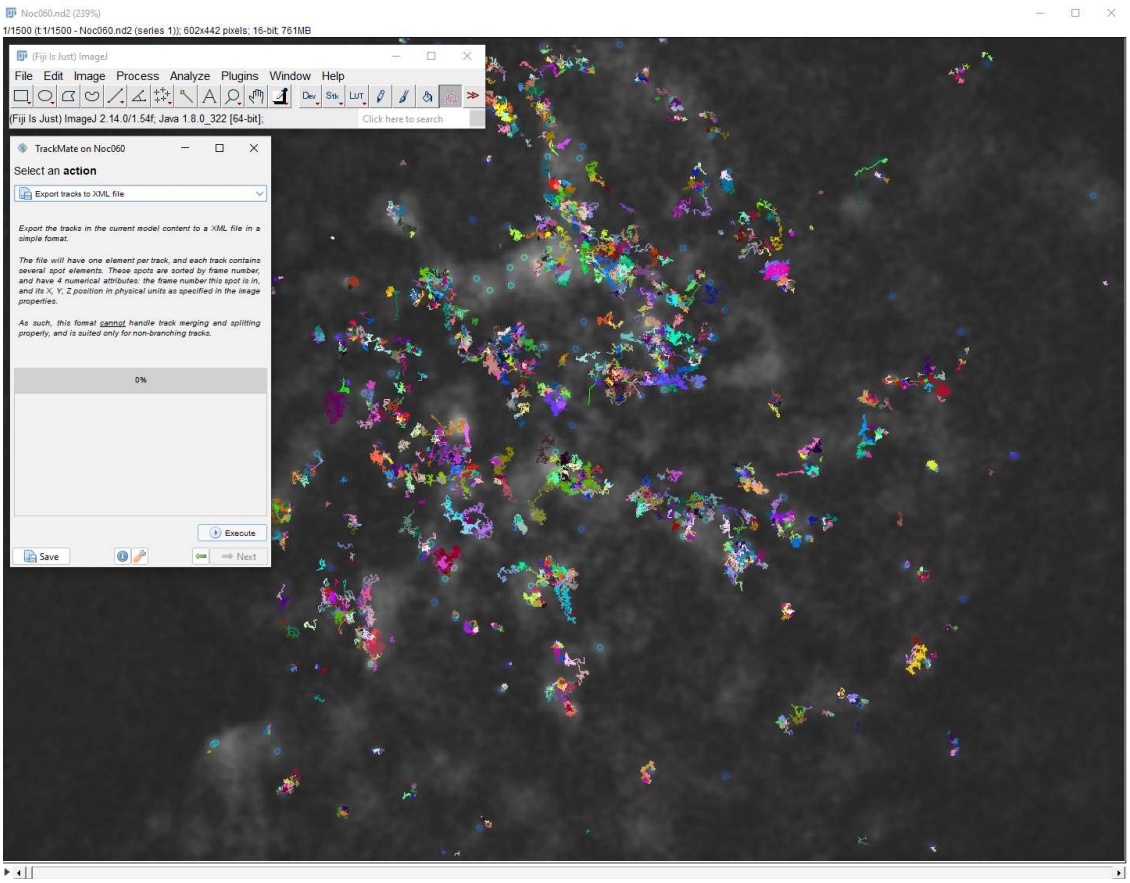


**Figure D.15:** Exporting trajectories as an XML file.

# Appendix E

# Codes for File Processing & Analysis in MATLAB

## E.1 Converting XML to TXT

'TrackMateOutputConversionV3TrueTime.m'

```
%%
clear all
close all
%clc
filename='C:\Users\ryanr\OneDrive\Desktop\Krapf Research\RNA data analysis\Trajectories\05-16-23 (cyclo)\Dish 6 - our_incubator\Sample6010_+29min_Tracks.xml'; %file to read
savefile='C:\Users\ryanr\OneDrive\Desktop\Krapf Research\RNA data analysis\Trajectories\05-16-23 (cyclo)\Dish 6 - our_incubator\Sample6010_+29min_Tracks.txt'; %filename to write to
pixelsize=0.130; %pixel size in micrometers (if in pixels, use 1)
Max=1500; %maximum track length in frames used in the movie length

%% Import tracks, output of trackMate plugin and display them
[tracks, metadata] = importTrackMateTracks(filename);
%%
[M,N]=size(tracks);
B(1:Max,1:2*M)=NaN;
format = '';
title = '';
fid = fopen(savefile, 'w');
traj_counter = 0;
for i=1:M
    A=tracks{i,1};
    [Q,P]=size(A);
    B(1:Q,2*i-1)=A(:,2) * pixelsize;  % x coordinate
    B(1:Q,2*i)=A(:,3) * pixelsize;  % y coordinate
    format = [format,'%12.4f\t%12.4f\t'];
    title = [title, '      ' 'X' num2str(traj_counter) '      ' '\t' '      ' 'Y' num2str(traj_counter) '      ' '\t'];
    traj_counter = traj_counter + 1;
end

%% Write
fprintf(fid, [title,'\r\n']);
fprintf(fid,[format,'\r\n'] ,B');
fclose(fid);
```

**Figure E.1:** MATLAB script for converting raw XML files from Fiji export to TXT files of XY trajectories. This is the first step necessary for any and all analyses that we do.

## E.2 Concatenating TXT Files: 'ConcatenateTrajFiles.m'

## E.3 Segmenting Trajectories Using Convex Hull

'segmentAllTrajectoriesConvHullV2.m'

## E.4 Removal of First Confined Segment

'RemoveFirstImmobilePartV2.m'

```
% Filter trajectories of minimum length and concatenate all files into
% a single one for future ensemble analysis.
%
directory='C:\Users\ryanr\OneDrive\Desktop\Krapf Research\Tracking\Concatenated\4 planes\New';
pattern='Filtered_min64_T0_Capture_??.txt'; %Common pattern to all files to combine
minlength=64; %minimum trajectory length
savefilename='Conc_Filtered_T0_4planes-'; % do not add directory or .txt extension. Minlength is added automatically also.
%%
% Do not change anything after this line

tracks_headers=1;
%%
filenames=GetFileNames(directory,pattern);
directory=strcat(directory,'\');
L=[];
alldata=[];

for i=1:size(filenames,2)
    [~,file_name,ext] = fileparts(char(filenames(i)));
    %file_name=strcat(file_name,ext);

    disp(file_name)
    %save_file_name=strcat('length260',file_name,'_nm',ext);
    file_name=strcat(directory,file_name,ext);

    A0 = importdata(file_name, '\t', tracks_headers);
    header=A0.textdata;
    A0 = A0.data;
    p1=size(A0,1);

    if p1>=minlength
        % Filter trajectories according to length
        lengths=lengthsTrajFunction(A0); %lengths of all trajectories
        len=NaN(1,length(lengths)*2);
        len(1:2:length(len)-1)=lengths; %X
        len(2:2:length(len))=lengths;   %Y
        A0(:,len<minlength)=[];
        header(len<minlength)=[];
        A0=A0(1:minlength,:);
        p2=size(A0,2);
        %
        alldata=[alldata A0]; %data
        L=[L;p2]; %lengths
    end
end

dlmwrite(strcat(directory,savefilename,string(minlength),'.txt'),alldata,'delimiter','\t','precision','%.3f');
```

**Figure E.2:** MATLAB script for concatenating similar TXT files into one large TXT file. This is used for combining all trajectories with the same lag time/frame rate and minimum length to get statistics on grouped trajectories that have the same properties.

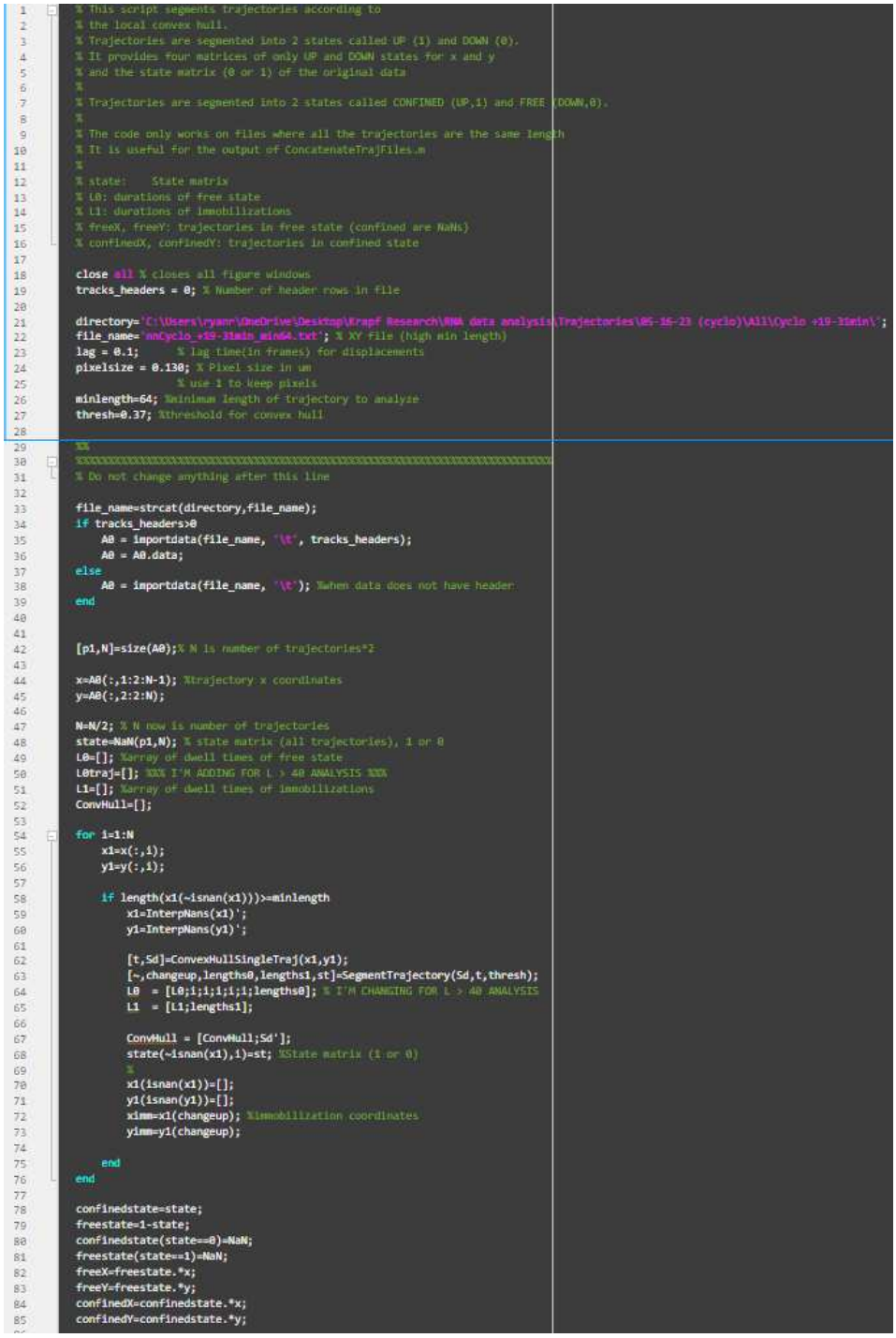

```
% This script segments trajectories according to
% the local convex hull.
% Trajectories are segmented into 2 states called UP (1) and DOWN (0).
% It provides four matrices of only UP and DOWN states for x and y
% and the state matrix (0 or 1) of the orlginal data
%
% Trajectories are segmented into 2 states called CONFINED (UP,1) and FREE (DOWN,0).
%
% The code only works on files where all the trajectories are the same length
% It is useful for the output of ConcatenateTrajFiles.m
%
% state:    State matrix
% L0: durations of free state
% L1: durations of immobilizations
% freeX, freeY: trajectories in free state (confined are NaNs)
% confinedX, confinedY: trajectories in confined state

close all % closes all figure windows
tracks_headers = 0; % Number of header rows in file

directory='C:\Users\ryann\OneDrive\Desktop\Krapf Research\RNA data analysis\Trajectories\05-16-23 (cyclo)\All\Cyclo +19-31min\';
file_name='AnCyclo_+19-31min_min64.txt'; % XY file (high min length)
lag = 0.1;      % lag time(in frames) for displacements
pixelsize = 0.130; % Pixel size in um
                % use 1 to keep pixels
minlength=64; %minimum length of trajectory to analyze
thresh=0.37; %threshold for convex hull

%%
%%%%%%%%%%%%%%%%%%%%%%%%%%%%%%%%%%%%%%%%%%%%%%%%%%%%%%%%%%%%%%%%%%%%%%%%%%%%%%%
% Do not change anything after this line

file_name=strcat(directory,file_name);
if tracks_headers>0
    A0 = importdata(file_name, '\t', tracks_headers);
    A0 = A0.data;
else
    A0 = importdata(file_name, '\t'); %when data does not have header
end


[p1,N]=size(A0);% N is number of trajectories*2

x=A0(:,1:2:N-1); %trajectory x coordinates
y=A0(:,2:2:N);

N=N/2; % N now is number of trajectories
state=NaN(p1,N); % state matrix (all trajectories), 1 or 0
L0=[]; %array of dwell times of free state
L0traj=[]; %%% I'M ADDING FOR L > 40 ANALYSIS %%%
L1=[]; %array of dwell times of immobilizations
ConvHull=[];

for i=1:N
    x1=x(:,i);
    y1=y(:,i);

    if length(x1(~isnan(x1)))>=minlength
        x1=InterpNans(x1)';
        y1=InterpNans(y1)';

        [t,Sd]=ConvexHullSingleTraj(x1,y1);
        [~,changeup,lengths0,lengths1,st]=SegmentTrajectory(Sd,t,thresh);
        L0  = [L0;i;i;i;i;i;i;lengths0]; % I'M CHANGING FOR L > 40 ANALYSIS
        L1  = [L1;lengths1];

        ConvHull = [ConvHull;Sd'];
        state(~isnan(x1),i)=st; %State matrix (1 or 0)
        %
        x1(isnan(x1))=[];
        y1(isnan(y1))=[];
        ximm=x1(changeup); %immobilization coordinates
        yimm=y1(changeup);

    end
end

confinedstate=state;
freestate=1-state;
confinedstate(state==0)=NaN;
freestate(state==1)=NaN;
freeX=freestate.*x;
freeY=freestate.*y;
confinedX=confinedstate.*x;
confinedY=confinedstate.*y;
```

**Figure E.3:** MATLAB script for using convex hull to segment trajectories into mobility states. This is done for the purpose of analyzing mobility states separately (e.g. waiting times or MSD), given that more than one mode of motion is found.

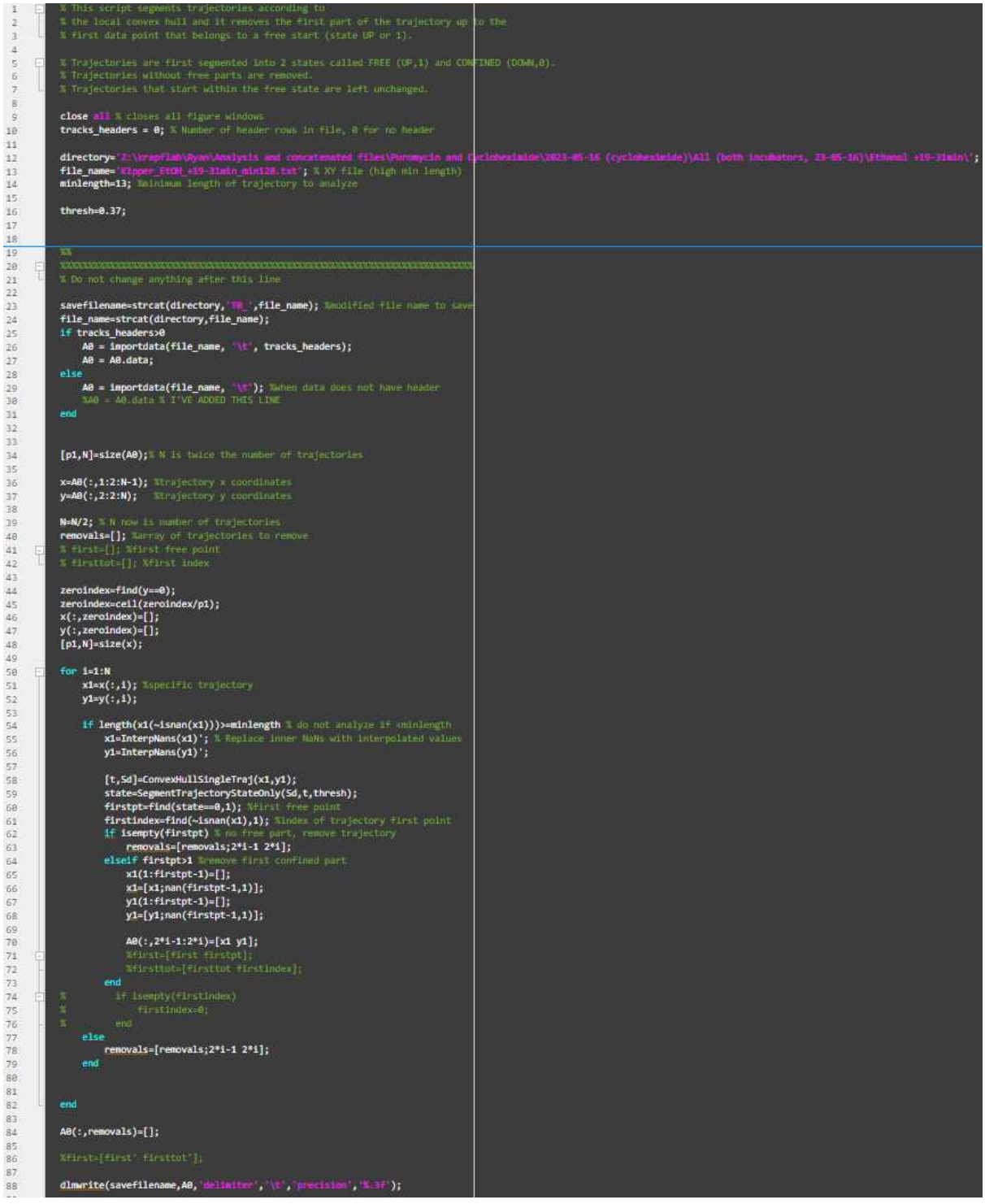

```
% This script segments trajectories according to
% the local convex hull and it removes the first part of the trajectory up to the
% first data point that belongs to a free start (state UP or 1).

% Trajectories are first segmented into 2 states called FREE (UP,1) and CONFINED (DOWN,0).
% Trajectories without free parts are removed.
% Trajectories that start within the free state are left unchanged.

close all % closes all figure windows
tracks_headers = 0; % Number of header rows in file, 0 for no header

directory='Z:\krapflab\Ryan\Analysis and concatenated files\Puromycin and Cyclohexiamide\2023-05-16 (cyclohexiamide)\All (both incubators, 23-05-16)\Ethanol +19-31min\';
file_name='Klipper_EtOH_+19-31min_min128.txt'; % XY file (high min length)
minlength=13; %minimum length of trajectory to analyze

thresh=0.37;


%%
%%%%%%%%%%%%%%%%%%%%%%%%%%%%%%%%%%%%%%%%%%%%%%%%%%%%%%%%%%%%%%%%%%%%%%%%%%%%%%%
% Do not change anything after this line

savefilename=strcat(directory,'TR_',file_name); %modified file name to save
file_name=strcat(directory,file_name);
if tracks_headers>0
    A0 = importdata(file_name, '\t', tracks_headers);
    A0 = A0.data;
else
    A0 = importdata(file_name, '\t'); %when data does not have header
    %A0 = A0.data % I'VE ADDED THIS LINE
end


[p1,N]=size(A0);% N is twice the number of trajectories

x=A0(:,1:2:N-1); %trajectory x coordinates
y=A0(:,2:2:N);   %trajectory y coordinates

N=N/2; % N now is number of trajectories
removals=[]; %array of trajectories to remove
% first=[]; %first free point
% firsttot=[]; %first index

zeroindex=find(y==0);
zeroindex=ceil(zeroindex/p1);
x(:,zeroindex)=[];
y(:,zeroindex)=[];
[p1,N]=size(x);

for i=1:N
    x1=x(:,i); %specific trajectory
    y1=y(:,i);

    if length(x1(~isnan(x1)))>=minlength % do not analyze if <minlength
        x1=InterpNans(x1)'; % Replace inner NaNs with interpolated values
        y1=InterpNans(y1)';

        [t,Sd]=ConvexHullSingleTraj(x1,y1);
        state=SegmentTrajectoryStateOnly(Sd,t,thresh);
        firstpt=find(state==0,1); %first free point
        firstindex=find(~isnan(x1),1); %index of trajectory first point
        if isempty(firstpt) % no free part, remove trajectory
            removals=[removals;2*i-1 2*i];
        elseif firstpt>1 %remove first confined part
            x1(1:firstpt-1)=[];
            x1=[x1;nan(firstpt-1,1)];
            y1(1:firstpt-1)=[];
            y1=[y1;nan(firstpt-1,1)];

            A0(:,2*i-1:2*i)=[x1 y1];
            %first=[first firstpt];
            %firsttot=[firsttot firstindex];
        end
%         if isempty(firstindex)
%             firstindex=0;
%         end
    else
        removals=[removals;2*i-1 2*i];
    end


end

A0(:,removals)=[];

%first=[first' firsttot'];

dlmwrite(savefilename,A0,'delimiter','\t','precision','%.3f');
```

**Figure E.4:** MATLAB script for removing the first confined segment of each trajectory. This is done under the assumption that the free state waiting times are exponentially distributed (i.e., a Markov process), and makes it so all trajectories begin in the free state where there is no memory.

```
% Plots any specific trajectory from an XY file
%
trajectory_file='C:\Users\ryanr\OneDrive\Desktop\Krapf Research\RNA data analysis\Filtered_min64_T001_Tracks.txt';
trajectorynumber=13; % number of the trajectory to plot
%%
trajectories = importdata(trajectory_file, '\t', 1);
trajectories=trajectories.data;
x=trajectories(:,trajectorynumber*2-1);
y=trajectories(:,trajectorynumber*2);
figure(1)
%plot(x/0.193,y/0.193) %%% divided by 0.193 to get original pixels in imageJ %%%
plot(x,y, 'LineWidth',1.5);
xlabel('X (\mum)');
ylabel('Y (\mum)');
%set(gca, 'YDir','reverse') % I'VE ADDED THIS LINE
%hold on
% ------------------------------
% I'VE ADDED PER STEP 3c
% plot(t,Sd)
% xlabel('Time');
% ylabel('Convex Hull');
% ------------------------------
%
%xx=trajectories(:,1:2:length(trajectories)-1);
%yy=trajectories(:,2:2:length(trajectories));
%plot(xx,yy)
daspect([1 1 1])

%figure(2)
%plot(x)
%hold on
%plot(y)
```

**Figure E.5:** MATLAB script for plotting/viewing individual trajectories. This is a simple code that is useful for cross−checking and verifying the 'RemoveFirstImmobilePartV2.m' script, as well as graphics for presentations.

## E.5 Plotting single trajectories

'plottrajectory.m'

## E.6 Calculating Displacements

'Displacements.m'

## E.7 Calculating MSDs

'TAMSDacrossXYV2.m'

## E.8 Calculating Aging MSDs

'TAMSDacrossXYAgingV2.m'

```
% Computes Displacements at given lag time for all trajectories
% it also computes displacements normalized to each trajectory standard
% deviation.
%
% Export data from origin and label variables
% XX and YY absolute displacements
% xx and yy normalized displacements

directory='Z:\krapflab\Ryan\Analysis and concatenated files\All concatenated trajectories (221109 - 230303)\Nocodazole (10 uM)\';
file_name='T0_ConcNoc_All128.txt';
tracks_headers = 0; % Number of header rows in file

dt=1; % Delta frames for Displacements

%%
%%%%%%%%%%%%%%%%%%%%%%%%%%%%%%%%%%%%%%%%%%%%%%%%%%%%%%%%%%%%%%%%%%%%%%%%%%%%%%%
% Do not change anything after this line

%% Read data
%
file_name=strcat(directory,file_name);
if tracks_headers>0
    A0 = importdata(file_name, '\t', tracks_headers);
    A0 = A0.data;
else
    A0 = importdata(file_name, '\t'); %when data does not have header
end

[n0,m]=size(A0); % frames, columns
%
%% Compute displacements

AA = A0((dt+1):n0,:)-A0(1:(n0-dt),:);  %obtain displacements
sigmas=std(AA,"omitnan"); % st. dev. of displacements for each column
aa=AA./sigmas; %normalize displacements to each st. dev.

XX=AA(:,2:2:m); %select X coordinate - displacements
YY=AA(:,1:2:m-1); %select X coordinate - displacements

xx=aa(:,2:2:m); %select X coordinate - norm displacements
yy=aa(:,1:2:m-1); %select X coordinate - norm displacements

% Eliminate NaNs
XX(isnan(XX))=[];
YY(isnan(YY))=[];
xx(isnan(xx))=[];
yy(isnan(yy))=[];

% Convert to single column
XX=XX(:);
YY=YY(:);
xx=xx(:);
yy=yy(:);


%% plot histograms of X
figure
histogram(XX)
title('Absolute x displacements')
figure
histogram(xx)
title('Normalized x displacements')

%% Data for Origin
label=["DX "+dt "DY "+dt "normDX "+dt "normDY "+dt];
origin= [XX YY xx yy];
```

**Figure E.6:** MATLAB script for calculating absolute and normalized displacements. This is one analysis we do, which can elucidate the degree of heterogeneity across different trajectories and within individual trajectories.

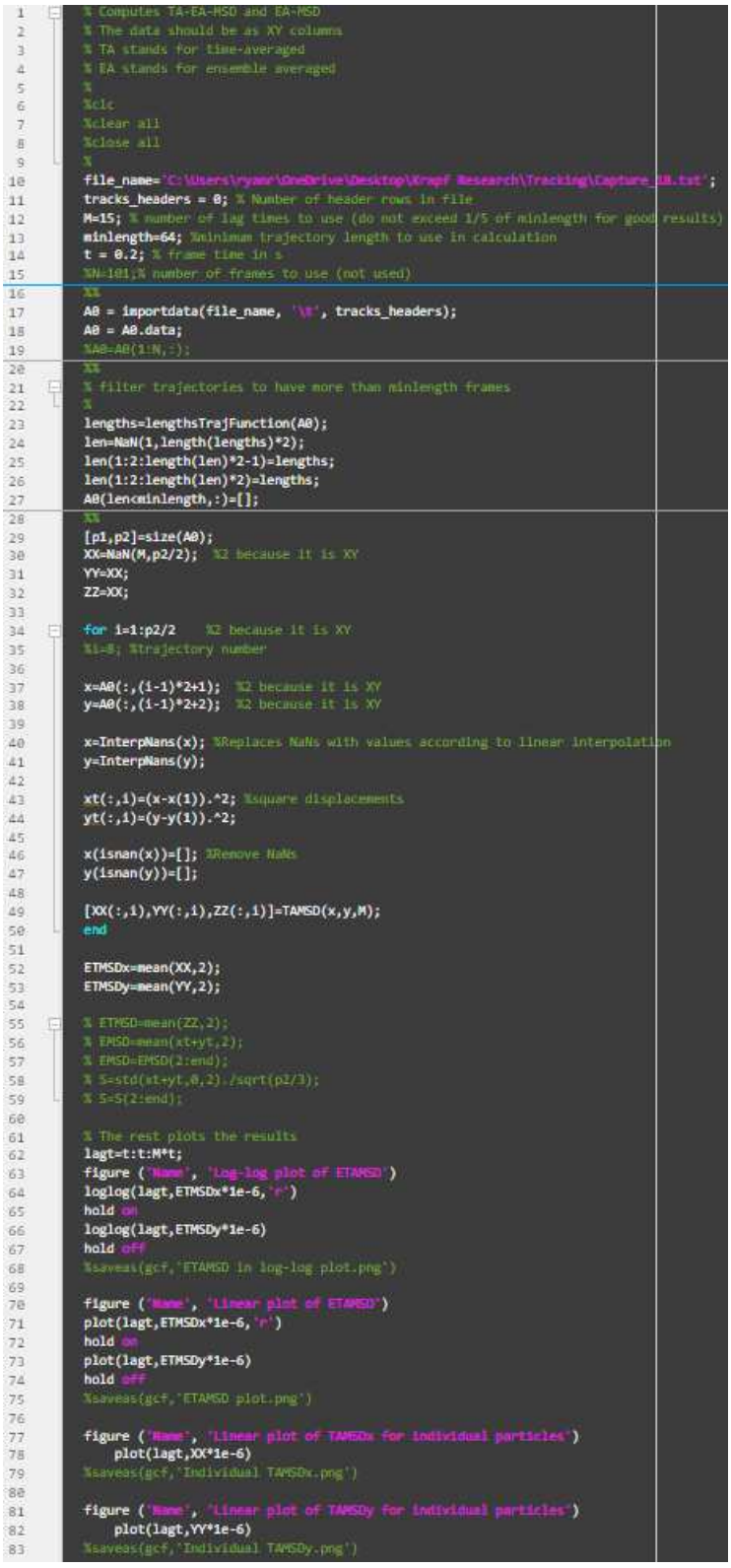

```
% Computes TA-EA-MSD and EA-MSD
% The data should be as XY columns
% TA stands for time-averaged
% EA stands for ensemble averaged
%
%clc
%clear all
%close all
%
file_name='C:\Users\ryanr\OneDrive\Desktop\Krapf Research\Tracking\Capture_18.txt';
tracks_headers = 0; % Number of header rows in file
M=15; % number of lag times to use (do not exceed 1/5 of minlength for good results)
minlength=64; %minimum trajectory length to use in calculation
t = 0.2; % frame time in s
%N=101;% number of frames to use (not used)
%%
A0 = importdata(file_name, '\t', tracks_headers);
A0 = A0.data;
%A0=A0(1:N,:);
%%
% filter trajectories to have more than minlength frames
%
lengths=lengthsTrajFunction(A0);
len=NaN(1,length(lengths)*2);
len(1:2:length(len)*2-1)=lengths;
len(1:2:length(len)*2)=lengths;
A0(len<minlength,:)=[];
%%
[p1,p2]=size(A0);
XX=NaN(M,p2/2);  %2 because it is XY
YY=XX;
ZZ=XX;

for i=1:p2/2    %2 because it is XY
%i=8; %trajectory number

x=A0(:,(i-1)*2+1);  %2 because it is XY
y=A0(:,(i-1)*2+2);  %2 because it is XY

x=InterpNans(x); %Replaces NaNs with values according to linear interpolation
y=InterpNans(y);

xt(:,1)=(x-x(1)).^2; %square displacements
yt(:,1)=(y-y(1)).^2;

x(isnan(x))=[]; %Remove NaNs
y(isnan(y))=[];

[XX(:,i),YY(:,i),ZZ(:,i)]=TAMSD(x,y,M);
end

ETMSDx=mean(XX,2);
ETMSDy=mean(YY,2);

% ETMSD=mean(ZZ,2);
% EMSD=mean(xt+yt,2);
% EMSD=EMSD(2:end);
% S=std(xt+yt,0,2)./sqrt(pi/3);
% S=S(2:end);

% The rest plots the results
lagt=t:t:M*t;
figure ('Name', 'Log-log plot of ETAMSD')
loglog(lagt,ETMSDx*1e-6,'r')
hold on
loglog(lagt,ETMSDy*1e-6)
hold off
%saveas(gcf,'ETAMSD in log-log plot.png')

figure ('Name', 'Linear plot of ETAMSD')
plot(lagt,ETMSDx*1e-6,'r')
hold on
plot(lagt,ETMSDy*1e-6)
hold off
%saveas(gcf,'ETAMSD plot.png')

figure ('Name', 'Linear plot of TAMSDx for individual particles')
    plot(lagt,XX*1e-6)
%saveas(gcf,'Individual TAMSDx.png')

figure ('Name', 'Linear plot of TAMSDy for individual particles')
    plot(lagt,YY*1e-6)
%saveas(gcf,'Individual TAMSDy.png')
```

**Figure E.7:** MATLAB script for calculating EA-MSD, TA-MSD and ET-MSD. This is one of the main analyses we do using 2D trajectories (XY). This is done after concatenating similar trajectories and/or separating mobility states.

**Figure E.8:** MATLAB script for aging MSDs. This script works the same way as 'TAMSDacrossXY.m', only it calculates MSDs using different realization times in order to investigate a relationship between statistics and observation time.

## E.9 Calculating PSDs

'PSDExperimentalTrajectoriesV3.m'

## E.10 Extract Particle Intensities (from Fiji)

'ExtractIntensitiesRyan.m'

## E.11 Analyze Average Particle Intensity vs. $K_\alpha$ and $\alpha$ in One Dimension

'DKalpha1D.m'

```
% Computes Power Spectral Density (PSD)
% The data should be as XY columns

clear
directory='C:\Users\ryanr\OneDrive\Desktop\Krapf Research\RNA data analysis\2022-11-09\Removed - dn6, th0.55\';
file_name='nTracks_T0_Conc128.txt';
tracks_headers = 0; % Number of header rows in file
time1=0.1; %t_step (frames in s)
minlength=128; %minimum trajectory length to use in calculation
Ns = [2^4 2^5 2^6 2^7];  % set of times to assess aging
leg = {'t=16','32','64','128'}; % same times as Ns for figure legend

%%
% No need to change anything after this line

%% Read data
%
file_name=strcat(directory,file_name);
if tracks_headers>0
    X0 = importdata(file_name, '\t', tracks_headers);
    X0 = X0.data;
else
    X0 = importdata(file_name, '\t'); %when data does not have header
end

m=size(X0,2);
%% Select X coordinate and filter trajectories for minlength frames
%
lengths=lengthsTrajFunction(X0); %lengths of all trajectories
X0=X0(:,1:2:m-1); %select X coordinate
X0(:,lengths<minlength)=[];
[frames,m]=size(X0);
% Interpolate and remove initial NaNs
for j=1:m
    X0(:,j)=InterpNans(X0(:,j));
    x1=X0(:,j);
    x1(isnan(x1))=[];
    X0(1:length(x1),j)=x1;
    if length(x1)<frames
        X0(length(x1)+1:frames,j)=NaN(frames-length(x1),1);
    end
end

%%
%initialize whole arrays
p3=Ns(length(Ns))/2+1;  %number of frequencies
pmeanx=NaN(p3,length(Ns));
freqs=NaN(p3,length(Ns));
%
count=0;
for N = Ns
    display(N);
    j=(0:N/2)';
    w=j./(N*time1); %frequencies
    x=X0(1:N,:)-X0(1,:); %subtract first frame
    [pxx,f] = periodogram(x,[],w,1/time1);
    pxx=pxx/2;   % need to change to pxx/2
    f=f*2*pi;

    p3=length(f);
    count=count+1;
    pmeanx(1:p3,count)=mean(pxx')';  %mean PSD
    freqs(1:p3,count)=f;
end

pmeanx=pmeanx*2;

loglog(freqs,pmeanx)
legend(leg)
xlabel('\omega')
ylabel('\langle S(\omega,t)\rangle')
%title(['m=' num2str(m) ', \alpha=' num2str(alpha) ', H=' num2str(H)])
%load gong
%sound(y,Fs)
```

**Figure E.9:** MATLAB script for calculating the PSD for an aging process with various realization times. This is another common analysis we do; the code works similarly to 'TAMSDacrossXY.m', only it calculates the power spectrum of position, rather than the mean square displacement.

```m
%%
clear all
close all
%clc
% filename is CSV table with intensities
filename='Z:\krapflab\Ryan\Analysis and concatenated files\Snehal miRNA\13 fps, single plane\Spots_table_C2-Cell4_armed_0z_13fps_MMStack_Pos0.csv'; %CSV file to read
minlength = 64;

%%

% Read csv table
T = readtable(filename);
% Display available opts
opts = detectImportOptions(filename)
% Filter for these opts
opts.SelectedVariableNames = {'TRACK_ID','TOTAL_INTENSITY_CH1'};
% New table with Track ID and Total Intensity
T1 = readtable(filename,opts);
% Convert to an array
T2 = table2array(T1);

% Rearrange T-1
track_ID_col = T2(:,1);
D = diff(track_ID_col); % Finds where each track ends
track_rows = find(D); % Every row where a track ends

% First row = 0 for first trajectory
track_rows = track_rows';
M=size(T2,1); % Row of last trajectory
track_rows = [0 track_rows M];
traj_lengths = diff(track_rows);
Max = max(traj_lengths);

% T3 is template for intensity columns
T3(1:Max,1:length(track_rows)-1) = NaN;
col_counter = 2;
%for i = 1:out(col_counter) % i=1-13, 1-77, etc.
for i = 1:length(track_rows)-1
    % T3(row 1:13/77/etc, col 1/2/3...) = T2(row 1/13/77/etc:13/77/etc,2)
    T3(1:traj_lengths(i),i) = T2(track_rows(col_counter-1)+1:track_rows(col_counter-1)+1 + traj_lengths(i)-1,2);
    col_counter = col_counter + 1;
end

nanCt = sum(~isnan(T3(:,:))); % Get trajectory lengths per column
short_trajectories = find(nanCt < minlength); % Find columns < minlength
T3(:,short_trajectories) = []; % Remove columns < minlength
% Check that it worked
new_nanCt = sum(~isnan(T3(:,:)));
min_traj = min(new_nanCt);

% Avg Intensities
Tavg = mean(T3, 'omitnan');
% For plotting in Origin
Tavg = Tavg';
```

**Figure E.10:** MATLAB script for extracting the average molecule intensity per trajectory. This creates an average trajectory intensity from a CSV table of total spot intensities (i.e. the total intensity per molecule per frame), which is exported from Fiji. We do this to investigate potential associations between molecule intensity and diffusivity/dynamics under the hypothesis that relatively high intensity particles may be clusters or aggregates of molecules and thus behave differently, whereas low intensity particles are single RNA molecules.

```
% Computes alpha and K from MSD=2K t^alpha
% Also computes D and sigma2 where MSD=2Dt+sigma2
%
% N is number of times to use
%
clear all
close all
%tracks_headers = 1; % Number of header rows in file it can also be 2
file_name='Z:\krapflab\Ryan\Analysis and concatenated files\Snehal miRNA\13 fps, single plane\DKalpha_Cell4_min64.txt'; %File with MSD organized as
                                    %Time in first column
                                    %MSDs in all other columns
N=11;       % number of times to use in fit (8 points)

A0 = importdata(file_name);
%A0 = importdata(file_name, '\t', tracks_headers);
%A0 = A0.data;
times=A0(1:N,1);
A0=A0(1:N,2:end); % First column is time
[p1,p2]=size(A0);

alpha=NaN(p2,1);
K=alpha;
D=alpha;
sigma2=alpha;

for i=1:p2
%i=5; %trajectory number for tests
MSD=A0(:,i);
Plog = polyfit(log(times),log(MSD),1);  %linear fit (log-log scales)
Plinear = polyfit(times,MSD,1); %linear fit
alpha(i) = Plog(1); % Slope from linear fit (log-log scale)
K(i) = exp(Plog(2))/2; % (e^(intercept))/2 (log-log scale)
D(i) = Plinear(1)/2; %in um^2/s
sigma2(i) = Plinear(2); %intercept in um^2
end

K_alpha_D_sigma2=[K alpha D sigma2];
% dlmwrite('K_alpha_D_sigma2Y.txt',K_alpha_D_sigma2,'\t');

plot(K,alpha,'+')
xlabel('K') % x-axis label
ylabel('alpha') % y-axis label
```

**Figure E.11:** MATLAB script for comparing average molecule intensity per trajectory versus $K_\alpha$ and $\alpha$. This code calculates individual $K_\alpha$ and $\alpha$ values per trajectory, which are then compared with the average intensities from 'ExtractIntensitiesRyan.m'.